3-2001

# Simulating Wet Deposition of Radiocesium from the Chernobyl Accident

Aaron M. Kinser


# SIMULATING WET DEPOSITION OF RADIOCESIUM FROM THE CHERNOBYL ACCIDENT

THESIS

Aaron M. Kinser, Captain, USAF

AFIT/GM/ENP/01M-05

**DEPARTMENT OF THE AIR FORCE**
**AIR UNIVERSITY**

**AIR FORCE INSTITUTE OF TECHNOLOGY**

**Wright-Patterson Air Force Base, Ohio**

The views expressed in this thesis are those of the author and do not reflect the official policy or position of the Department of Defense or the United States Government.

AFIT/GM/ENP/01M-5

# SIMULATING WET DEPOSITION OF RADIOCESIUM FROM THE CHERNOBYL ACCIDENT

THESIS

Presented to the Faculty of the Department of Engineering Physics
Graduate School of Engineering and Management
of the Air Force Institute of Technology
Air University
In Partial Fulfillment of the
Requirements for the Degree of
Master of Science

Aaron M. Kinser, B.S.
Captain, USAF

March 2001

AFIT/GM/ENP/01M-5

# SIMULATING WET DEPOSITION OF RADIOCESIUM FROM THE CHERNOBYL ACCIDENT

Aaron M. Kinser, B.S.

Captain, USAF

Approved:

| | |
|---|---|
| Lt. Col. Michael K. Walters (Chairman) | 12 MAR 01 Date |
| Maj. Vincent J. Jodoin (Member) | 12 MAR 01 Date |
| Dr. Dennis W. Quinn (Member) | 12 MAR 01 Date |

*Acknowledgements*

Craig Sloan from AFTAC offered the initial inspiration for this research, and his continued coordination has been crucial to the work. He also personally introduced me to Roland Draxler, paving the way for our productive relationship. The greatest and most generous contributions to this work came from the lead author of HySPLIT software, Roland Draxler of NOAA's Air Resources Laboratory. He has convincingly earned the title of Chief Scientific and Technical Advisor for this thesis. The amount and variety of work, knowledge, and collaboration he contributed (almost totally via e-mail) merits serious consideration as co-author. Thank you, Roland.

Thesis Committee Chairman and inspiring mentor, Lt Col Michael Walters, laid critical groundwork of scientific principles and theory during my graduate level studies at AFIT. Major Vince Jodoin helped me catch the excitement of modeling nuclear events, and quickly got me back on the track whenever I derailed my "nuclear" train of thought. Dr. Dennis Quinn introduced sound, fundamental approaches to the data at hand, and I have fed on his contagious optimism and enthusiasm.

My appreciation goes also to Peter J. Rahe, AFIT Meteorology Laboratory Technician, for equipment set-up and software installation. I am grateful to Capt Lisa C. Shoemaker, Air Force weather officer and AFTAC Meteorologist, for technical advice, data templates, and "been there" encouragement. Ginger Caldwell from UCAR granted and coordinated access to ECMWF data at NCAR. Joey Comeaux from NCAR supplied download and conversion instructions for their mass storage system. He also assembled a program for reading and processing GRIB format data. Thanks to the European Center for Medium-range Weather Forecasting (ECMWF) for reanalyzing and sharing ECMWF model data with the global weather research community.

Noted editor and scientist, Giovanni Graziani, from the European Commission's Joint Research Centre (JRC) in Ispra, Italy contributed deposition data files, key information on handling their contents, the full Radioactivity Environmental Monitoring (REM) Chernobyl database report, and a handsome atlas of European caesium deposition.

I dedicate this thesis to a hard-working heroine, my beautiful wife,

Aaron M. Kinser

*Table of Contents*

## *List of Figures*

## *List of Tables*

## *Abstract*

In response to the Chernobyl nuclear power plant accident of 1986, cesium-137 deposition was measured in Europe at sites equipped to do so. The resulting deposition dataset is uniquely applicable to atmospheric transport model validation. Most of the airborne Chernobyl cesium was wet deposited, i.e., either via interception by falling raindrops (below-cloud scavenging) or via absorption into cloud droplets destined to become raindrops (in-cloud scavenging). The model used in this work is the Hybrid Single-Particle Lagrangian Integrated Transport (HySPLIT) model developed at Air Resources Laboratory. A cloud base modification is tested and appears to slightly improve the accuracy of one HySPLIT simulation of daily Chernobyl cesium-137 deposition over the course of the accident at isolated European sites, and degrades the accuracy of another HySPLIT simulation of deposition in Germany and Austria accumulated in the month of April, 1986. Large uncertainties in the emission specifications, model precipitation fields, and deposition measurements prevent designating the results as conclusive, but most evidence points to improved performance within 500km of the emission source. Trial and error lessons learned from hundreds of preliminary model runs are documented, and the exact HySPLIT settings of successful and meaningful simulations are appended.

# SIMULATING WET DEPOSITION OF RADIOCESIUM FROM THE CHERNOBYL ACCIDENT

## *I. Introduction*

The United States Air Force Technical Applications Center (AFTAC) is charged with observing global environmental conditions to detect and identify activities peculiar to nuclear weapons testing. AFTAC's global array of seismic, atmospheric, and other environmental sensors makes up the U.S. Atomic Energy Detection System (USAEDS). By means of USAEDS and a full complement of world-class analytical laboratories, AFTAC monitors signatory nations' compliance with international nuclear test ban treaties (Hagans 00). In a role supporting this mission, AFTAC meteorologists generate routine and special atmospheric pollutant transport simulations. The simulations can, from a given source, gauge how much pollutant will arrive where and when. Long-range meteorological simulations require accounting for precipitation scavenging, both in-cloud and below-cloud. In-cloud scavenging (or rain-out), hereafter referred to as ICS, is the process of cloud droplets or ice crystals assimilating pollutant within clouds, aggregating, and falling to the ground. Below-cloud scavenging (or wash-out), hereafter referred to as BCS, is the process of pre-formed precipitation cleansing pollutant from the air below clouds on its way to the surface. The combined processes of ICS and BCS result in wet deposition at the earth's surface, and play a significant role in removing long-term pollutants from the atmosphere. So, improvements to wet deposition modeling are important to improving the accuracy of long-range transport simulations. Because wet deposition dominated the other long-range Chernobyl fallout deposition mechanisms, the Chernobyl case, though severely limited by uncertainty in initial conditions and deficiencies in measurement data, is uniquely applicable to wet deposition scheme

validation. AFTAC meteorologists have proposed tests of wet deposition schemes in Chernobyl deposition simulations using the Hybrid Single-Particle Lagrangian Integrated Trajectory (HySPLIT) model (Draxler 98b). The rest of this document expands on the motivations, procedures, and results of requested HySPLIT simulations of the Chernobyl accident fallout deposition.

### *1.1 Problem and Objective*

Reasonable cloud base parameterization is crucial to realistic model assignments of ICS and BCS. To that end, the sensitivity of wet deposition modeling to ICS is tested, then used to interpret results of a test of a HySPLIT modified-cloud-base scheme, namely, reducing cloud bases to 75% relative humidity over land masses from 80%, in pursuit of improved HySPLIT wet deposition parameterization.

### *1.2 Thesis Organization*

The chapters of this thesis are structured so as to clarify specific challenges to modeling wet deposition of Chernobyl Cs-137. Chapter II provides background on aspects of the Chernobyl accident relevant to wet deposition modeling, including emission characteristics and prevalent weather patterns. Chapter II also puts major atmospheric transport studies in perspective with respect to wet deposition modeling. Chapter III describes the methods used to introduce weather variables, validates the basic simulation parameters by comparison to previous work, and details the methods used for further simulation runs of ICS sensitivity and cloud base modification. Chapter IV presents separately the results of said sensitivity runs and cloud base modification runs. Chapter V ties the other chapters together and gives the reader direction for further wet deposition investigation. The appendix is designed to aide the reader in reconstructing and customizing the simulations herein. The reader may find the Glossary of Acronyms in Appendix A frequently useful.

# *II. Background*

## *2.1 Background Overview*

This chapter includes a review of the Chernobyl nuclear power plant accident of April 1986 with emphasis on the role of Cs-137 deposition, a brief description of prevailing weather conditions, a short discussion of major long-range transport studies, and an overview of HySPLIT, the transport model used for all Chernobyl simulations in this thesis. These topics provide a foundation both for an ICS sensitivity study described in Section 3.4, and for a cloud base modification study described in Section 3.5.

## *2.2 The Chernobyl Accident as a Wet Deposition Case Study*

At 2123 UTC (0123L) on 25 April 1986, during a sequence of tests, reactor unit number four at the Chernobyl nuclear power plant experienced an unmanageable increase in power due to a number of "design deficiencies and operator errors" (DeCort 98:11). Emergency actions by the attendant technicians were fruitless as increasing temperatures in the cooling system brought on two violent steam explosions, ejecting reactor components into the reactor room, blowing apart portions of the building including the roof, and setting dozens of fires at the site. Heat from the initial steam explosion and subsequent graphite fire lifted a cloud of radioactive particulates at least a kilometer up into the atmosphere. The emission rate gradually tapered off until 2 May when heroic efforts to contain the fire caused, instead, increasing emissions over the next four days. The ruptured unit was finally sealed in a concrete sarcophagus on 6 May (Klug 92:2). In total, the event released 6000-8000$kg$ of radioactive material and probably much more inactive material into the atmosphere. About one-third of the particles were transported more than 20$km$ from the power plant (Pöllänen 97). Over the course of the 10-*day* emission an estimated $85 \pm 26 PBq$ of Cs-137 was released (Métivier 95). Later, in Section 3.5.1,

complete Chernobyl emission specifications for simulations used in this thesis are described.

Wet deposition played a dominant role in long-range cesium deposition during the Chernobyl accident. Based on estimates of time-integrated concentrations and measured dry deposition velocities of cesium (or "caesium") after the accident, Lauritzen and Mikkelsen suggest "that only approx. 10% of the total deposition of caesium is due to dry deposition, while the remaining 90% stems from wet deposition" (Lauritzen 99). Wet deposition modeling, then, must be included in any realistic simulation of Chernobyl cesium deposition. Long-range (dry) transport is itself an inexact science. Superimposing another process as complicated as rain or snow modeling onto the dry transport process takes transport modeling to a new level of uncertainty. Lauritzen and Mikkelsen call the distribution of atmospheric transport deposition "multi-fractal" and believe that this randomness on all scales "implies that standard atmospheric dispersion models (i.e., deterministic models) cannot explain details of the deposition pattern, but only its gross, average structure" (Lauritzen 99:3271). Case studies of wet deposition are difficult and rare because of this compounded uncertainty. Severe patchiness in deposition measurements from the localizing effects of precipitation scavenging oblige transport experiment designers to carefully schedule experiments so as to avoid the complications of precipitation effects. Likewise, nuclear weapons tests are performed on clear days, avoiding dangerous radioactive hot spots associated with precipitation (Glasstone 77:418). The Chernobyl accident is a unique case study in that it involves a massive quantity of radioactive tracer wet-deposited and measured hundreds and even thousands of miles away. Because the Chernobyl case is a unique case of measured wet deposition, it presents a unique opportunity to validate wet deposition in transport and dispersion models.

### *2.3 Weather Patterns During the Chernobyl Accident*

Although Chernobyl pollutants were eventually detected throughout the northern hemisphere, much of Chernobyl's emissions were deposited in Europe because of low level circulations and widespread precipitation typical for the season. The weather patterns during the accident provided a range of changing conditions throughout the continent. Figure 1 presents simplified surface weather charts for the first four days of the accident from Knap, 1988 (Knap 88:151). Synoptic weather analysis reveals a prevailing cold continental high pressure system to the northeast of Chernobyl. Meanwhile, a North Atlantic semi-permanent low pressure system off the west coast of Great Britain spawned a series of precipitating troughs across western and central Europe during all phases of the Chernobyl accident emissions. While the effects of large-scale features west and east of Central Europe on the Chernobyl plume were apparent during the time of the accident, the plume was often directly steered by smaller, weaker weather features such as the shallow fronts associated with these short-wave troughs.

### *2.4 Cesium-137 Transport from the Chernobyl Accident*

For particles to travel far enough (100's to 1000's of $km$) to be considered long-range emissions, they must be aerodynamically small enough for turbulence to keep them suspended and carried on the wind for days. The Chernobyl fire generated massive quantities of sub-micron particles carrying Cs-137 (cesium-137). Small particles, $1\mu m$ in aerodynamic diameter and smaller, have a fall speed of less than about $1.0mm/s$. Accordingly, the dry processes that have the greatest influence on their transport and deposition are turbulent eddies and Brownian diffusion (small particles spread out by random collisions with air molecules) (Pöllänen 97). Particles that tiny remain suspended long enough for precipitation, when present, to play a major role in their deposition. Large particles, $20\mu m$ in aerodynamic diameter and larger, have a fall speed of greater than about $10.0mm/s$ in the lower

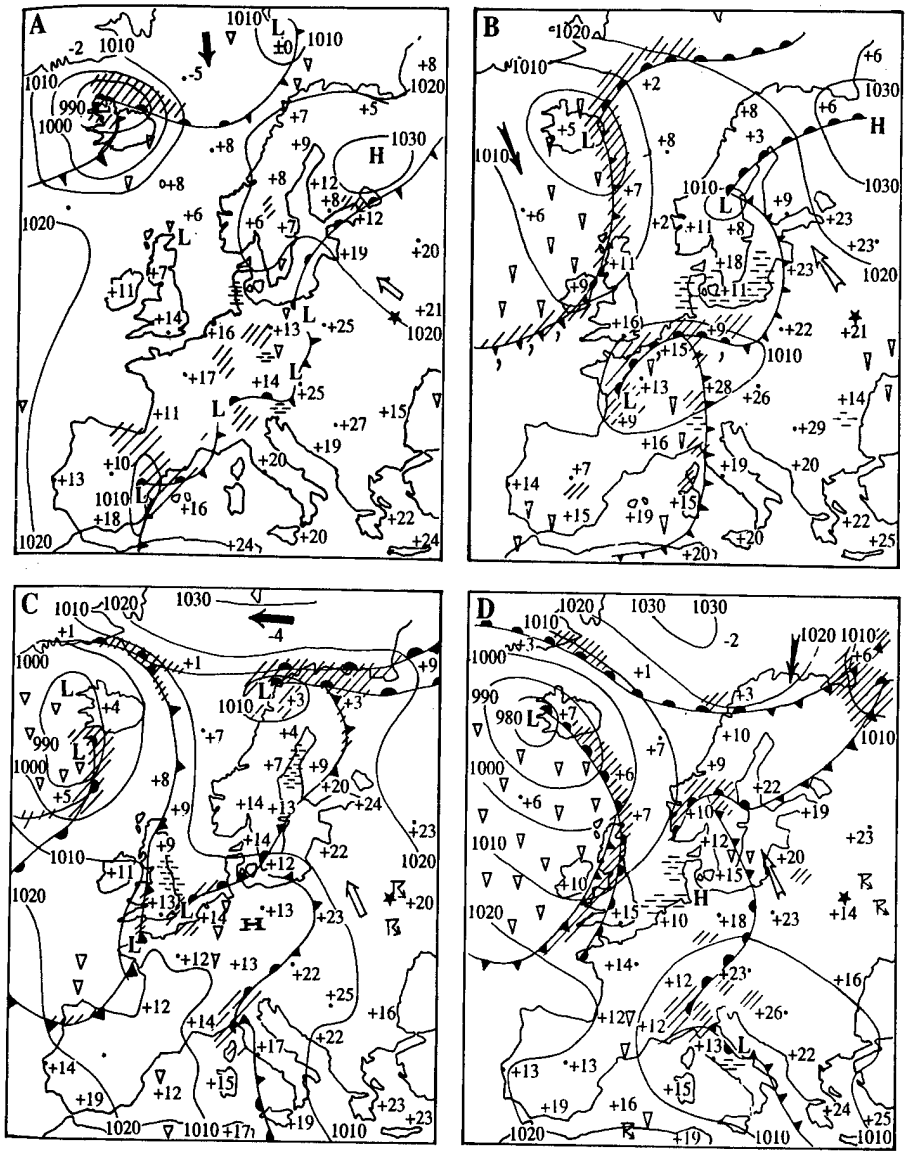


Figure 1 Simplified 12Z surface weather maps for 25 - 28 Apr, 1986 (Knap 88)

atmosphere. As a result, the processes that have the greatest influence on their deposition are gravitational settling (large particles pulled earthward) and turbulent dispersion (particle-bearing air mass grows by entrainment). The relatively short transport life of large particles prevents rain from playing a significant role in their deposition. Particles with a size between small and large present a special challenge to the transport and deposition modeler. A single fall speed parameterization for medium-sized particles is elusive. Which dry transport mechanisms determine the effective fall speed of medium-size particles depends on whether the particles are large-medium or small-medium and on several specific weather conditions at each location (Seinfeld 86). Fortunately for Chernobyl plume modelers, particles from the Chernobyl accident containing Cs-137 are confined mainly to the small category because of how they were formed in the fire and smoke at Chernobyl.

Cs-137 and Sr-90 (strontium-90) are signature long-range fallout isotopes both of nuclear power production and of nuclear weapons testing. The human body is less susceptible to harm from ingesting Cs-137 than from ingesting the same amount of Sr-90. The biological half-life of Cs-137 is 50 to 200$days$. Sr-90, on the other hand, is chemically similar to calcium, so the body tends to concentrate the isotope in bone tissue where it remains in the body much longer. So, even though Cs-137 is just as easy to measure, has a slightly longer radioactive half-life, and is slightly more abundant than Sr-90 in nuclear weapons fallout, nuclear scientists normally characterize long-range weapons fallout by patterns of Sr-90 deposition (Glasstone 77:604). The accident at Chernobyl, due to the nature of the explosion and fire, produced relatively little Sr-90 outside the 30-$km$ evacuation zone (DeCort 98:13). Therefore, Cs-137 is the best species for characterizing the long-range radioactive deposition pattern from the Chernobyl accident as a whole (Klug 92).

Because Cs-137 is radioactive, it is detectable in very small concentrations, an ideal property for a long-range plume tracer. The radionuclide itself has a radioactive decay half-life of more than thirty years (Serway 92). Such a long half-

life affords meaningful cumulative measurements over periods of months and even years. More details are available in Appendix B, a primer on radioactivity and Cs-137. An experiment releasing sub-micron particles bearing Cs-137 would, in theory, be ideal for validating and improving operational wet deposition modeling. Atmospheric nuclear weapon tests in the 1950's and 1960's injected radiocesium into the stratosphere which, to this day, continues to trickle radioactive particles back into the troposphere, especially at mid-latitudes near the jetstream, although one could argue that the amount is negligible (Glasstone 77:448). At any rate, a large and hazardous emission would be required to discern long-range experimental concentrations above measurement background noise, and the political repercussions of such an experiment would be prohibitive. An experimental case study using Cs-137 as a tracer is not feasible. So, the Chernobyl case is likely to remain a unique opportunity to model and compare Cs-137 deposition on a large scale.

### *2.5 Other Long-Range Transport Modeling Exercises*

In November 1986, an international effort emerged to coordinate a transport modeling study within the context of the Chernobyl accident. In response to the accident and its environmental repercussions, the IAEA (International Atomic Energy Agency) collaborated with the WMO (World Meteorological Organization) to develop the Atmospheric Transport Model Evaluation Study (ATMES). The study was designed both to test the emergency response capability of current transport modeling agencies, and to "intercalibrate" their various models (Klug 92:v). Twenty-two agencies from fourteen countries volunteered their transport models for the study. Each model was developed independently, some for purposes other than nuclear accident response, so results varied widely. Some models were designed for meso-scale application and were specially adapted for the ATMES exercise. Some simulated puff emissions, others tracked individual particles. Some were based on integrations in an Eulerian frame, others were based on Lagrangian integrations. Each

model's configuration and results were compiled in the ATMES Report along with comparisons to each other and to available measured deposition data. The writers of the ATMES Report constructed a contour plot of accumulated Cs-137 deposition (Figure 2) from available surface-based measurement data. Though based on all available deposition measurements at the time, the figure is not representative of the whole pattern of Chernobyl Cs-137 deposition. For instance, even though the highest concentrations of Cs-137 were found near Chernobyl at 51.38° latitude, 30.1° longitude, Figure 2 suggests a minimum there. So, due to large data sparse regions, it appears Figure 2's content may be less representative of area-averaged Cs-137 deposition values than of the geographical density of observation sites in the ATMES Cs-137 deposition dataset (map in Section 3.5.4).

A key result of the ATMES project was the realization of the strong need for an experimental case, i.e. a transport experiment with known emission specifications and synchronized, homogeneous measurements, to confidently evaluate even the relative performance of long-range transport models (Klug 92). Controlled experiments have several advantages over accidental cases. To date, major long-range atmospheric transport modeling experiments have all released non-depositing tracers to maintain detectable pollutant concentrations over distance and remove uncertainties involved in deposition. Controlled experiment observations are planned at regular time and space intervals to generate output grids that are homogeneous (Rodriguez 95:800). Perhaps most importantly, the source rate and height are known precisely in a controlled experiment, in stark contrast to the typically vague specifications of accidental emissions.

Following the guidance from ATMES conclusions, and the lessons learned from the Across North America Tracer EXperiment (ANATEX), the same agencies that organized the ATMES Report designed and executed the European Tracer Experiment, or ETEX (Rodriguez 95). This time, NOAA's Air Resources Laboratory (ARL) was a participant in the study, contributing deposition simulations created

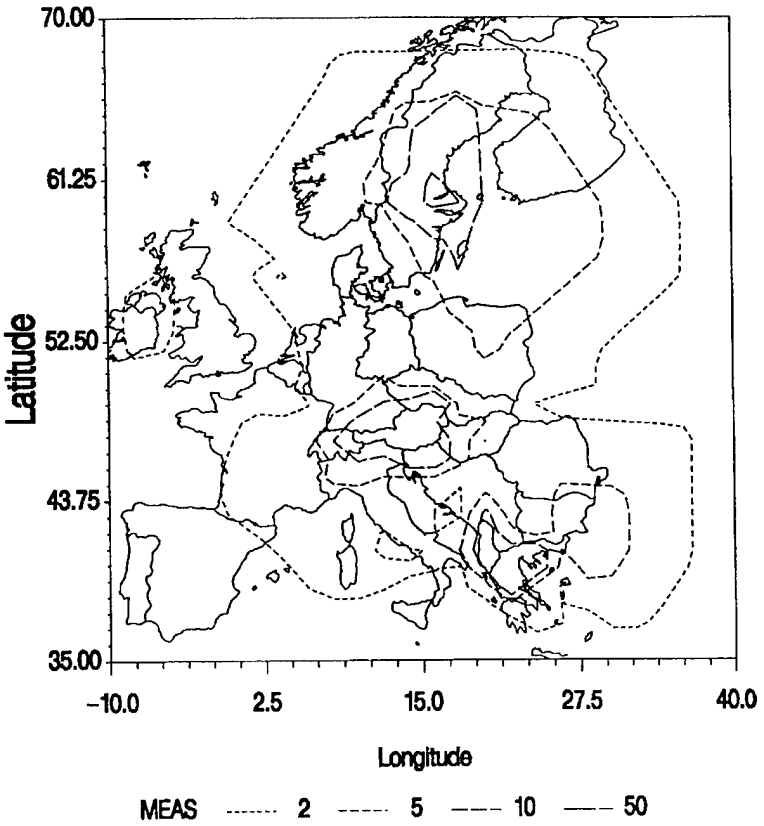


Figure 2 Geographic plot of contours of accumulated Cs-137 deposition $[kBq/m^2]$ from 27Apr1986 to 10May1986. ATMES Report Figure 10 (Klug 92).

with HySPLIT Version 4.0 (ARL 00b). The organizers of ETEX, like the ANATEX designers, chose a non-soluble perfluorcarbon chemical as a tracer species. The chemical resists deposition by both wet and dry mechanisms, optimizing the homogeneity of the tracer's transport pattern, and so making for better simulation comparisons. Both ANATEX and ETEX were initiated in part to provide a dataset for future model evaluations. The careful completeness of each experiment's design makes them ideal for long-range (dry) transport model evaluations and improvements. However, since the tracer could not be rained out, their datasets are not suited for a wet deposition study (Graziani 97). Again, the Chernobyl accident

stands alone as a case study for validating long-range wet deposition schemes against in situ measurements.

### *2.6 HySPLIT Model Description*

HySPLIT, the Hybrid Single-Particle Lagrangian Integrated Transport model calculates either the trajectories of air parcels, or the transport, dispersion and deposition of pollutant particles or puffs. User-supplied inputs for HySPLIT calculations are pollutant species characteristics, emission parameters, gridded meteorological fields, and output deposition grid specifications. Input meteorological fields can be on Polar Stereographic, Lambert Conformal, or Mercator map projections. The horizontal deformation of the wind field, the wind shear, and the vertical diffusivity profile are used to compute dispersion rates. The model can be configured to treat the pollutant as particles, or as Gaussian puffs, or as top-hat puffs. The term hybrid refers to the additional capability of HySPLIT to treat the pollutant as a Gaussian or top-hat puff in the horizontal, while treating the pollutant as a particle for the purposes of calculating vertical dispersion. An advantage to the hybrid approach is that the higher dispersion accuracy of the vertical particle treatment is combined with the spatial resolution benefits of horizontal puff-splitting. All model runs for this work were made in the default hybrid particle/top-hat mode.

HySPLIT calculates wet deposition by scavenging pollutant from portions of the plume in (ICS) and below (BCS) precipitating model clouds. All of the scavenged pollutant is assumed to deposit on the ground directly below the clouds. To identify precipitating model clouds, HySPLIT's wet deposition algorithm checks the input meteorological data at each surface gridpoint for precipitation. Where precipitation is non-zero, it searches upward from the top of the surface layer (i.e., no fog modeling) for the lowest model level with an RH (relative humidity) greater than or equal to 80%. This 80% threshold establishes the modeled cloud base. A 75% threshold is tested later in Chapter III. The cloud top is determined by the lowest level above

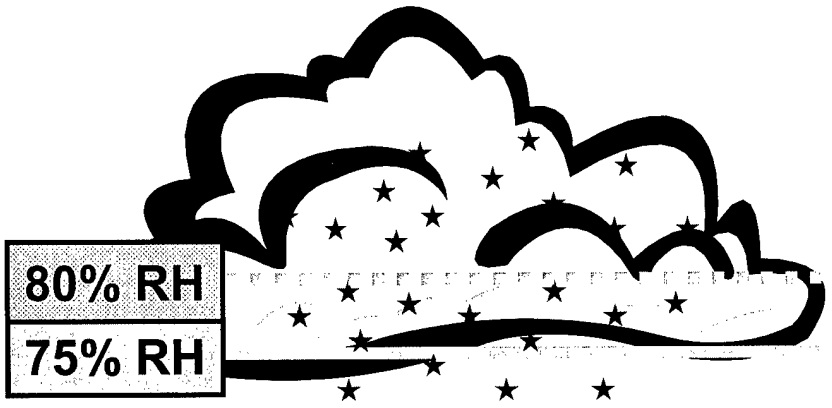


Figure 3 Illustration of cloud representation in HYSPLIT. Stars represent pollutant plume. 80% RH is the default cloud base, 75% RH is the tested modification.

the base where the RH is below 60%. Above the first (lowest) cloud layer, HySPLIT diagnoses no more clouds. Figure 3 illustrates a precipitating cloud, both modeled cloud bases, and a pollutant plume.

Below the bases of precipitating clouds HySPLIT scavenges the pollutant plume, reducing its concentration by an amount equal to the product of the pollutant concentration, the user-specified BCS rate $[s^{-1}]$ (below-cloud scavenging rate), and the time increment $[s]$. The amount of below-cloud pollutant reduction (concentration reduction times plume volume) is then added to the surface deposition output grid. Deposition from ICS (in-cloud scavenging) is calculated (and in-cloud pollutant concentration is reduced accordingly) using a user-specified ICS efficiency $[L/L]$ defined as the ratio of pollutant concentration in air (grams of plume pollutant per liter of air) to pollutant concentration in rain (grams of deposited pollutant per liter of precipitated water). The amount of deposition from ICS is found by multiplying the in-plume pollutant concentration $[L^{-1}]$ by the rain accumulation $[mm]$ and dividing by the ICS efficiency as derived in the equations below (unit conversion: $1m^2 \times 1mm = 1Liter = 0.001m^3$). This approach to ICS requires rain rate $[mm]$

from the input meteorological grid. HySPLIT is not able to calculate wet deposition without input precipitation fields (Draxler 98a:16).

$$\frac{\text{In-Cloud Plume Concentration}}{\text{Rain Concentration}} = \text{ICS Efficiency}$$

$$\text{Rain Pollutant}[g/L] = \frac{\text{Air Pollutant}[g/L]}{\text{ICS Efficiency}}$$

$$\text{Rain Pollutant}[g/m^2] \text{ / Rain}[mm] = \frac{0.001 \times \text{Air Pollutant}[g/m^3]}{\text{ICS Efficiency}}$$

$$\text{Rain Pollutant}[g/m^2] = \frac{0.001(\text{Air Pollutant}[g/m^3])(\text{Rain}[mm])}{\text{ICS Efficiency}}$$

# *III. Methodology*

## *3.1 Methodology Chapter Overview*

HySPLIT has seen frequent algorithm updates to assimilate current findings in the field of atmospheric transport modeling, and HySPLIT's user interface has been continually enhanced to improve its usability as an operational tool. This chapter supplies the details on exactly how to use HySPLIT to perform selected atmospheric transport simulations. Section 3.2 describes how meteorological fields including wind, temperature, pressure, humidity, and precipitation data were incorporated in simulations for this thesis. To ensure that correct meteorological fields and other inputs are being used, a duplicate Cs-137 deposition simulation is attempted and compared to results produced by ARL. Section 3.3 explains how the attempted duplicate simulation is performed. Section 3.4 describes the method used to evaluate the sensitivity of a Chernobyl simulation to various scavenging rates. Finally, Section 3.5 describes the procedures used to validate a proposed cloud base modification in the model against Chernobyl deposition measurements. Results of sensitivity runs and of cloud base modification runs are presented later, in Chapter IV.

## *3.2 Incorporation of Meteorological Input Fields*

The meteorological input fields for all simulations are reanalyzed ECMWF data from NCAR. Using HySPLIT for Chernobyl plume transport and deposition calculations requires conversion of ECMWF GRIB format meteorological fields to ARL packed format (Draxler 99). The conversion utility program provided with HySPLIT requires platform-dependent GRIB decoder libraries typically available from the source of raw GRIB data, in this instance NCAR. As it converts a file to ARL-packed format, the utility interpolates the data linearly to a polar stereographic lat/lon grid in the horizontal, and to internal terrain-following sigma levels in the vertical. HySPLIT uses the smallest domain of input meteorological fields as the

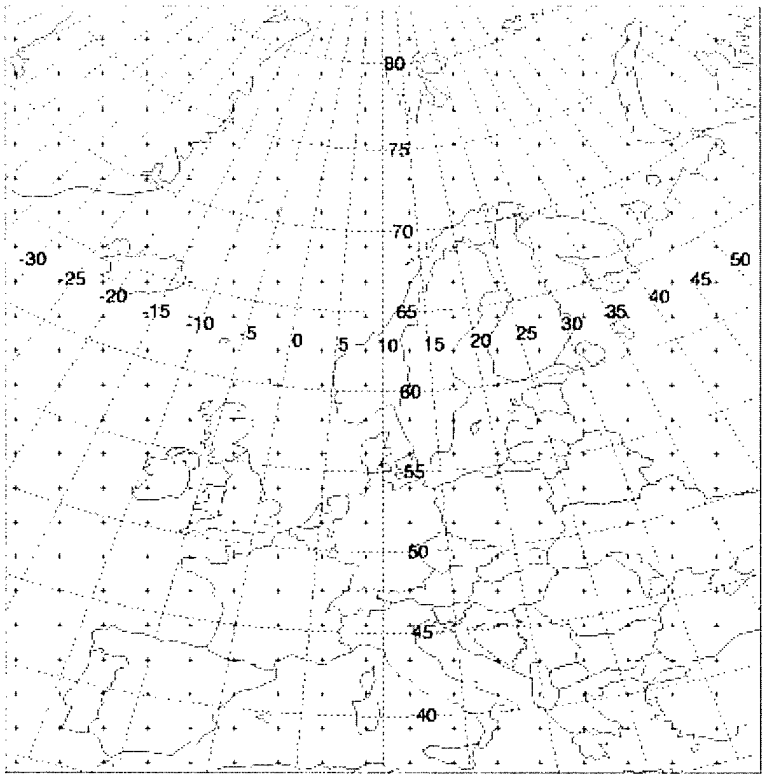


Figure 4 Model domain and resolution of ECMWF meteorological input data grid, also used for concentration calculations in HySPLIT. Crosses at every fourth gridpoint for clarity. .

total domain for a given simulation. The domain and resolution of the ECMWF input files for all simulations in this work is depicted in Figure 4. Upper air data fields for all simulations include temperature in [°C], $u$ and $v$ wind components in $[m/s]$, $w$ wind component in $[hPa/hr]$, and specific humidity in $[g/kg]$. The surface data fields provided are 2-$m$ temperature in [°C], 10-$m$ $u$ and $v$ wind components in $[m/s]$, surface pressure in $[hPa]$, and 6-$hr$ prior accumulated precipitation in $[mm]$. For comparison to simulations and for informal diagnosis of wet deposition effects, a full set of six-hourly ECMWF re-analyzed precipitation fields over the model domain for the first five days of the accident are provided as shaded plots in Appendix C.

### *3.3 Comparison to Chernobyl Simulation by ARL*

Before addressing the methods for sensitivity runs and cloud base modification runs (Sections 3.4 and 3.5), evidence is presented here to show that the working installation of HySPLIT is performing as designed, and that appropriate meteorological fields and user-specified parameterization settings are being utilized properly. The evidence takes the form of results from an attempted duplicate of web-published Chernobyl deposition contours generated at ARL (Air Resources Laboratory) (ARL 00a). The attempted duplicate simulation uses an abbreviated Chernobyl source term, releasing pollutant at a constant rate for $24hrs$ only. Gross features of the 84-$hr$ deposition patterns from the ARL simulation (Figure 5) and the attempted duplicate (Figure 6) are in agreement, suggesting that HySPLIT is functioning properly, the proper time period of meteorological data has been applied, wet scavenging is actually being modeled, etc. Differences (e.g., deposition southeast of Chernobyl) between the ARL simulation and the attempted duplicate are attributable to ARL's undocumented inclusion of some emissions beyond the first 24 hours (Draxler 00a). A copy of the control file settings used to create the HySPLIT duplicate simulation is furnished in Section D.2 of Appendix D. The setup for this simulation serves as a baseline for simulation setups for the remainder of this work.

### *3.4 In-Cloud Wet Scavenging Rate Sensitivity Runs*

To gauge the relative importance of ICS in wet deposition modeling, a simplified scenario is required mainly because the actual emissions from Chernobyl were continuous for days, making it difficult to attribute given deposition to a particular release time. So, an abbreviated emission is used in the sensitivity run, and the country of Germany is chosen as the deposition domain because the weather conditions modeled there also apply to cloud base modification studies in Section 3.5. The sensitivity run emission rate, $6.65 \times 10^{14} Bq/hr$, and the emission's uniform vertical profile from $1250m$ to $1750m$, mirror the first phase of the Chernobyl emission

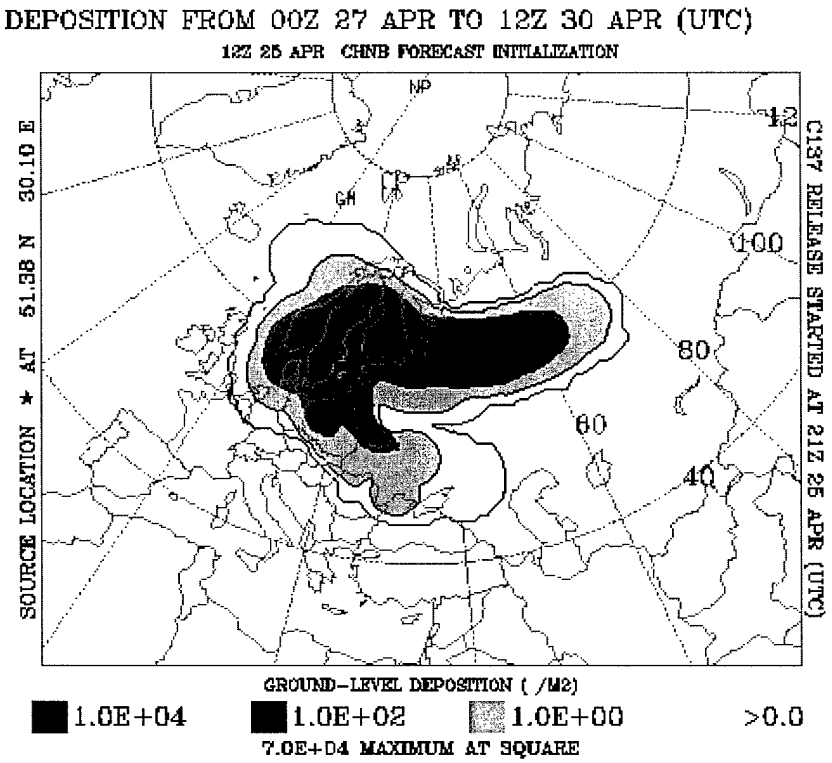


Figure 5 Chernobyl Cs-137 deposition as modeled by ARL. Deposition velocity set at $0.1 cm/s$. In-cloud scavenging ratio set at $3.2 \times 10^5 l/l$. Below-cloud scavenging rate set at $5.0 \times 10^{-5} s^{-1}$. Deposition contoured on a logarithmic scale

simply because it is useful to verify the model's ability to accommodate values with these magnitudes. Apr 26 is the chosen time period because precipitation is present that day. Six-hourly accumulations of pollutant deposition are recorded to coincide with the time resolution of the precipitation fields. The coordinate 48.0° latitude, 11.0° longitude is the chosen release location because the spot is immediately upstream from Germany during the chosen period. If the modeled release were chosen at Chernobyl, it would not be possible to observe the immediate influence of ICS.

ARL suggests a value of $3.2 \times 10^5$ for the user-specified ICS efficiency after Hicks (Hicks 86) and an empirical mean value of $5.0 \times 10^{-5} s^{-1}$ for the BCS rate. To evaluate the sensitivity of HySPLIT's wet deposition scheme to ICS parameters,

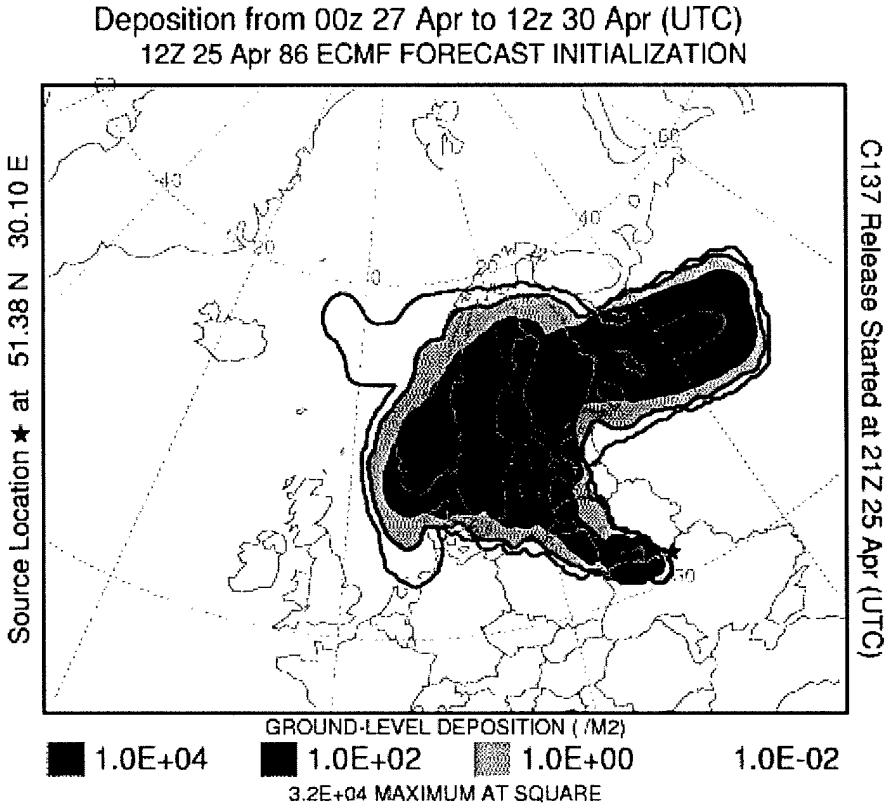


Figure 6 Attempted duplicate of ARL's Chernobyl Cs-137 deposition. Source modeled as uniform vertical line source from $750m$ to $1500m$ at a rate of $10^{15}Bq/hr$ for 24 hours. Deposition velocity set at $0.1cm/s$. In-cloud scavenging ratio set at $3.2 \times 10^5 l/l$. Below-cloud scavenging rate set at $5.0 \times 10^{-5}s^{-1}$. Deposition contoured on a logarithmic scale.

these ARL-recommended values are employed as the baseline values for the sensitivity control run. In addition to the sensitivity control run, a simulation is performed for each of these ICS efficiencies: $3.232 \times 10^5$, $3.36 \times 10^5$, $3.52 \times 10^5$, $3.168 \times 10^5$, $3.04 \times 10^5$, $2.88 \times 10^5$. These values reflect boosts and reductions of the ICS efficiency by 1%, 5%, and 10%. HySPLIT control file settings for the sensitivity control run are recorded in Section D.3 of Appendix D. HySPLIT output concentration grid files are converted using HySPLIT utility program, 'con2bin.exe' to GRADS format for field differencing. Results of the sensitivity simulations accompanied by plots of simultaneous accumulated model precipitation are presented in Section 4.1.

## *3.5 Modeled Cloud Base Modification*

In this Section, a method is presented for assessing performance of a modified-cloud-base height parameterization in simulations of Chernobyl Cs-137 deposition. Subsection 3.5.1 develops a reasonable source term (emission specification). Subsection 3.5.2 gives the motivation and procedure for the specific cloud base modification tested later. The available dataset lends itself best to two main model comparisons: a comparison to simulations of daily deposition 1986Apr28 - 1986May15 at 21 measurement sites spread across Europe described in Subsection 3.5.3, and a separate comparison to simulations of April-cumulative deposition from the onset of Chernobyl emissions at 2123Z, 1986Apr25, up to 0000Z, 1986May01 at a cluster of 395 measurement sites in Germany and Austria, described in Subsection 3.5.4.

*3.5.1 Daily Phases of Chernobyl Emissions.* The best-guess Chernobyl source term (i.e., the emission specifications) is segmented into daily phases, except that the plume is treated separately during the first seven hours because it is believed to have risen significantly higher than subsequent emissions. The twelve phases, I through XII, used in this research are adapted from Table 1 of the ATMES Report (Klug 92:358). The ATMES Report provided a daily Cs-137 emission rate, specified a center of mass height for each phase of emission, and required that a step-function be used for the project's simulations. However, the ATMES organizers "still gave a certain degree of freedom to the participants, e.g. on the mass distribution with height" (Klug 92:2). According to the ATMES report, revised Russian release height estimates presented to the ATMES Steering Committee in January, 1989 are the only authoritative estimates (Klug 92:1,2). Today, though some documented evidence supports a change to the official release height, the source term estimate has not yet been updated by consensus (Graziani 00). Generally, it is accepted that the initial plume escaped the boundary layer, and that, after the first two days, the initial plume did not exceed an altitude of $400m$ (Persson 87). For this research, Phases I and II were recalculated (based on equal total emission amounts to 0000Z, 27Apr)

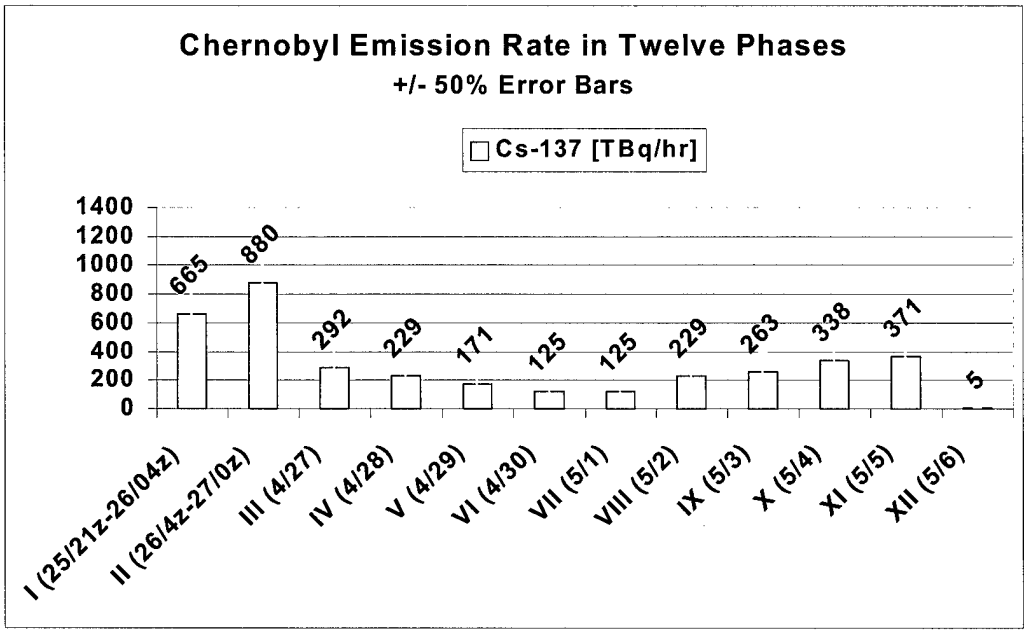


Figure 7 Complete Chernobyl Cs-137 modeled source term in twelve phases. Plume modeled as uniform vertical line source at an hourly rate in becquerels. Phase I initial plume 1250-1750$m$, Phases II and III initial plumes 350-850$m$, Phases IV through XII initial plumes 200-400$m$.

as a compromise between ATMES' 26.0000Z 6-$hr$ initial plume and the known time of Chernobyl's initial explosion, 25.2123Z. Each phase was modeled in HySPLIT as a uniform vertical line source. Figure 7 displays the resulting twelve Chernobyl emission phases.

The first few hours of Chernobyl emissions are the release time period with the greatest vertical location uncertainty. It is agreed that the initial steam explosion and ensuing fire at Chernobyl launched radioactive particles well above the accident-averaged boundary layer top at roughly $500m$. Pollanen et al. present evidence for a higher release height based on large particle trajectory calculations.

> "In northeastern Poland, 500-700 $km$ from Chernobyl, particles up to $\sim 60$ *microns* in aerodynamic diameter were found. Their sedimentation velocity is so large (up to $\sim 0.1ms^{-1}$) that turbulent dispersion, rapid transport in a prefrontal low-level jet, warm frontal conveyor belt ... or

even effective release height of 3000 $m$ cannot explain these findings" (Pöllänen 97:3581).

A series of four preliminary 84-$hr$ Chernobyl simulations is accomplished here to demonstrate how much the pattern of modeled pollutant deposition in Europe changes for a range of distinct, reasonable point source heights, namely, $1500m$, $3000m$, $4000m$, and $5000m$. These preliminary simulations are not referenced outside of this section of the thesis. Each simulation's emission mirrors Chernobyl's initial emission rate of $6.65 \times 10^{14} Bq/hr$ (see Subsection 3.5.1 for a complete time profile of best-guess Chernobyl emissions). Other particle parameterizations are empirical estimates of those properties typical of Cs-137-bearing particles from a nuclear reaction. The four preliminary simulations are identical except for release height. Exact HySPLIT settings used for the 1500-$m$ run are presented in Section D.1 of Appendix D along with detailed descriptions of each setting. These descriptions serve to familiarize the reader with HySPLIT concentration model setup. Should the reader consider downloading and using HySPLIT, further instructions are available on the internet from ARL (and more details are in Appendix D). A surface deposition concentration grid is computed in each simulation over the lat/lon grid centered at 48°/13° and spanning 26° of latitude, 36° of longitude. The main difference between a 1500-$m$ release (Figure 8) and a 3000-$m$ release (Figure 9) is an overall decrease in deposition, presumably because the particles take longer to settle from a higher release point, and because greater wind speeds at $3000m$ carry more particles beyond deposition grid boundaries. Changing the release height to $4000m$ (Figure 10) produces a distinct southward shift in the 84-$hr$ deposition pattern. Less pollutant deposits in the Nordic countries (e.g., none in Finland), while higher and more widespread pollutant concentrations are modeled from Ukraine and Romania to Italy, France and even Algeria. A release height of $5000m$ (Figure 11) produces a further southward shift in the deposition pattern: less deposition from Lithuania and Belarus to Sweden, more deposition from Ukraine and Romania to

Italy and Algeria. For the reader's reference, Appendix E offers a map of Europe with current political boundaries.

The pollutant is transported completely across the Mediterranean Sea into Algeria when the initial plume exceeds $3000m$. The concentration of modeled deposition is on the order of only $1Bq/m^2$, well below background levels of 2000 - $3000Bq/m^2$. However, modeled deposition underestimates hot spots due to precipitation field smoothing. So, if the model is broadly accurate in the region, detection would not be impossible, especially if daily measurements are available within deposition hot spots. Though beyond the scope of this work, this clue would be of special interest to those interested in refining the Chernobyl source term. There is a distinct shift in the deposition pattern to include deposition south and east of Chernobyl for release heights above $3500m$. This change in general plume direction supports the view that release heights above $3000m$ would seriously alter the deposition pattern of Chernobyl's day one emissions.

*3.5.2 Modified-Cloud-Base Motivation and Procedure.* Since empirical values for Cs-137 ICS efficiency and BCS rate have been documented, a logical place to look for wet deposition improvement is the cloud base parameterization since it directly determines vertically where modeled BCS stops and modeled ICS begins. The complexities of cloud formation are immense and many. Sophisticated prognostic cloud models are available, but are computationally expensive and gain little accuracy over diagnostic parameterizations since large uncertainties remain in the accounting of "advective transports of cloud variables, sub-grid scale processes, cloud microphysics, and cloud optical properties" (Tiedke 93:3040). Most current transport models and even some global meteorological models still use simple diagnostic schemes to model clouds. Future generations of transport models may just accommodate liquid and ice cloud fields from the input meteorological model rather than calculating their own cloud limits. For now, a parameterization is still needed and HySPLIT's simple scheme of cloud diagnosis from relative humidity is considered

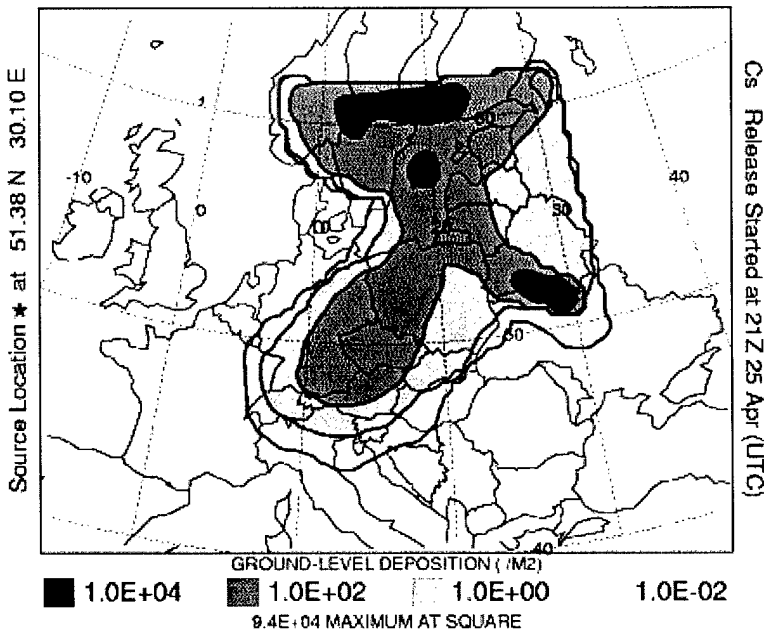


Figure 8 Chernobyl deposition $[Bq/m^2]$ from 00Z 1986Apr26 to 00Z 1986May01. Emission from 2123Z Apr25 for $24hrs$ at Chernobyl (star in the graphic) at $6.65 \times 10^{14} Bq/hr$ from 1500-$m$ point source height.

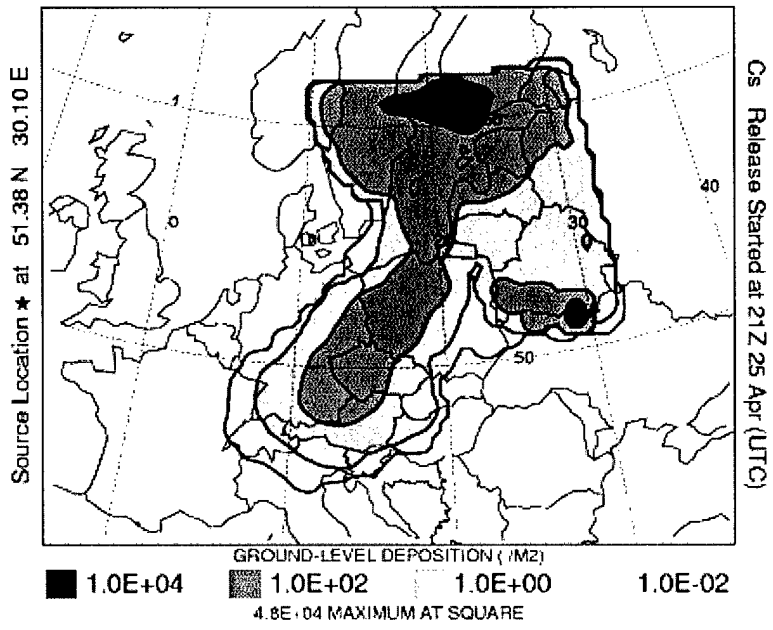


Figure 9 Chernobyl deposition $[Bq/m^2]$ from 00Z 1986Apr26 to 00Z 1986May01. Emission from 2123Z Apr25 for $24hrs$ at Chernobyl (star in the graphic) at $6.65 \times 10^{14} Bq/hr$ from 3000-$m$ point source height.

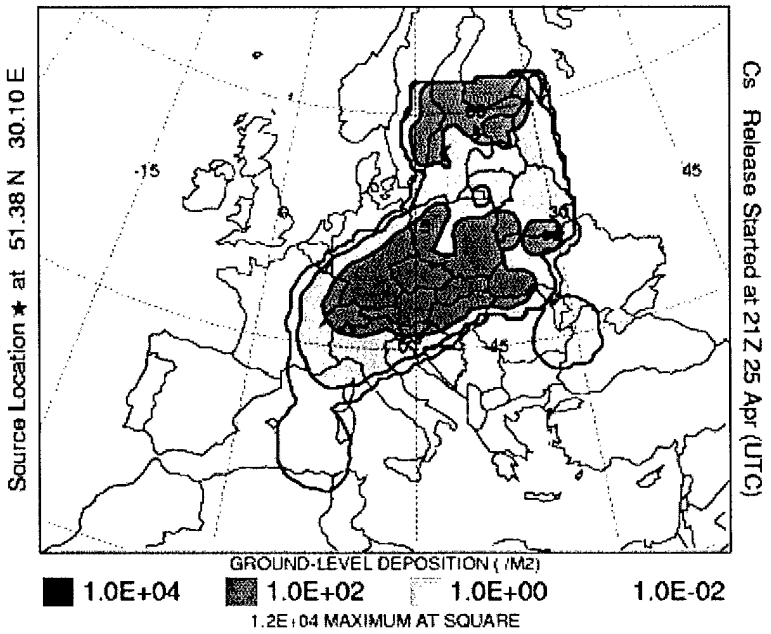


Figure 10 Chernobyl deposition $[Bq/m^2]$ from 00Z 1986Apr26 to 00Z 1986May01. Emission from 2123Z Apr25 for $24hrs$ at Chernobyl (star in the graphic) at $6.65 \times 10^{14} Bq/hr$ from 4000-$m$ point source height.

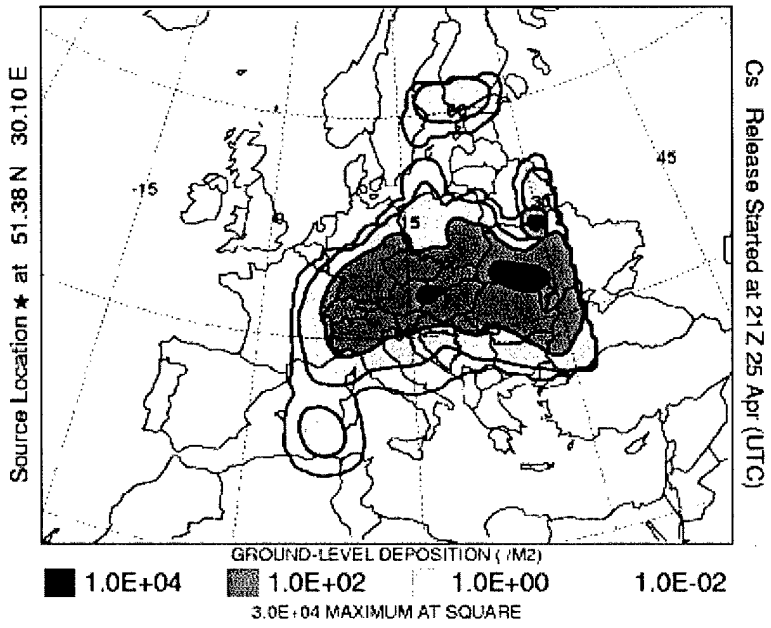


Figure 11 Chernobyl deposition $[Bq/m^2]$ from 00Z 1986Apr26 to 00Z 1986May01. Emission from 2123Z Apr25 for $24hrs$ at Chernobyl (star in the graphic) at $6.65 \times 10^{14} Bq/hr$ from 5000-$m$ point source height.

an over-generalization (Draxler 00b). To attempt an improvement to HySPLIT's cloud base parameterization simple enough to test in a short time, and as a starting point for exploring cloud base parameterization, a simple HySPLIT modification is proposed following work at NCEP (National Center for Environmental Prediction). As part of a comprehensive cloud model algorithm in NOAA's Meso ETA model, meteorologists at NCEP split the cloud base scheme into a marine part and a terrestrial part. It is believed that an 80% RH cloud base over continents represents too little cloud condensation. Cloud bases over land are modeled at 75% RH while cloud bases over water are modeled at 80% RH (Staudenmaier 96). HySPLIT's hard-wired 80% RH cloud base is not unreasonable. If limited to a single value, long-range transport models should weight a unified scheme in favor of the marine environment since the earth's surface is mostly water. So, if NCEP's scheme approximates reality, 80% RH-modeled global cloud bases should outperform 75% RH-modeled cloud bases on a global scale. However, since HySPLIT has the ability to distinguish land use types, there is no need to compromise. The requisite cloud base modification in HySPLIT requires a change to the model source code as given in Appendix F. HySPLIT source code was provided for this thesis courtesy of Roland Draxler at ARL. Once the source code is edited and recompiled, the comparison runs can be accomplished identically to the April deposition control runs. Test results of April deposition control runs and April deposition modification runs against the April deposition data are presented in Section 4.2.

*3.5.3 Modified-Cloud-Base Procedures, Simulation of Daily Deposition.*
The available dataset used for comparing surface-based Cs-137 measurements to simulation data is from the REM (Radioactivity Environmental Monitoring) Chernobyl archives at the JRC/Ispra (Joint Research Centre - Ispra, Italy) of the EC (European Commission) (DeCort 90). Deposition from above-ground nuclear weapon tests in the mid 1950's and early 1960's has blanketed the surface of the entire globe with a thin layer of Cs-137. Just before the Chernobyl accident, typical Cs-137 concentra-

tions on the ground in Europe were between 2000 and $3000 Bq/m^2$ (DeCort 98:15). Post-accident deposition measurements on the ground near that range of values cannot be attributed to Chernobyl with confidence unless measurements were recorded at the same site before the accident. Since measurement records were mainly near large cities and near other nuclear power plants, pre-accident measurement data is sparse and geographically irregular. These limitations prevent construction of a more complete surface-based measurement dataset. Aerial gamma spectrometry measurements were taken over Eastern Europe and Western Russia weeks after the accident and deposition maps of these measurements exist (DeCort 98). However, these data were not available for this research, so this work is based entirely on the available surface-based Cs-137 measurements (DeCort 90). The surface-based deposition data for the Chernobyl case, available from the JRC, are segregated into two distinct datasets: a daily deposition dataset described in this section, and a cumulative deposition dataset described in Section 3.5.4. Figure 12 identifies, for the period during and just after Chernobyl's emission, the 23 sites where daily deposition readings are available and the first date at each site that daily measurements were recorded. Section 4.2.1 presents a bar graph for each city with daily deposition measurements.

Daily deposition data in the REM dataset is recorded at most sites in $[Bq/m^2]$. Passau, Koblenz, Glasgow, and Berkeley reported deposition in $[Bq/L]$, i.e., becquerels per liter of rain. For calculation of daily deposition totals at these sites, the REM dataset supplies daily precipitation amounts in $[mm]$ for some sites. For those sites with measurements in $[Bq/L]$ and no precipitation, precipitation at the nearest weather station is used to convert to $[Bq/m^2]$. No weather station precipitation was recorded for Koblenz, so model precipitation amounts are used to convert measurements from $[Bq/L]$ to $[Bq/m^2]$ for the Koblenz data only. European weather station precipitation records are courtesy of the Air Force Combat Climatology Center (AFCCC). Precipitation is missing from the Koblenz record in the REM dataset

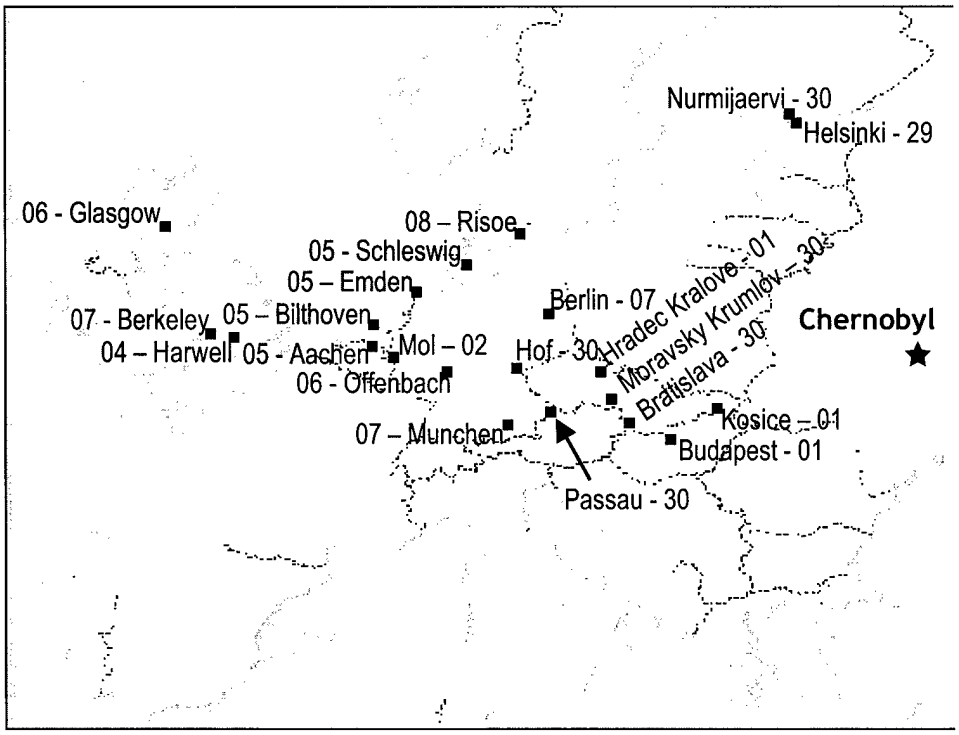


Figure 12 European cities where daily Cs-137 deposition measurements were taken with measurement start dates. Dates 29-30 are April 1986, 01-08 are May 1986

and from precipitation records supplied by AFCCC. Absent human-recorded precipitation, ECMWF model precipitation is substituted for the conversion of Koblenz deposition from $[Bq/L]$ to $[Bq/m^2]$. HySPLIT limits pollutant release specifications to a constant emission rate, so twelve separate runs are required to model emissions from the entire accident, one for each phase of emission. Time series of surface deposition at measurement sites are extracted from the daily deposition control run output grids of each run and summed. To produce corresponding deposition time series modeled with the proposed cloud base modification, the process is repeated exactly as the daily deposition control run, but executed with a recompiled HySPLIT model. The resulting daily deposition control and modification time series are presented and examined in Section 4.2.1. To allow the reader to reproduce the

simulations, HySPLIT settings used to produce Phase I model output from the daily deposition control run are given in Section D.4 of Appendix D.

*3.5.4 Modified-Cloud-Base Procedures, Simulation of April Deposition in Germany and Austria.* Measurement sites from the REM cumulative deposition dataset are depicted geographically in Figure 13, from ATMES Report Figure 8. It is evident from Figure 13 that the dataset's data points in Germany, Austria, and Greece are uniquely dense and homogeneous. Further examination reveals that the German, Austrian, and Grecian data in the cumulative dataset is also simultaneous. Because isolated measurement data points are not generally representative of a region due to unpredictable hot spots and holes in the long-range deposition pattern, the portion of the REM cumulative Cs-137 deposition dataset in these three countries is extracted for cloud modification run comparisons in this thesis. Unfortunately, the HySPLIT April deposition control run with best-guess Chernobyl source term and reanalyzed meteorological input data (Section 4.2.2) does not yield any deposition in Greece up to 86.05.01.00Z, while several separate measurements taken on that day in Greece indicate cumulative Cs-137 concentrations above $10^5 Bq/m^2$. Appendix G addresses possible reasons for the exclusion of Greece from modeled April deposition patterns in this thesis. May 1 German and Austrian deposition data remains the most homogeneous cumulative Chernobyl deposition data and is used exclusively for the April-cumulative model comparison (results in Section 4.2.2).

Because HySPLIT only accommodates a constant emission rate, a separate model run must be accomplished for each phase of Chernobyl emissions to account for the total Cs-137 emission, then the deposition from each phase can be added together. To minimize the number of deposition simulations required to model April-cumulative Chernobyl deposition on Germany and Austria, air parcel trajectories are calculated for each of the first six phases of Chernobyl emissions. Figures 14 through 19 are the modeled atmospheric trajectories of air parcels from Chernobyl during April (86.04.25.21Z - 86.04.30.24Z). The six figures correspond to the first six

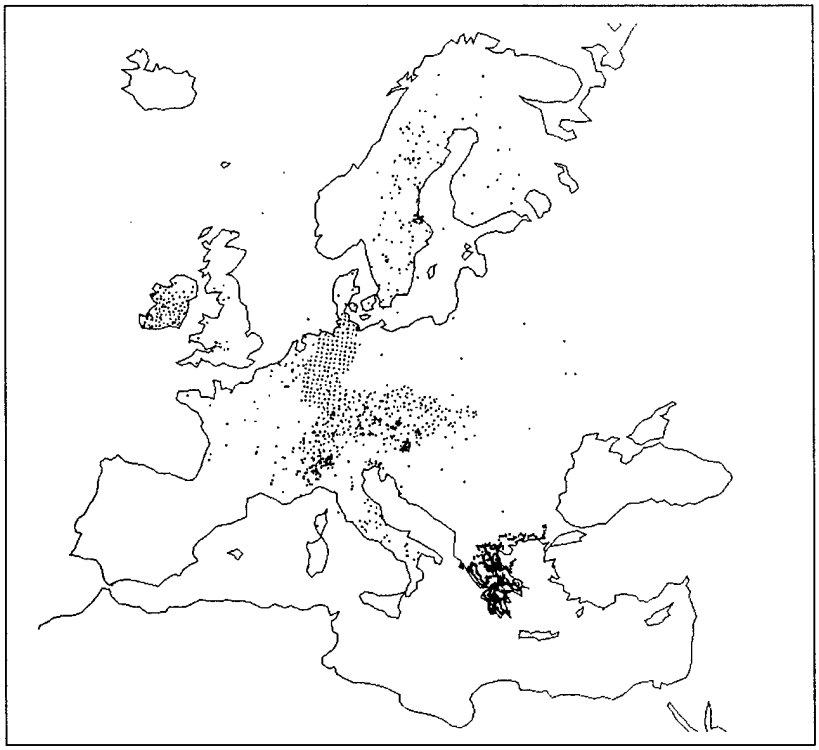

Figure 13 All surface-based cesium-137 measurement sites, daily deposition sites and cumulative deposition sites following the Chernobyl accident, from ATMES Report Figure 8 (Klug 92).

phases (I through VI) of Chernobyl emissions from Figure 7. Each line represents the path of an air parcel initiated at a discrete point and at the onset of the appropriate emission phase, terminating at 00Z on 1May1986. The starting heights of air parcel trajectories are chosen at the limits and the middle of the vertical line source of the corresponding source term phase in Figure 7. Each trajectory is calculated with HySPLIT default settings for typical Cs-137-bearing nuclear fallout, specifically, a deposition velocity of $1mm/s$, ICS efficiency of $3.2 \times 10^5$, and BCS rate of $5.0 \times 10^{-5}s^{-1}$.

During the first two days of emissions, the modeled plume above the boundary layer flowed around the northeast high, away from Germany and Austria, as evidenced in Figure 14 (all trajectories) and Figure 15 (trajectory from $850m$). Figure

15 trajectories from $350m$ and $500m$ and Figure 16 trajectory from $850m$ imply that the only modeled Chernobyl accident air parcel trajectories that cross Germany or Austria in April originate from Phase II emissions (1986.04.26.04Z - 27.00Z) and Phase III emissions (27.00Z - 28.00Z). These three trajectories trace the plume's path northwestward toward the Baltic Sea under the influence of northeast high pressure before getting wrapped southwestward through Germany and Austria around the back side of a shallow, transient trough. The remainder of modeled April Chernobyl trajectories once again exhibit anticyclonic curvature, characteristic of a high pressure system, and curve away from Germany and Austria (Figures 17, 18, and 19). April 28 and 29, the northeast high retreats eastward leaving a loose arrangement of very weak frontal boundaries. Without a strong pressure gradient to boost winds, the plume trajectories slow and meander more. By April 30, high pressure to the west begins to build and move eastward.

Since only Phases II and III produced plumes over the area of interest (Germany and Austria), only two runs are required for each April cumulative deposition simulation. April deposition control run cumulative output concentration grids from HySPLIT are converted to GRADS format and summed in the GRADS program, available from the Institute of Global Environment and Society (IGES 01). The process is repeated using the recompiled HySPLIT model, and results for April deposition control run and April deposition modification runs are presented in Section 4.2.2. Exact HySPLIT settings for April cumulative Phase II model output from the April deposition control run over Germany and Austria are given in Section D.5 of Appendix D. To confirm that Phase I emissions did not diffuse from their mean path (i.e., the trajectories in Figure 14) all the way to Germany, the results of a full deposition simulation for Phase I appears in Figure 20. The results show that modeled Phase I emissions do not contribute in April to the initial 5-*day* deposition on Germany and Austria, but deposit instead largely in Belarus and Lithuania.

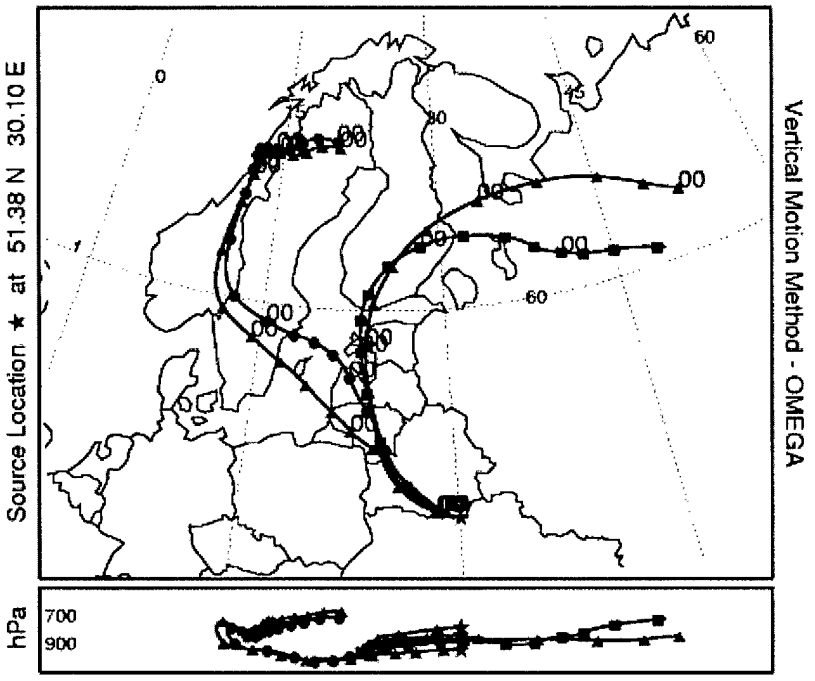


Figure 14 Modeled trajectories of Chernobyl air parcels in 6-hr increments. Originating at 2100Z on 25Apr1986 from 500m (triangles to Sweden), 1000m (circles), 1500m (squares), and 2000m(triangles to Russia)

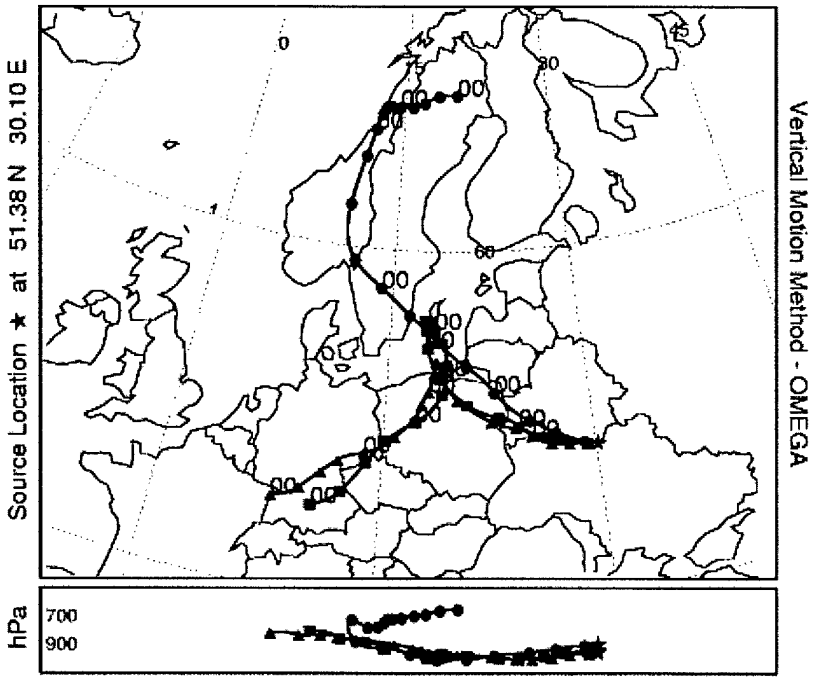


Figure 15 Modeled trajectories of Chernobyl air parcels in 6-hr increments. Originating at 0400Z on 26Apr1986 from 350m (triangles), 500m (squares), and 850m (circles)

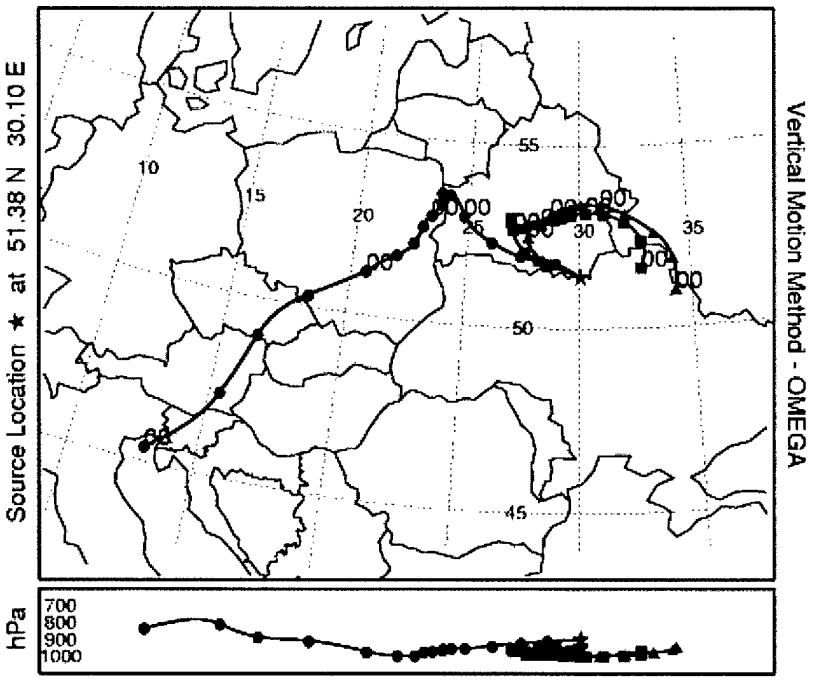


Figure 16 Modeled trajectories of Chernobyl air parcels in 6-hr increments. Originating at 0000Z on 27Apr1986 from 350m (triangles), 500m (squares), and 850m (circles)

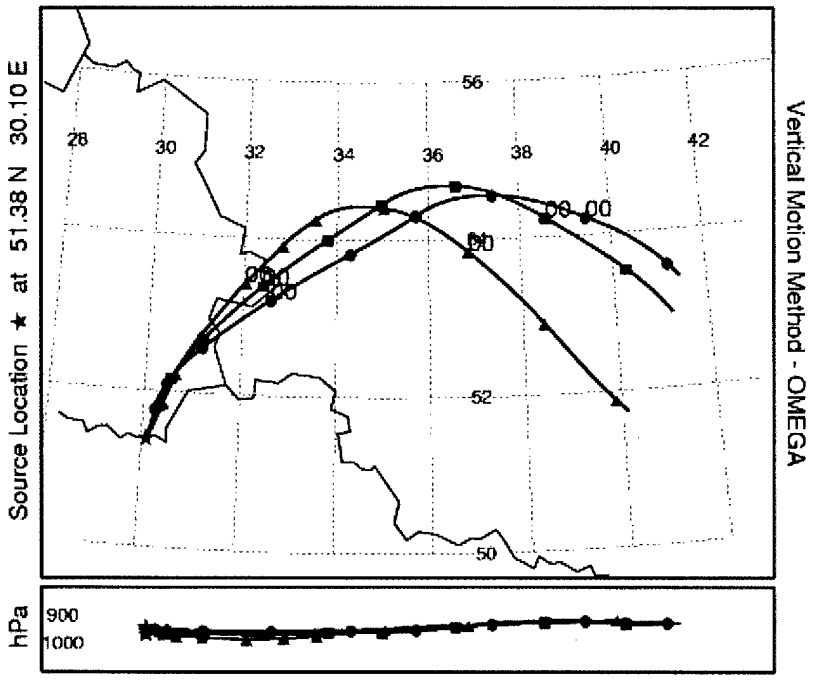


Figure 17 Modeled trajectories of Chernobyl air parcels in 6-hr increments. Originating at 0000Z on 28Apr1986 from 200m (triangles), 300m (squares), and 400m (circles).

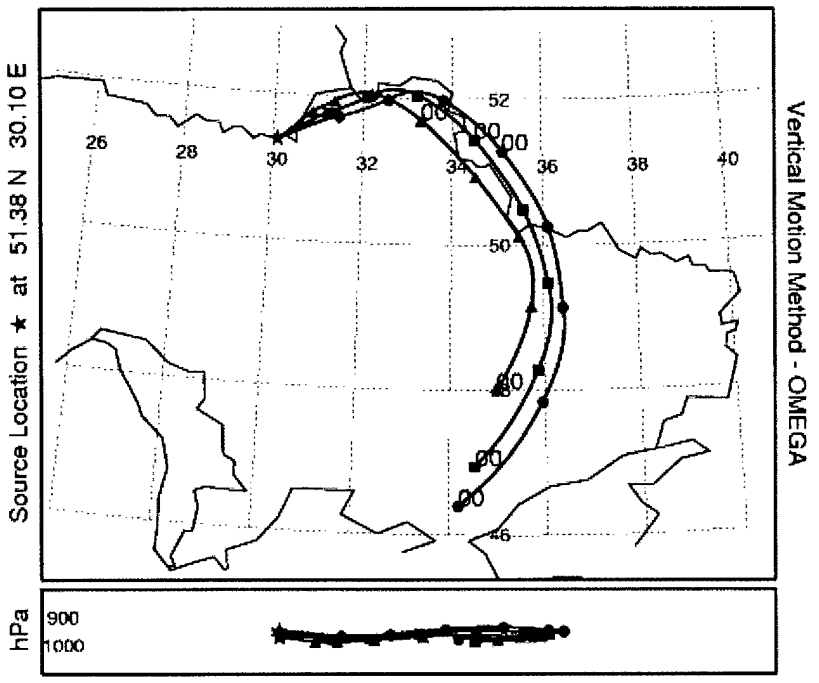


Figure 18 Modeled trajectories of Chernobyl air parcels in 6-hr increments. Originating at 0000Z on 29Apr1986 from 200m (triangles), 300m (squares), and 400m (circles)

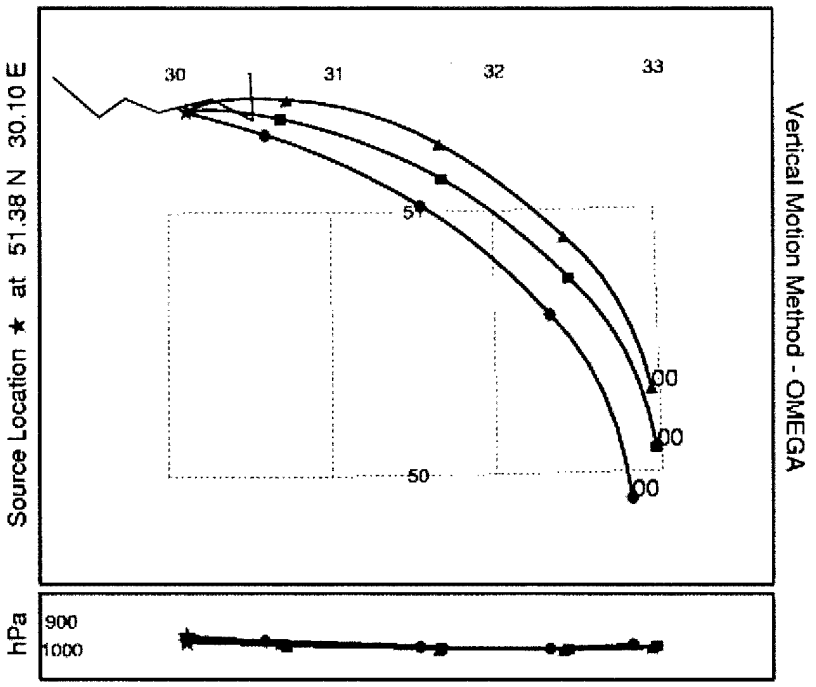


Figure 19 Modeled trajectories of Chernobyl air parcels in 6-hr increments. Originating at 0000Z on 30Apr1986 from 200m (triangles), 300m (squares), and 400m (circles).

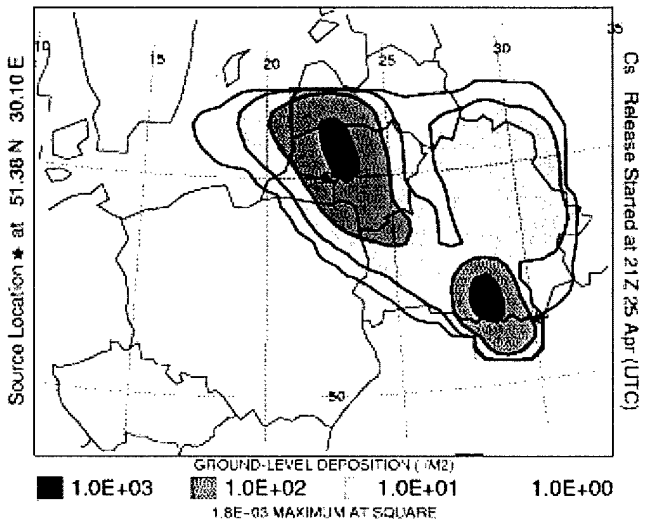


Figure 20 Modeled Deposition of Phase I Chernobyl Emissions Accumulated Over 04.25.21Z - 05.01.00Z

# *IV. Results*

## *4.1 In-Cloud Scavenging Sensitivity Test Results*

The results of seven diagnostic HySPLIT sensitivity test runs are explored in this section. Design of the runs follows the method for diagnosing ICS sensitivity presented in Section 3.4. The seven runs include the sensitivity control run, three runs with ICS efficiencies boosted by different amounts, and three runs with ICS efficiencies reduced by different amounts. The first time period, 86.04.26.00Z - 86.04.26.06Z, is examined in Subsection 4.1.1, then the second time period, 26.06Z - 26.12Z is examined in Subsection 4.1.2. In the sensitivity test scenario, a plume of particles like those carrying Cs-137 from a nuclear event is initiated in southernmost Germany at 48.0°N, 11.0°E and travels north-northeast as evidenced in deposition plots to follow. In HySPLIT, the units of emission per hour translate to the units of surface deposition per square meter. So, emissions in $[Bq/hr]$ translate to deposition in $[Bq/m^2]$.

*4.1.1 ICS Sensitivity Over Germany, 86.04.26.06Z.* Figure 21 provides 6-$hr$-accumulated precipitation from the model to aide interpretation of deposition plots in Figures 22, 23, 24, 25, 26, 27, and 28. For example, Figure 21 identifies a dry area (no rain) in southeast Germany that corresponds to a deposition minimum between two maximums in the sensitivity control run deposition plot in Figure 22. The effects of boosting and reducing default ICS efficiency by various percentages in deposition model runs can be seen clearly by subtracting sensitivity control run deposition from each test run's results. The amount of deposition difference from the sensitivity control run for each boosted-ICS or reduced-ICS test run appears in Figures 23 through 28.

In Figure 23 subtracting the sensitivity control run deposition from the (1% ICS efficiency boost) test run deposition yields a change in deposition on the order

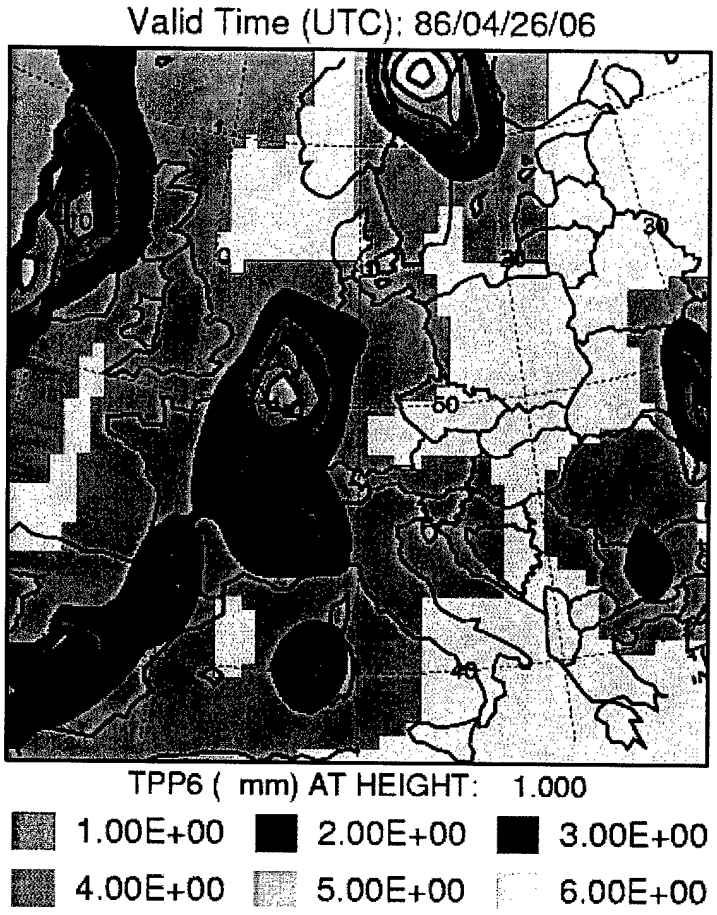


Figure 21 Reanalyzed ECMWF model precipitation in $[mm]$ accumulated from 86.04.26.00Z to 86.04.26.06Z for comparison to in-cloud scavenging sensitivity run. Contours in 1-$mm$ increments.

of $-0.5Bq/m^2$ near the source at 48.0°N, 11.0°E. Logic dictates that deposition should instead be initially heavier when ICS is boosted, and initially lighter when ICS is reduced. The deposition change in Figure 23 implies that the immediate result of boosted ICS is decreased deposition. About $100km$ further north (downstream) increased deposition is observed. Two questions arise from these observations. The first question is, "How could deposition change amounts be opposite in sign if scavenging efficiency is *increased only*?" The second question is, "Why does it appear that *increased* scavenging immediately causes a *decrease* in deposition?"

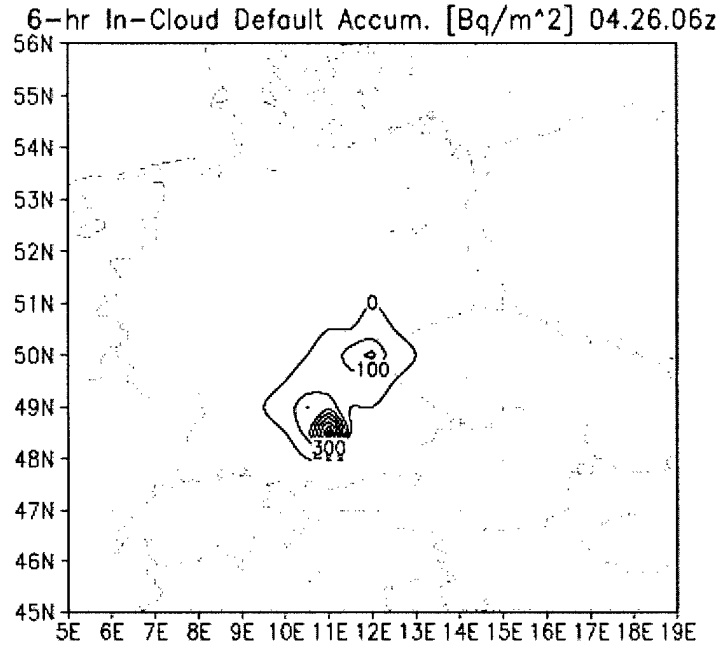


Figure 22 Six-hour-accumulated Cs-137 deposition $[Bq/m^2]$ from in-cloud scavenging sensitivity control run, 1986.04.26.06Z

In answer to the first question, the deposition differences from altered model scavenging can be opposite in sign upstream versus downstream from a point that could be termed the "scavenging error crossover point," or "SECP." At this unique point along the plume path, if total scavenging errors remain somewhat constant, the impact of the scavenging errors on deposition reverses. For example, if one assumes that modeled net scavenging is always and everywhere over-estimated, there must be a point in time and space where excess scavenging upstream has depleted the model plume so much that over-estimated scavenging downstream cannot make up for the concentration deficit in the plume. The resulting pattern of modeled deposition concentration would be too heavy upstream from the SECP and too light downstream from the SECP. Conversely, if net scavenging is always and everywhere under-estimated, the resulting deposition pattern would be too light near the source, and too heavy far from the source. The SECP principle applies as well to ICS errors alone if BCS and dry deposition are held constant as in these sensitivity tests.

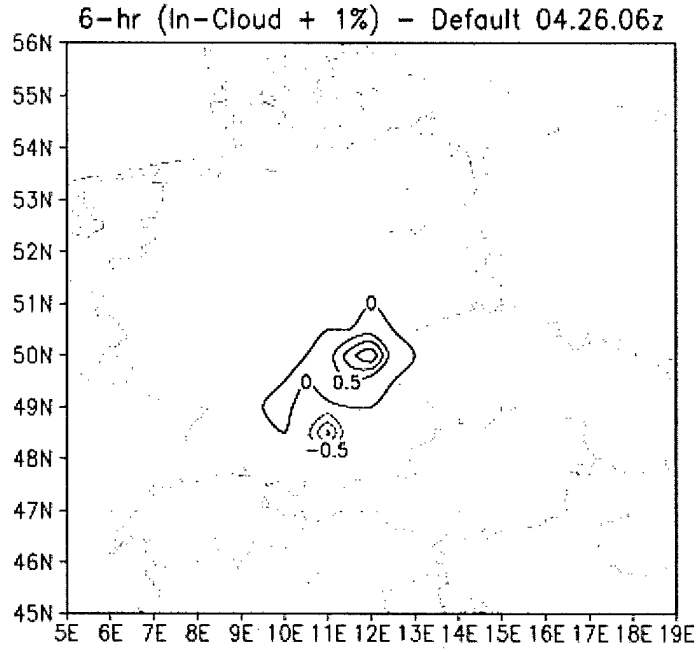


Figure 23 Difference in 6–*hr*-accumulated Cs-137 deposition $[Bq/m^2]$; Deposition from a test run with a 1% boost of in-cloud scavenging efficiency less deposition from control run, 86.04.26.06Z

However, in the tests, ICS efficiency changes do not necessarily apply everywhere and always (e.g., a 1% boost of the default constant ICS efficiency may be an over-estimate in some places and an under-estimate in others), so the SECP principle cannot be applied to model results blindly. In fact, the SECP principle cannot explain the answer to the second question. The SECP principle is noted, later, in Section 4.2.2 in an interpretation of deposition pattern changes from modifying the modeled cloud base.

In answer to the second question, increased model scavenging appears to immediately cause decreased model deposition due to grid resolution and interpolation issues within the model. The feature of interest at 48.5°N, 11.0°E in Figures 23 - 28, just north of the emission source, is not a physical phenomenon, but a computational one. HySPLIT only uses ICS efficiency (to calculate wet deposition) at gridpoints where precipitation is present. Since no precipitation is modeled at

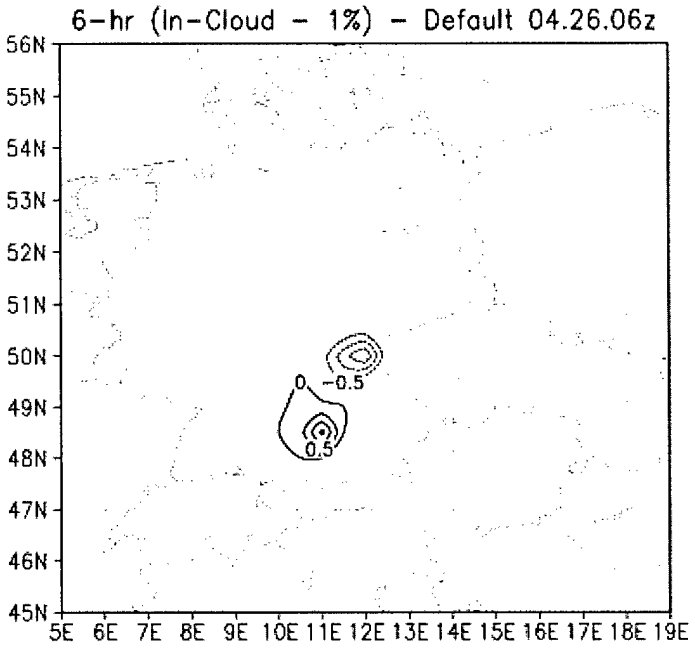


Figure 24 Difference in 6–*hr*-accumulated Cs-137 deposition $[Bq/m^2]$; Deposition from a test run with a 1% reduction of in-cloud scavenging efficiency less deposition from control run, 86.04.26.06Z

48.5°N, 11.0°E, and the only difference between the sensitivity control run and each test run is the ICS efficiency parameter, there must be a reason for the feature that is unrelated to ICS efficiency. The scale of the feature, the symmetry of the feature with the feature just north of it, as well as the persistence of both features in the nearly identical 12Z runs, leads one to believe that the cause of the phenomenon is initial deposition grid interpolations within HySPLIT. The impact of the feature on cloud base modification test results in Section 4.2 is negligible because of its relatively small magnitude, and is irrelevant because no deposition observations in the dataset selected for this work are available near Chernobyl to diagnose the cause of the feature. Further investigation of the phenomenon is beyond the scope of this work. Finally, to answer the second question explicitly, the immediate decrease in deposition is not caused by increased scavenging, but instead is likely an artifact of HySPLIT's interpolation of continuous variables using a discrete 60-*km* grid.

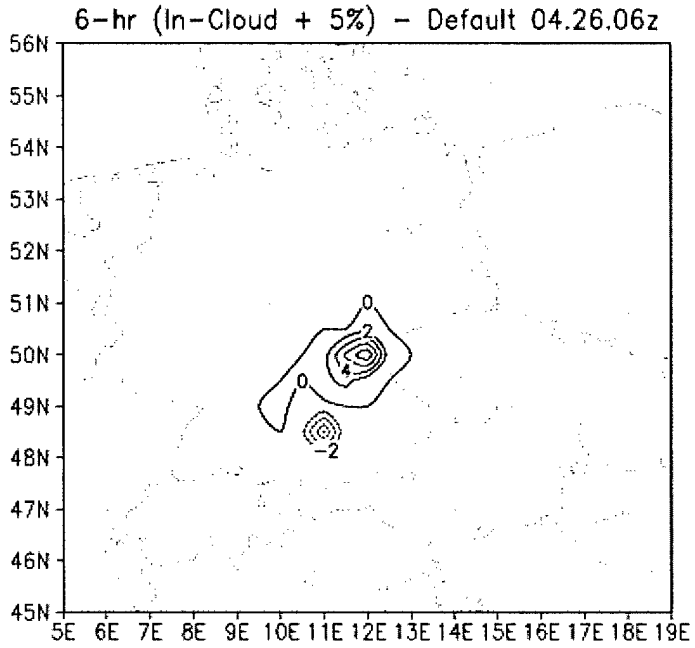


Figure 25 Six-hour-accumulated Cs-137 deposition $[Bq/m^2]$ difference from control run with a 5% boost of in-cloud scavenging efficiency, 86.04.26.06Z

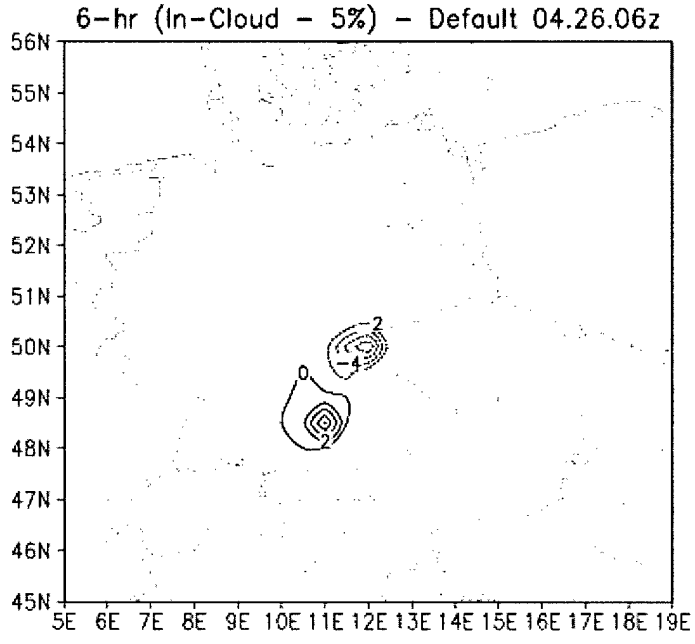


Figure 26 Six-hour-accumulated Cs-137 deposition $[Bq/m^2]$ difference from control run with a 5% reduction of in-cloud scavenging efficiency, 86.04.26.06Z

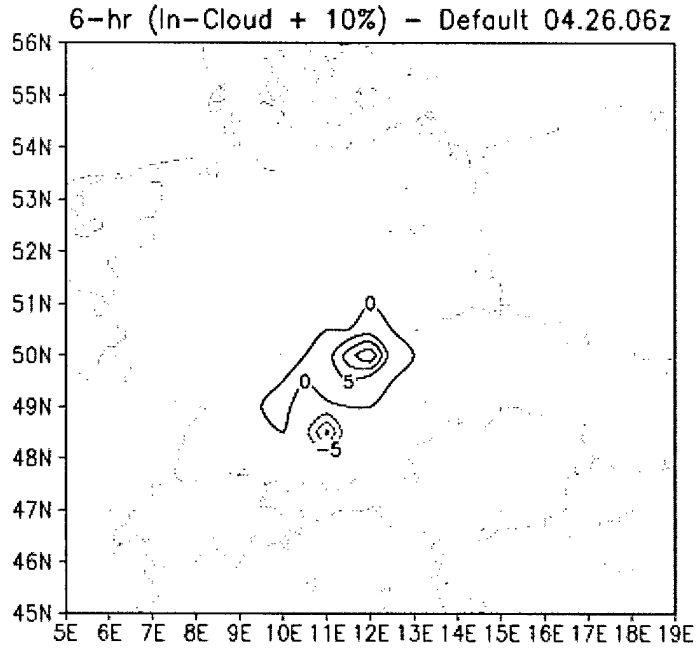


Figure 27 Six-hour-accumulated Cs-137 deposition $[Bq/m^2]$ difference from control run with a 10% boost of in-cloud scavenging efficiency, 86.04.26.06Z

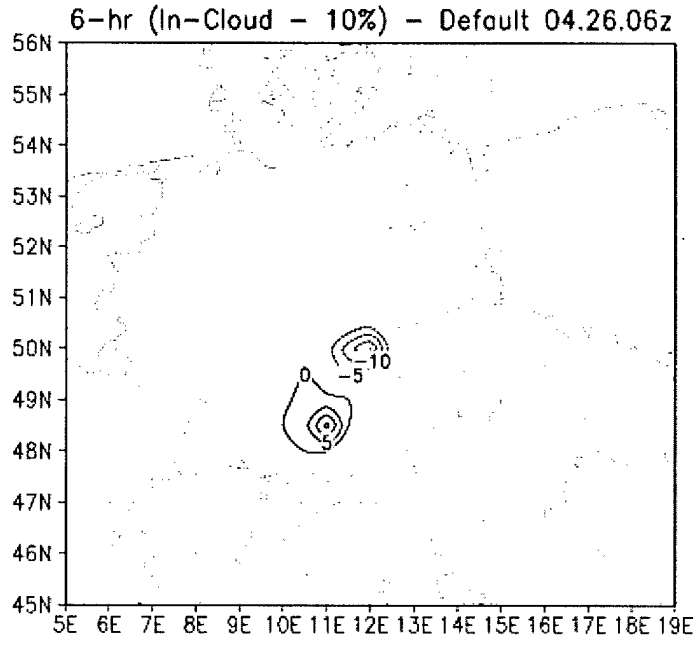


Figure 28 Six-hour-accumulated Cs-137 deposition $[Bq/m^2]$ difference from control run with a 10% reduction of in-cloud scavenging efficiency, 86.04.26.06Z

*4.1.2 ICS Sensitivity Over Germany, 86.04.26.12Z.* Because of the initial interpolation errors described in Subsection 4.1.1, a sensitivity test beyond the first six hours is required to estimate the impact of ICS on total deposition. A $12Z$ sensitivity test, covering the period 86.04.26.06Z - 86.04.26.12Z, is presented here. Figure 29 provides 6-$hr$-accumulated precipitation from the model to aide interpretation of the $12Z$ sensitivity test deposition plots in Figures 30 through 36. As in Subsection 4.1.1, sensitivity control run deposition is presented first, in Figure 30, then six figures displaying difference plots where sensitivity control run deposition is subtracted from the deposition from each test run. The $12Z$ sensitivity control run deposition is an order of magnitude greater than the $06Z$ sensitivity control run deposition. Each difference plot in Figures 31, 32, 33, 34, 35, and 36 exhibits the initial interpolation error like those in Subsection 4.1.1. However, after the plume travels about $100km$, the deposition pattern is straightforward. As expected, a boost of ICS efficiency results in increased deposition as generally indicated in Figures 31, 33, and 35. A reduction in ICS efficiency results in decreased deposition as generally indicated in Figures 32, 34, and 36. The response in the deposition pattern is approximately proportional to changes in the ICS efficiency, e.g., the change in deposition caused by a 5% boost in ICS efficiency (Figure 33) is approximately 5 times as much as the change in deposition from a 1% boost in ICS efficiency (Figure 31). It is also noted that, assuming the sensitivity control run is truth, a plume with a 10% error in ICS efficiency, traveling $600km$ in precipitation falling at $1mm/hr$, does not reach its SECP. Otherwise, there would be a change in sign of downstream portions of the deposition difference patterns, at least in Figures 35 and 36.

## *4.2 Modified-Cloud-Base Height Simulation Results*

*4.2.1 Modified-Cloud-Base Performance Over Time.* Daily deposition output from HySPLIT runs, produced as specified in Subsection 3.5.3, is presented in Figures 37 - 59 in order by earliest deposition measurement at each city. Raw

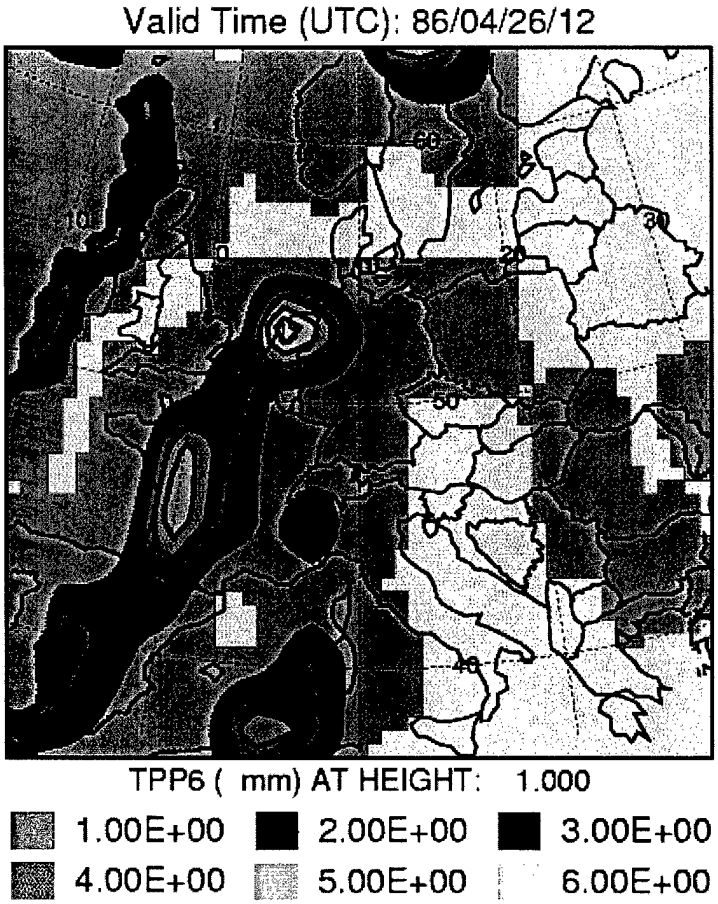


Figure 29 Reanalyzed ECMWF model precipitation in $[mm]$ accumulated from 86.04.26.06Z to 86.04.26.12Z for comparison to in-cloud scavenging sensitivity run. Contours in 1-$mm$ increments.

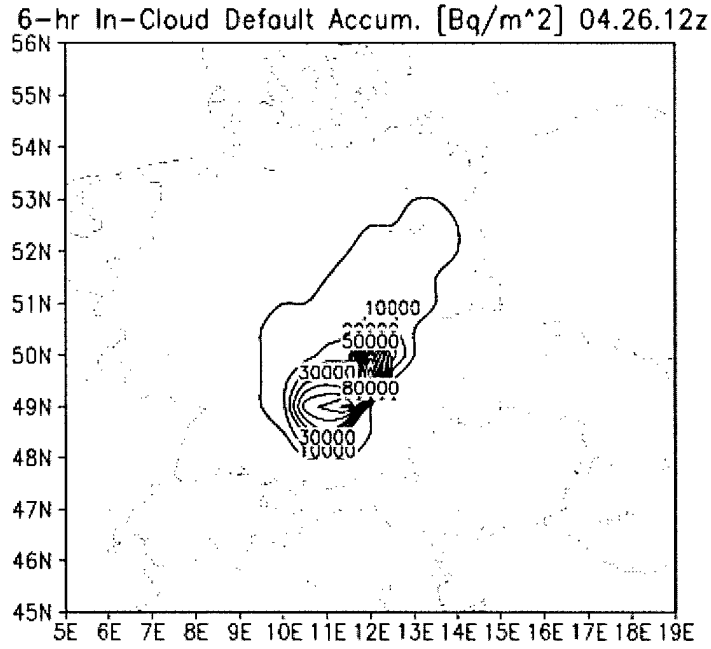


Figure 30 Six-hour-accumulated Cs-137 deposition $[Bq/m^2]$ from in-cloud scavenging sensitivity control run, 1986.04.26.12Z

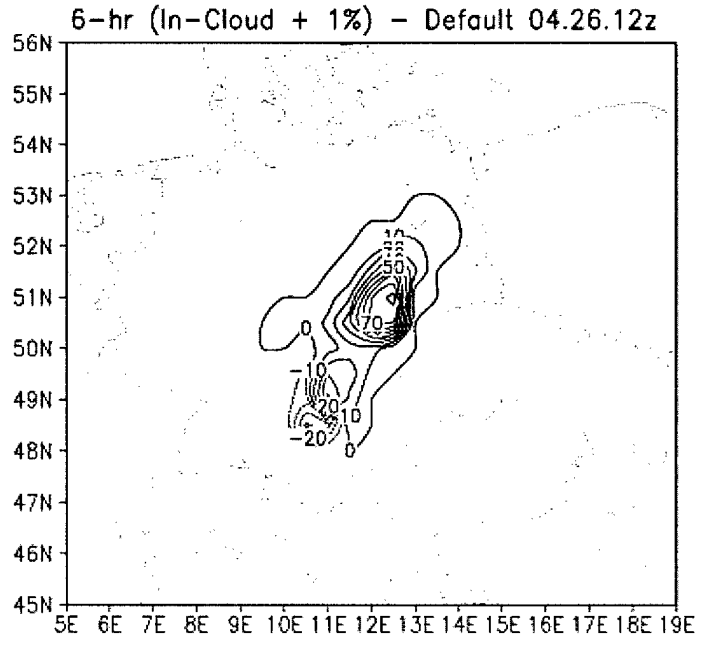


Figure 31 Six-hour-accumulated Cs-137 deposition $[Bq/m^2]$ difference from control run with a 1% boost of in-cloud scavenging efficiency, 86.04.26.12Z

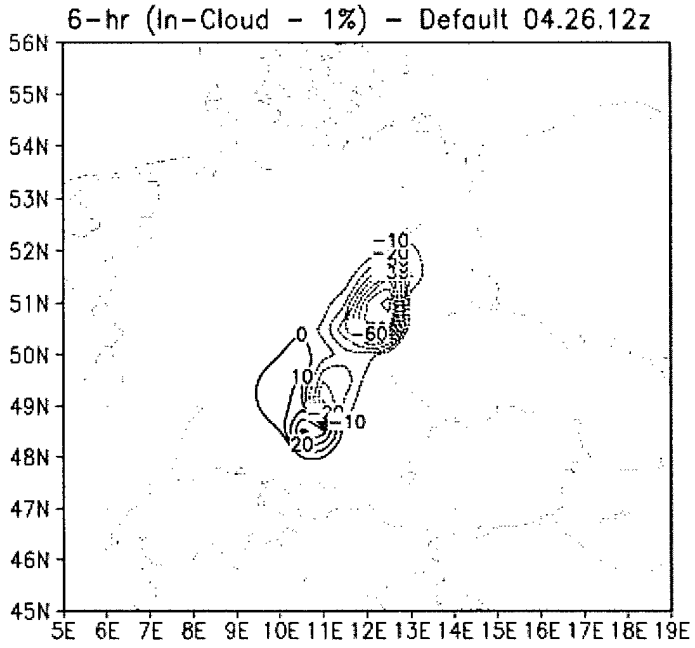


Figure 32 Six-hour-accumulated Cs-137 deposition $[Bq/m^2]$ difference from control run with a 1% reduction of in-cloud scavenging efficiency, 86.04.26.12Z

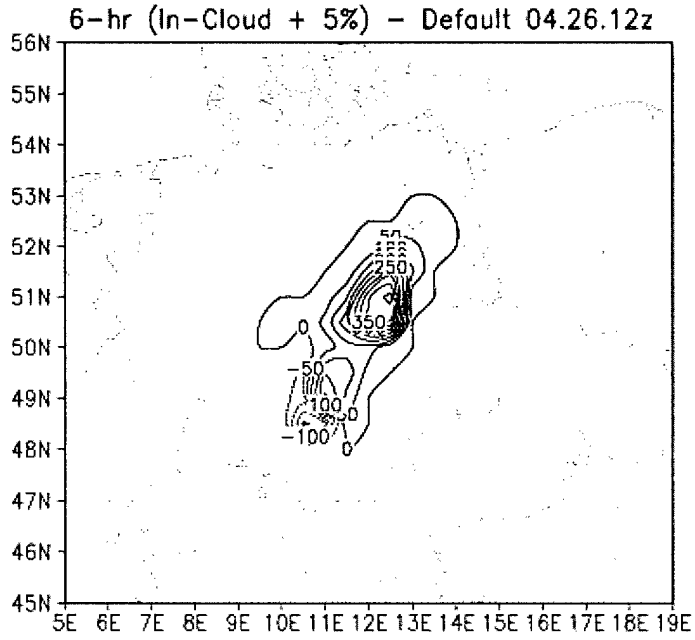


Figure 33 Six-hour-accumulated Cs-137 deposition $[Bq/m^2]$ difference from control run with a 5% boost of in-cloud scavenging efficiency, 86.04.26.12Z

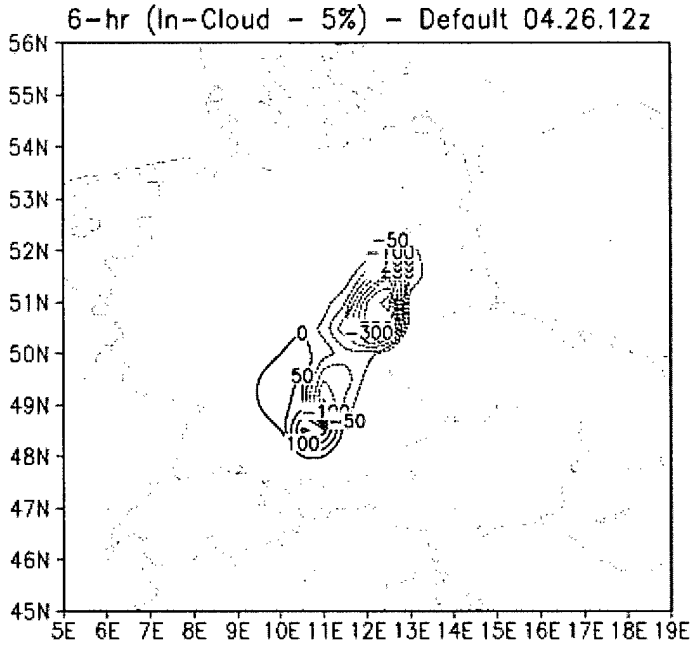


Figure 34 Six-hour-accumulated Cs-137 deposition $[Bq/m^2]$ difference from control run with a 5% reduction of in-cloud scavenging efficiency, 86.04.26.12Z

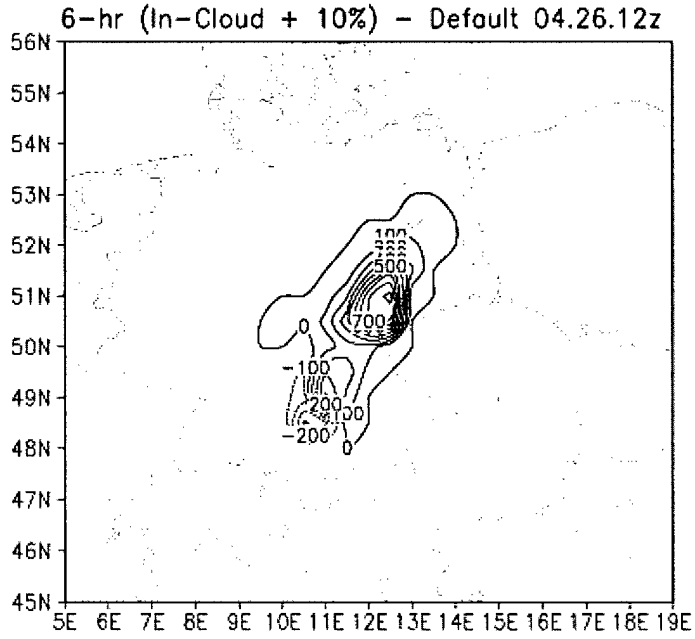


Figure 35 Six-hour-accumulated Cs-137 deposition $[Bq/m^2]$ difference from control run with a 10% boost of in-cloud scavenging efficiency, 86.04.26.12Z

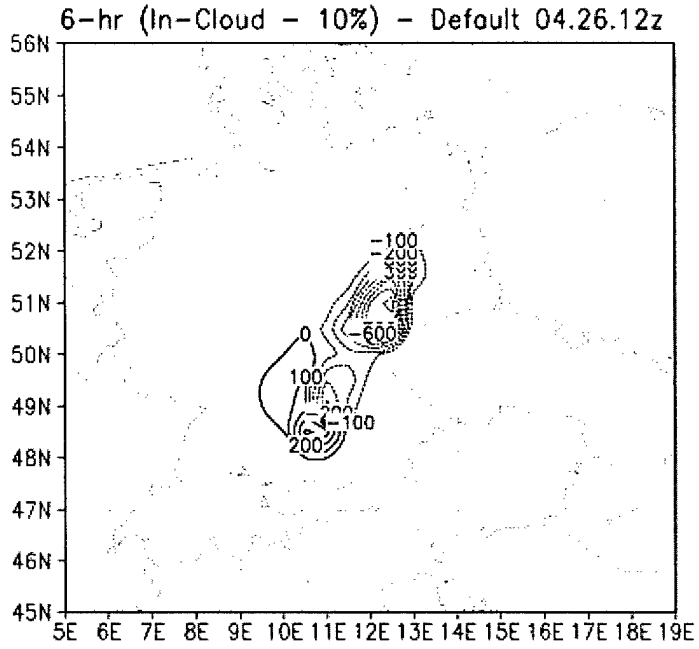


Figure 36 Six-hour-accumulated Cs-137 deposition $[Bq/m^2]$ difference from control run with a 10% reduction of in-cloud scavenging efficiency, 86.04.26.12Z

measurement data (bars with shade gradient) for all 23 figures are from the REM databank at JRC - Ispra, Italy, and are based on total daily Cs-137 deposition measurements (DeCort 90). At many cities, gross features of modeled deposition distribution are in good agreement with those of measured deposition distribution. For instance, bimodal distributions are often indicated in both the measurement data and the modeled data with peaks synchronized to within about one day. The Pearson correlation coefficient between the entire daily deposition control run dataset and the daily deposition measurements is 0.5037. The Pearson correlation coefficient between the daily deposition modified-cloud-base run dataset and the daily deposition measurements is 0.5050. The formula for correlation follows, where $n$ is the number of datapoints, and the variables $X$ and $Y$ are either daily measurement data and daily control run data, or daily measurement data and daily modified-cloud-base run

data.

$$Cor(X,Y)\frac{\sum_{j=1}^{n}(x_j-\overline{x})(y_j-\overline{y})}{\sqrt{\sum_{j=1}^{n}(x_j-\overline{x})^2\sum_{j=1}^{n}(y_j-\overline{y})^2}}$$

Often, the daily deposition control run and daily deposition modified-cloud-base runs produce identical deposition, even days after emissions begin. Three different scenarios could produce identical daily deposition control and modified-cloud-base amounts of deposition for a given day and site. If deposition for the whole day took place without the benefit of precipitation, no cloud base is calculated in HySPLIT, eliminating any cloud base modification effect. The second scenario finds precipitation on site, but no plume present between 75%-RH and 80%-RH levels above the deposition site, i.e., control run and modified-cloud-base run both find the plume either entirely beneath the cloud base, or entirely above the cloud base. The third scenario is a vertical resolution issue arising when the 75%-RH and 80%-RH are at effectively the same level. Such a discontinuity is possible in the model since the wet deposition algorithm uses discrete layers of humidity data. Even in some meteorological situations, such as a warm, moist air mass over-running a cold, dry air mass, a discontinuous relative humidity vertical profile is not an unreasonable approximation.

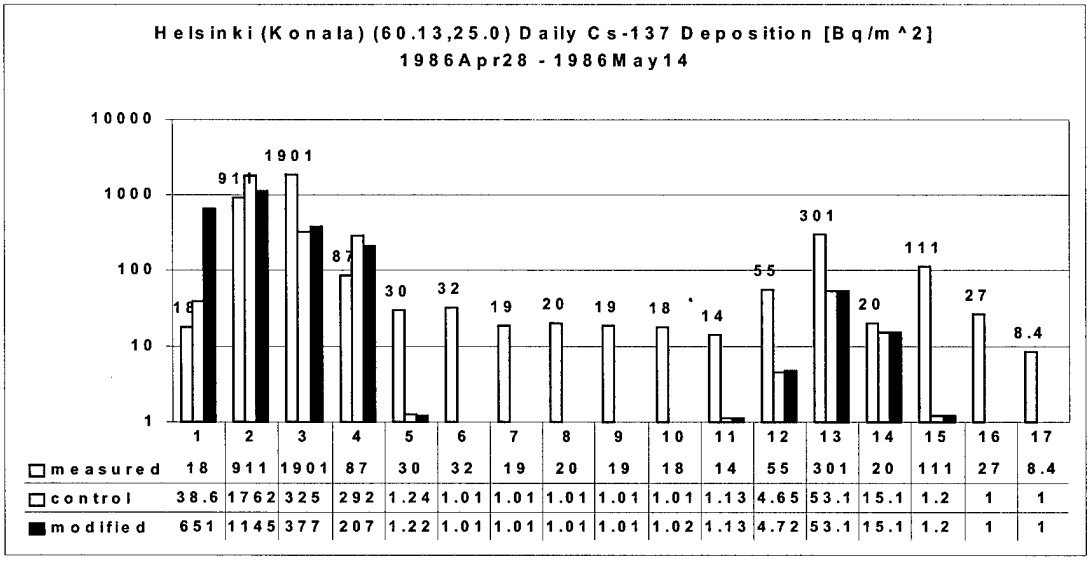


| | 1 | 2 | 3 | 4 | 5 | 6 | 7 | 8 | 9 | 10 | 11 | 12 | 13 | 14 | 15 | 16 | 17 |
|---|---|---|---|---|---|---|---|---|---|---|---|---|---|---|---|---|---|
| measured | 18 | 911 | 1901 | 87 | 30 | 32 | 19 | 20 | 19 | 18 | 14 | 55 | 301 | 20 | 111 | 27 | 8.4 |
| control | 38.6 | 1762 | 325 | 292 | 1.24 | 1.01 | 1.01 | 1.01 | 1.01 | 1.01 | 1.13 | 4.65 | 53.1 | 15.1 | 1.2 | 1 | 1 |
| modified | 651 | 1145 | 377 | 207 | 1.22 | 1.01 | 1.01 | 1.01 | 1.01 | 1.02 | 1.13 | 4.72 | 53.1 | 15.1 | 1.2 | 1 | 1 |

Figure 37 Summary of Helsinki (Lat,Lon in decimal degrees) daily total Cs-137 deposition 1986Apr27 - 1986May14; measured, control run, and modified cloud base run.

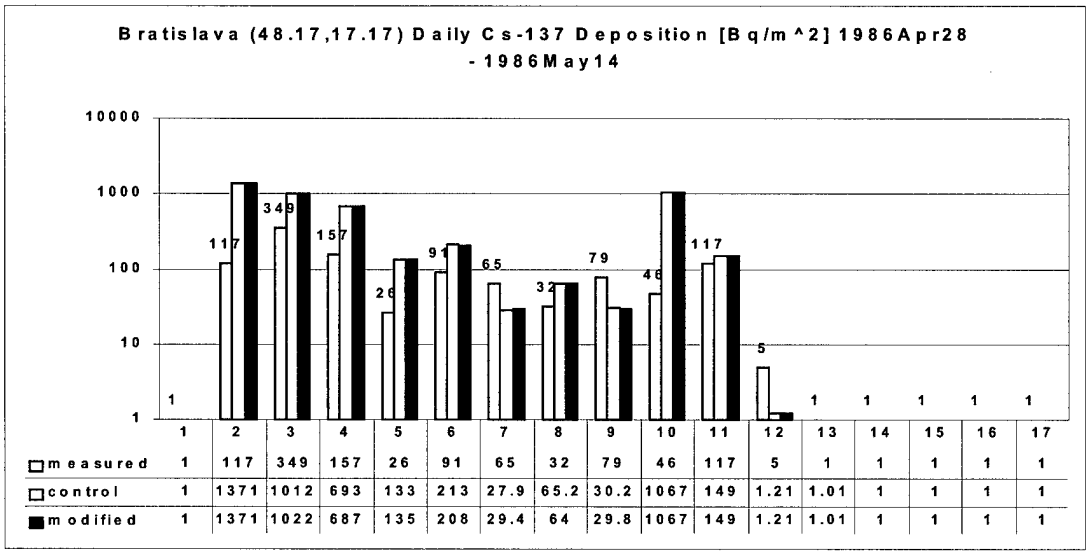


| | 1 | 2 | 3 | 4 | 5 | 6 | 7 | 8 | 9 | 10 | 11 | 12 | 13 | 14 | 15 | 16 | 17 |
|---|---|---|---|---|---|---|---|---|---|---|---|---|---|---|---|---|---|
| measured | 1 | 117 | 349 | 157 | 26 | 91 | 65 | 32 | 79 | 46 | 117 | 5 | 1 | 1 | 1 | 1 | 1 |
| control | 1 | 1371 | 1012 | 693 | 133 | 213 | 27.9 | 65.2 | 30.2 | 1067 | 149 | 1.21 | 1.01 | 1 | 1 | 1 | 1 |
| modified | 1 | 1371 | 1022 | 687 | 135 | 208 | 29.4 | 64 | 29.8 | 1067 | 149 | 1.21 | 1.01 | 1 | 1 | 1 | 1 |

Figure 38 Summary of Bratislava (Lat,Lon in decimal degrees) daily total Cs-137 deposition 1986Apr27 - 1986May14; measured, control run, and modified cloud base run.

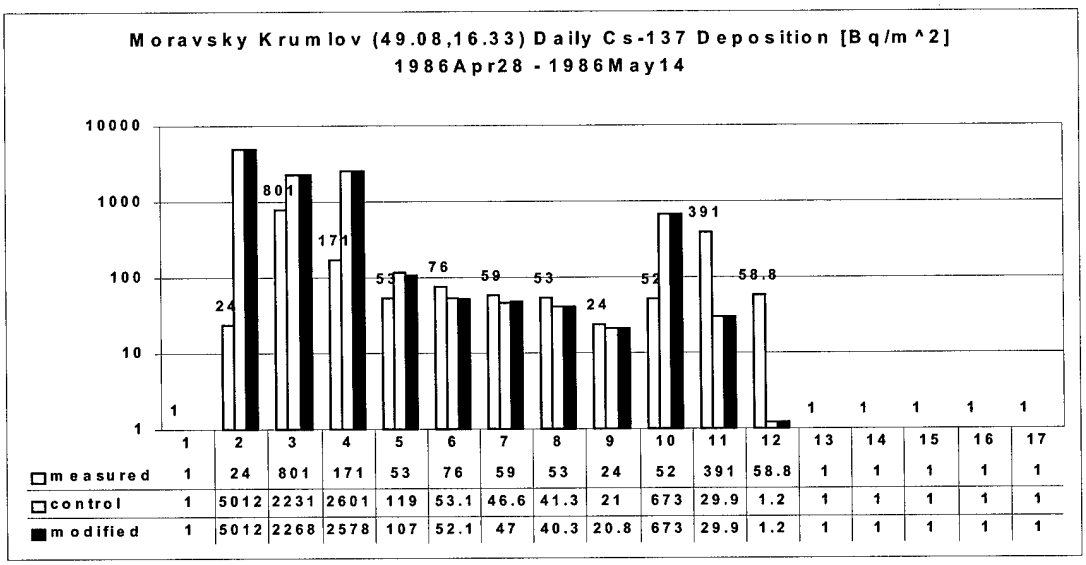


| | 1 | 2 | 3 | 4 | 5 | 6 | 7 | 8 | 9 | 10 | 11 | 12 | 13 | 14 | 15 | 16 | 17 |
|---|---|---|---|---|---|---|---|---|---|---|---|---|---|---|---|---|---|
| measured | 1 | 24 | 801 | 171 | 53 | 76 | 59 | 53 | 24 | 52 | 391 | 58.8 | 1 | 1 | 1 | 1 | 1 |
| control | 1 | 5012 | 2231 | 2601 | 119 | 53.1 | 46.6 | 41.3 | 21 | 673 | 29.9 | 1.2 | 1 | 1 | 1 | 1 | 1 |
| modified | 1 | 5012 | 2268 | 2578 | 107 | 52.1 | 47 | 40.3 | 20.8 | 673 | 29.9 | 1.2 | 1 | 1 | 1 | 1 | 1 |

Figure 39 Summary of Moravsky Krumlov (Lat,Lon in decimal degrees) daily total Cs-137 deposition 1986Apr27 - 1986May14; measured, control run, and modified cloud base run.

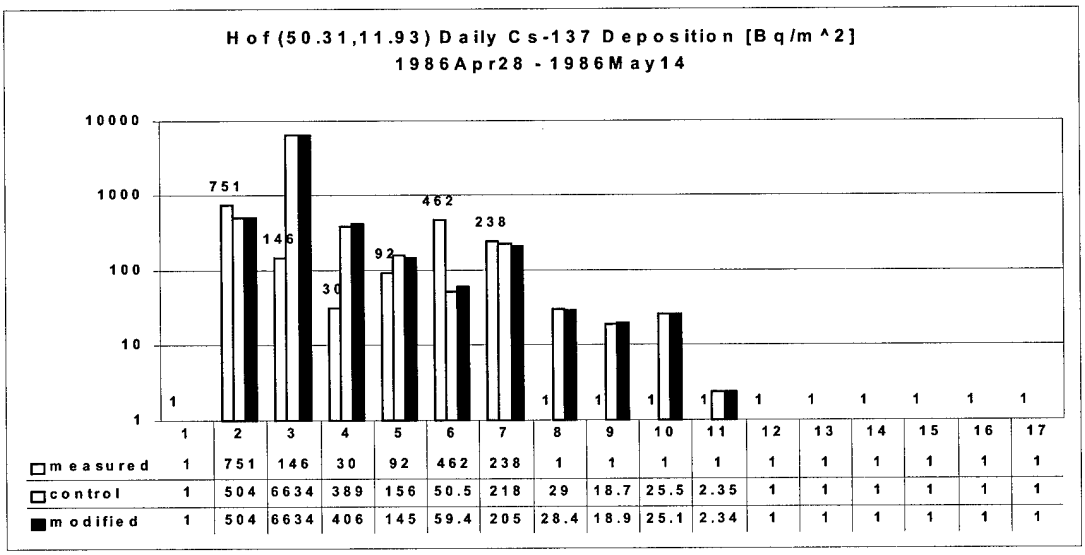


| | 1 | 2 | 3 | 4 | 5 | 6 | 7 | 8 | 9 | 10 | 11 | 12 | 13 | 14 | 15 | 16 | 17 |
|---|---|---|---|---|---|---|---|---|---|---|---|---|---|---|---|---|---|
| measured | 1 | 751 | 146 | 30 | 92 | 462 | 238 | 1 | 1 | 1 | 1 | 1 | 1 | 1 | 1 | 1 | 1 |
| control | 1 | 504 | 6634 | 389 | 156 | 50.5 | 218 | 29 | 18.7 | 25.5 | 2.35 | 1 | 1 | 1 | 1 | 1 | 1 |
| modified | 1 | 504 | 6634 | 406 | 145 | 59.4 | 205 | 28.4 | 18.9 | 25.1 | 2.34 | 1 | 1 | 1 | 1 | 1 | 1 |

Figure 40 Summary of Hof (Lat,Lon in decimal degrees) daily total Cs-137 deposition 1986Apr27 - 1986May14; measured, control run, and modified cloud base run.

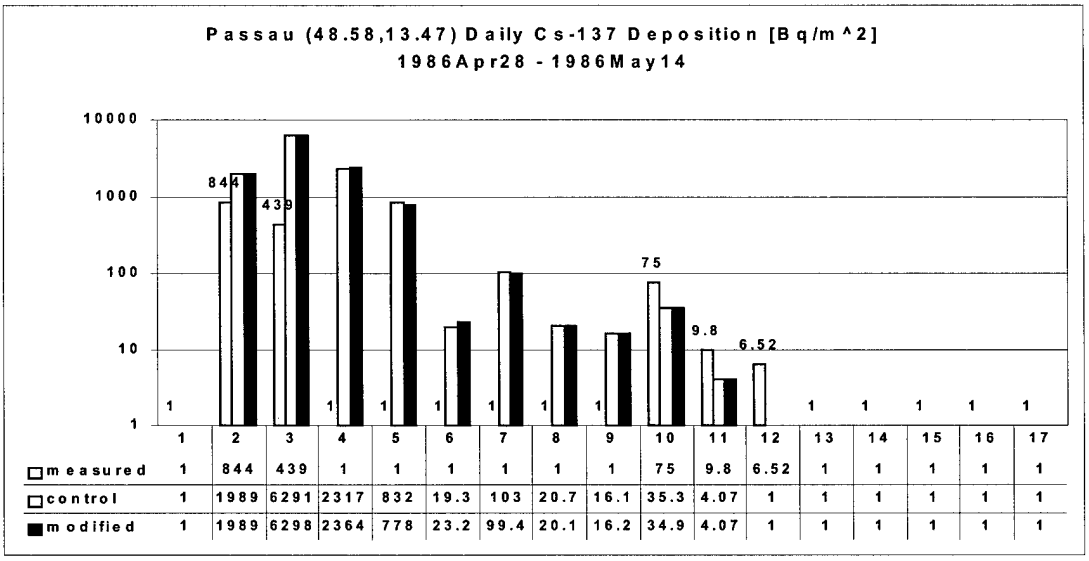


| | 1 | 2 | 3 | 4 | 5 | 6 | 7 | 8 | 9 | 10 | 11 | 12 | 13 | 14 | 15 | 16 | 17 |
|---|---|---|---|---|---|---|---|---|---|---|---|---|---|---|---|---|---|
| measured | 1 | 844 | 439 | 1 | 1 | 1 | 1 | 1 | 1 | 75 | 9.8 | 6.52 | 1 | 1 | 1 | 1 | 1 |
| control | 1 | 1989 | 6291 | 2317 | 832 | 19.3 | 103 | 20.7 | 16.1 | 35.3 | 4.07 | 1 | 1 | 1 | 1 | 1 | 1 |
| modified | 1 | 1989 | 6298 | 2364 | 778 | 23.2 | 99.4 | 20.1 | 16.2 | 34.9 | 4.07 | 1 | 1 | 1 | 1 | 1 | 1 |

Figure 41 Summary of Passau (Lat,Lon in decimal degrees) daily total Cs-137 deposition 1986Apr27 - 1986May14; measured, control run, and modified cloud base run.

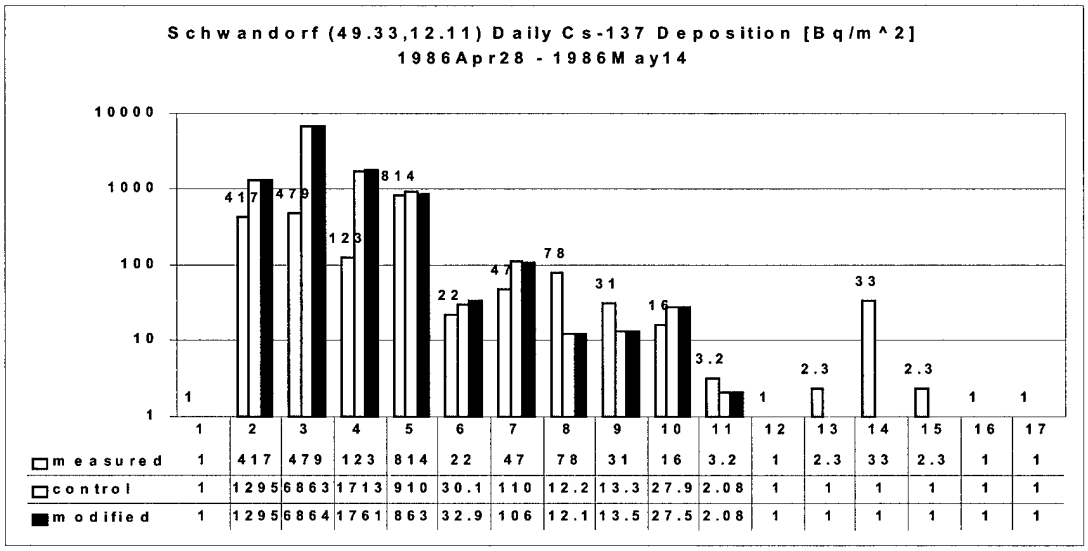


| | 1 | 2 | 3 | 4 | 5 | 6 | 7 | 8 | 9 | 10 | 11 | 12 | 13 | 14 | 15 | 16 | 17 |
|---|---|---|---|---|---|---|---|---|---|---|---|---|---|---|---|---|---|
| measured | 1 | 417 | 479 | 123 | 814 | 22 | 47 | 78 | 31 | 16 | 3.2 | 1 | 2.3 | 33 | 2.3 | 1 | 1 |
| control | 1 | 1295 | 6863 | 1713 | 910 | 30.1 | 110 | 12.2 | 13.3 | 27.9 | 2.08 | 1 | 1 | 1 | 1 | 1 | 1 |
| modified | 1 | 1295 | 6864 | 1761 | 863 | 32.9 | 106 | 12.1 | 13.5 | 27.5 | 2.08 | 1 | 1 | 1 | 1 | 1 | 1 |

Figure 42 Summary of Schwandorf (Lat,Lon in decimal degrees) daily total Cs-137 deposition 1986Apr27 - 1986May14; measured, control run, and modified cloud base run.

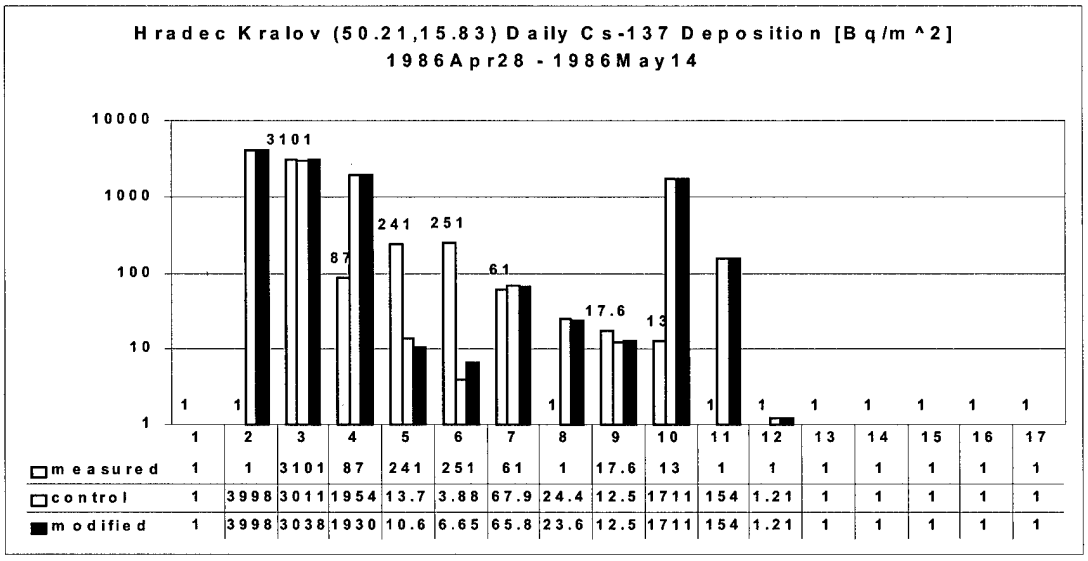


Figure 43 Summary of Hradec Kralov (Lat,Lon in decimal degrees) daily total Cs-137 deposition 1986Apr27 - 1986May14; measured, control run, and modified cloud base run.

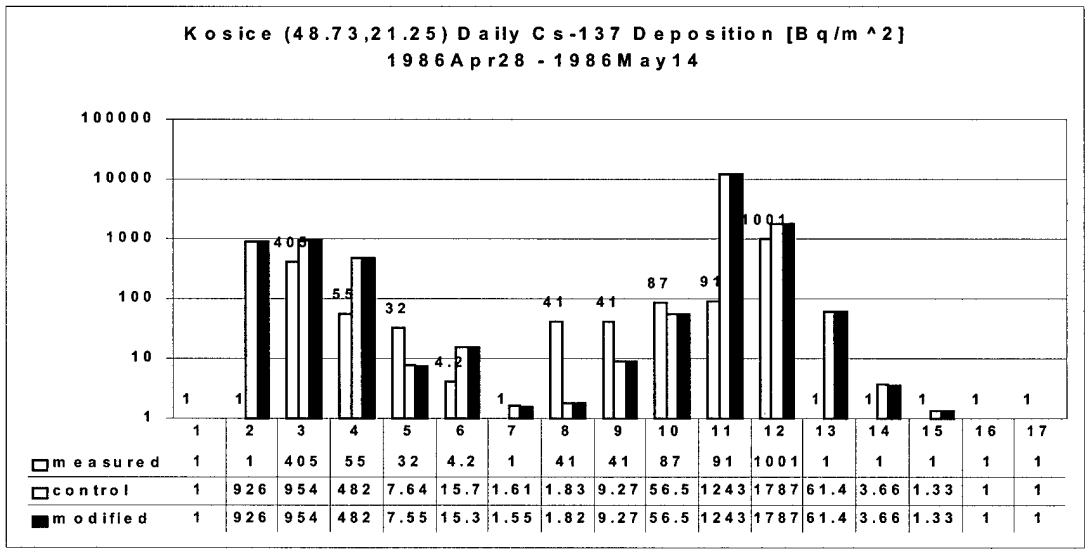


Figure 44 Summary of Kosice (Lat,Lon in decimal degrees) daily total Cs-137 deposition 1986Apr27 - 1986May14; measured, control run, and modified cloud base run.

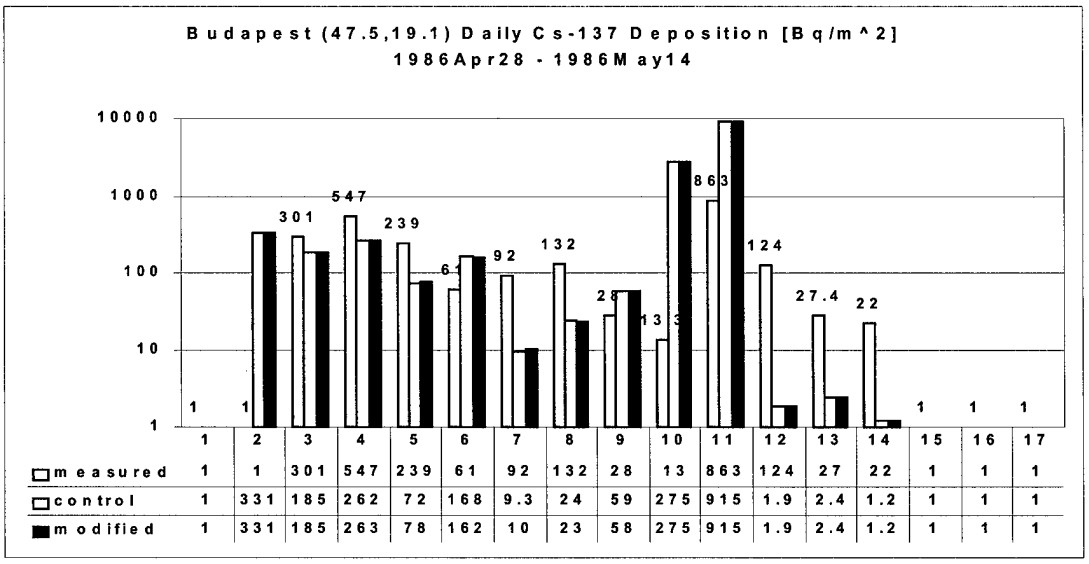


Figure 45 Summary of Budapest (Lat,Lon in decimal degrees) daily total Cs-137 deposition 1986Apr27 - 1986May14; measured, control run, and modified cloud base run.

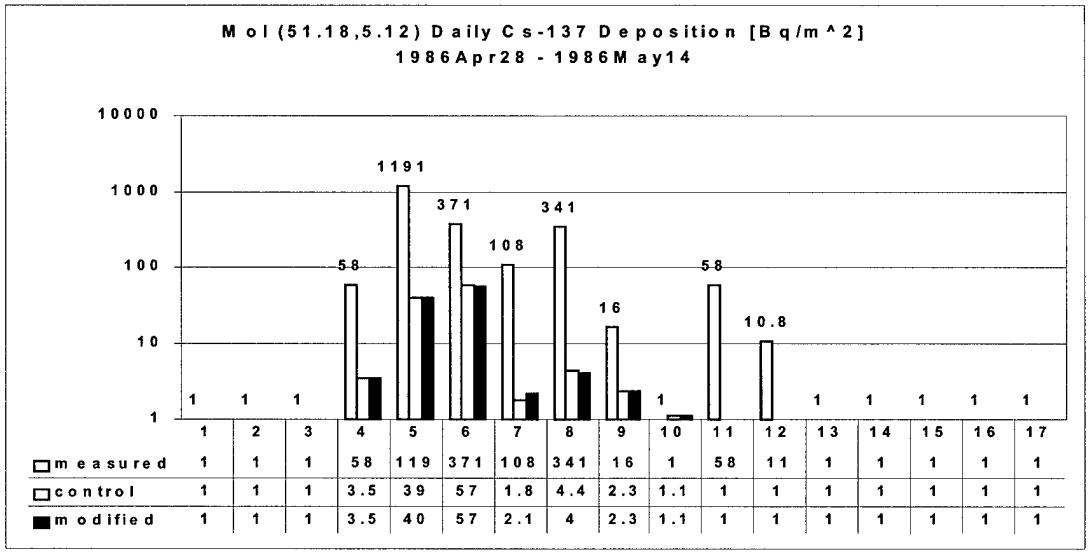


Figure 46 Summary of Mol (Lat,Lon in decimal degrees) daily total Cs-137 deposition 1986Apr27 - 1986May14; measured, control run, and modified cloud base run.

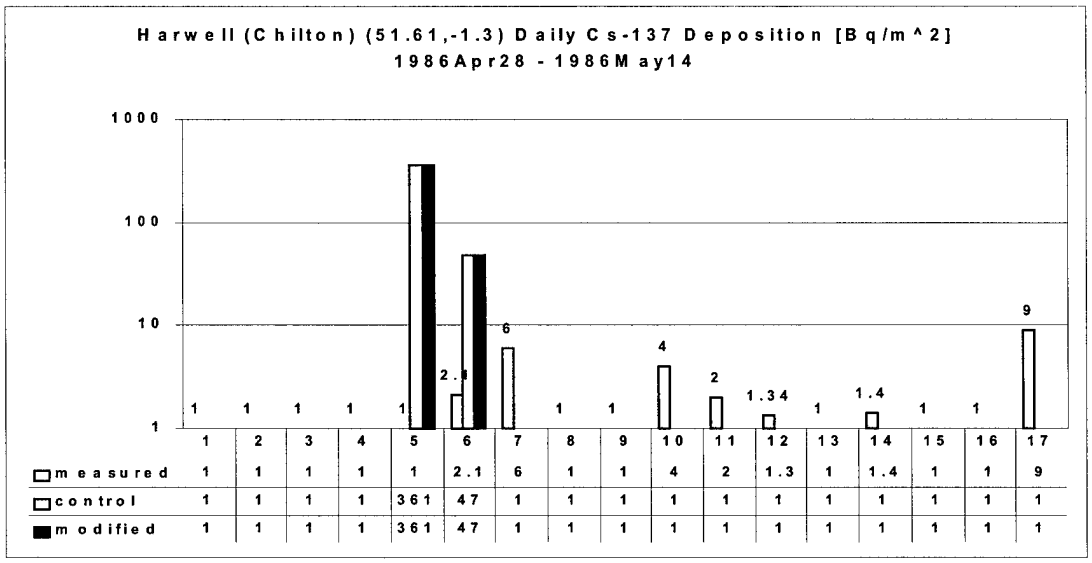


Figure 47 Summary of Harwell (Lat,Lon in decimal degrees) daily total Cs-137 deposition 1986Apr27 - 1986May14; measured, control run, and modified cloud base run.

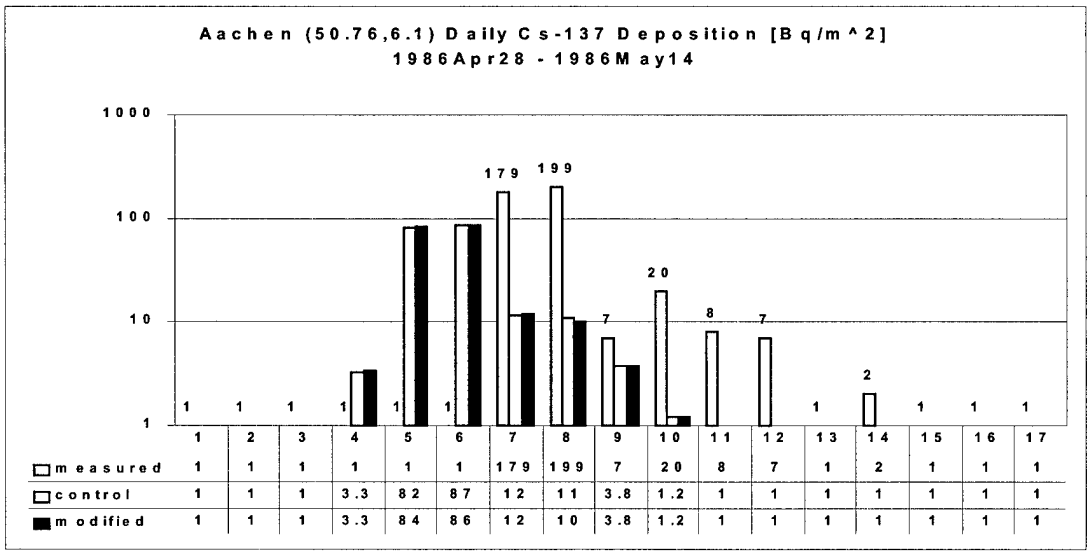


Figure 48 Summary of Aachen (Lat,Lon in decimal degrees) daily total Cs-137 deposition 1986Apr27 - 1986May14; measured, control run, and modified cloud base run.

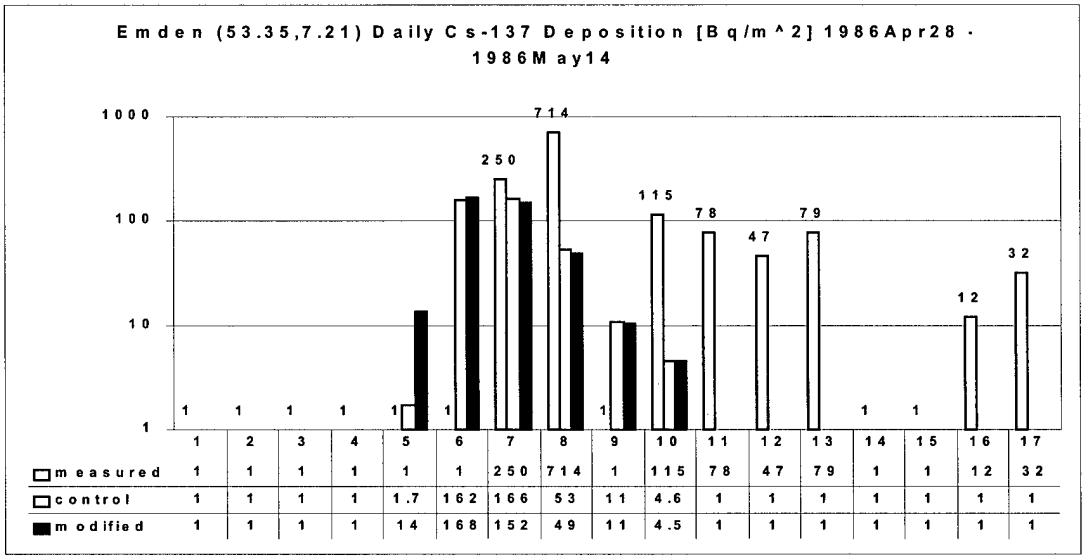


Figure 49 Summary of Emden (Lat,Lon in decimal degrees) daily total Cs-137 deposition 1986Apr27 - 1986May14; measured, control run, and modified cloud base run.

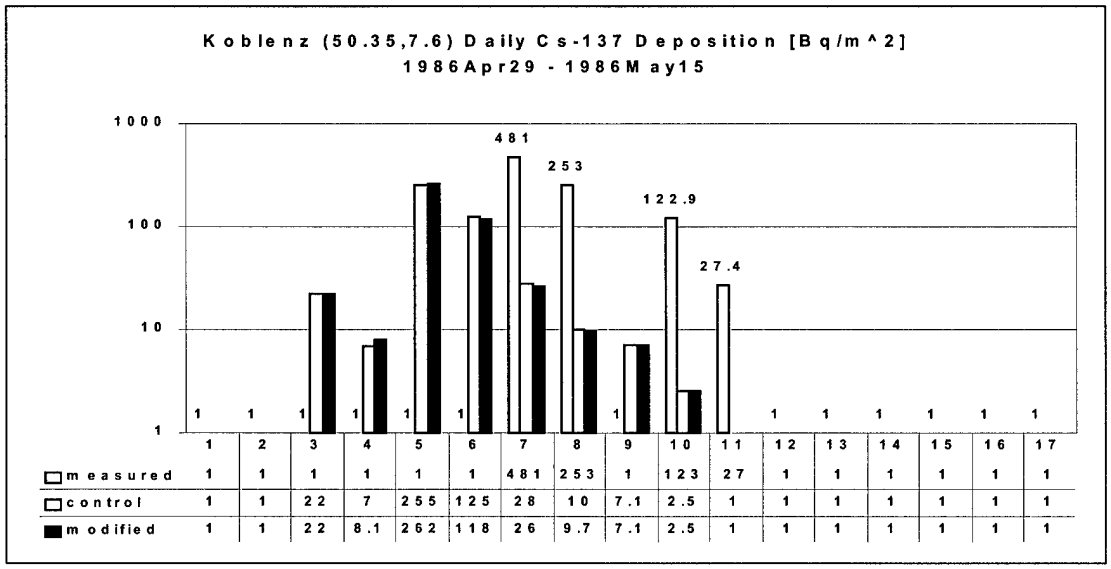


Figure 50 Summary of Koblenz (Lat,Lon in decimal degrees) daily total Cs-137 deposition 1986Apr27 - 1986May14; measured, control run, and modified cloud base run.

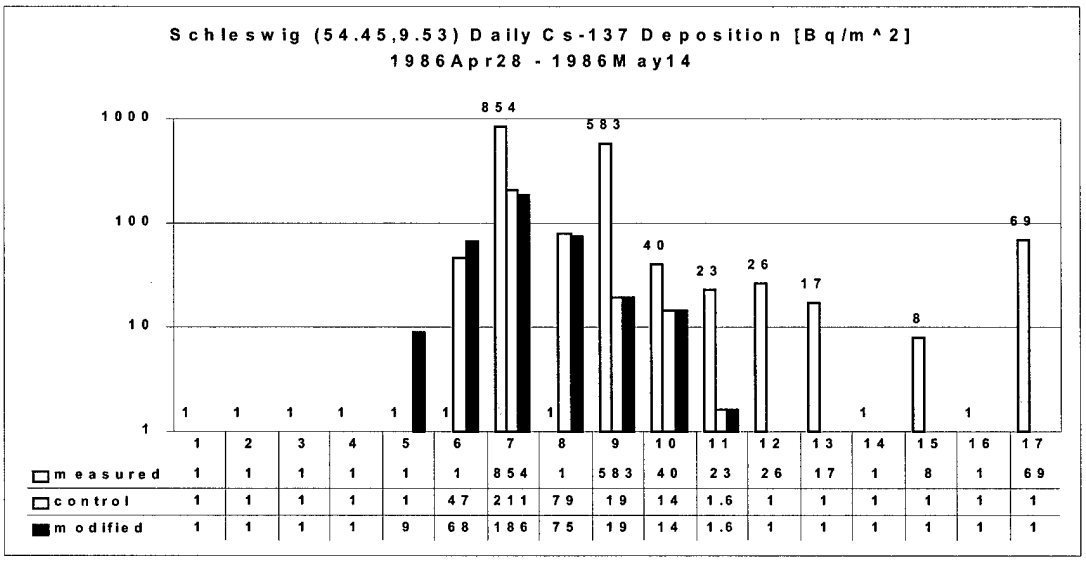


Figure 51 Summary of Schleswig (Lat,Lon in decimal degrees) daily total Cs-137 deposition 1986Apr27 - 1986May14; measured, control run, and modified cloud base run.

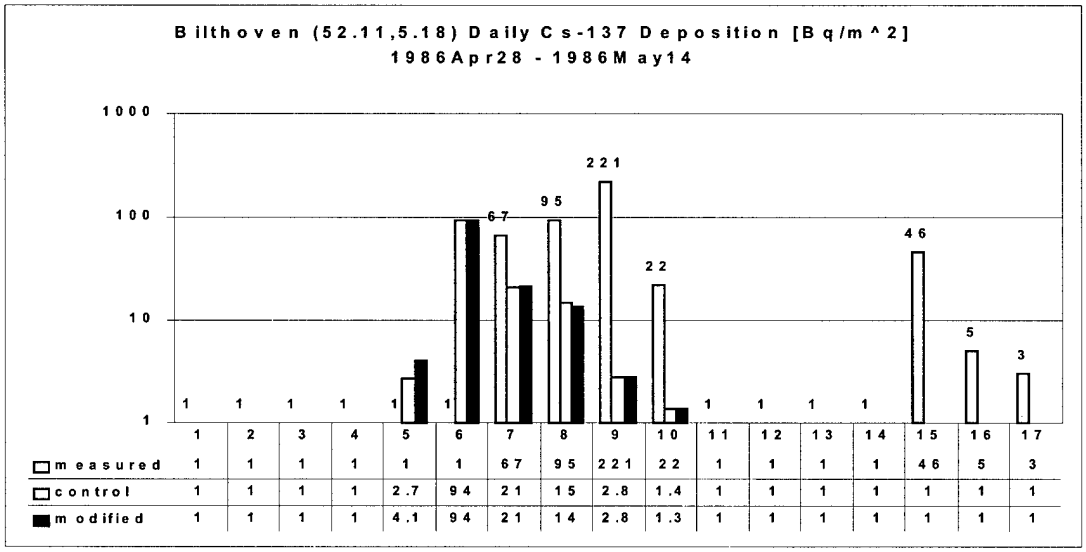


Figure 52 Summary of Bilthoven (Lat,Lon in decimal degrees) daily total Cs-137 deposition 1986Apr27 - 1986May14; measured, control run, and modified cloud base run.

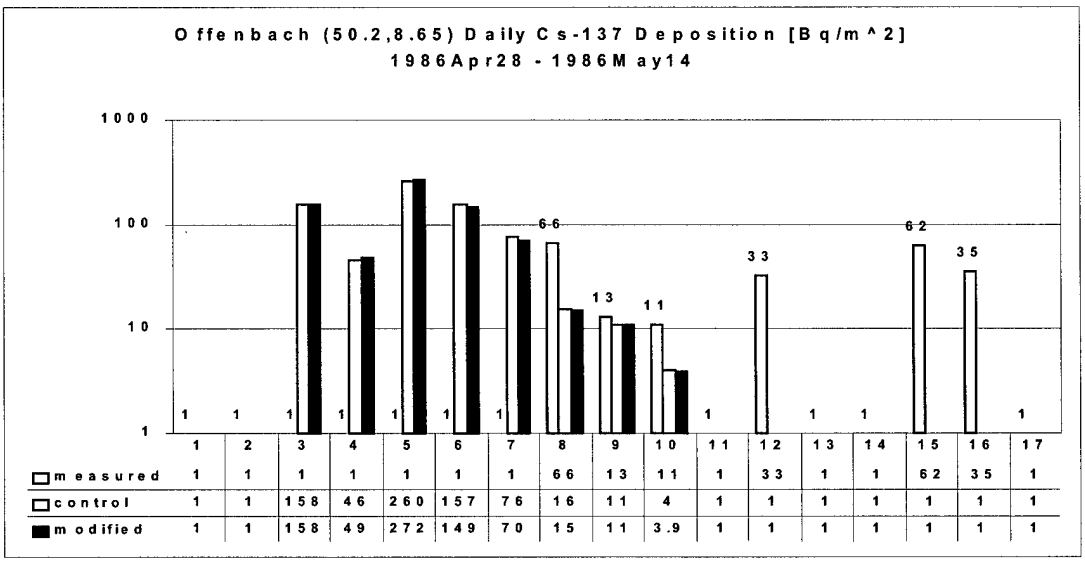


Figure 53 Summary of Offenbach (Lat,Lon in decimal degrees) daily total Cs-137 deposition 1986Apr27 - 1986May14; measured, control run, and modified cloud base run.

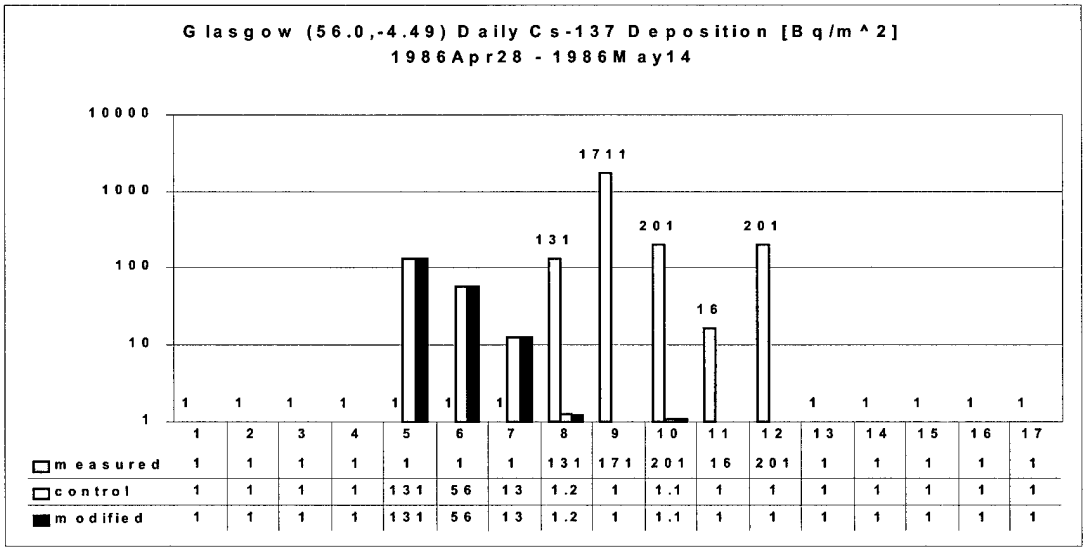


Figure 54 Summary of Glasgow (Lat,Lon in decimal degrees) daily total Cs-137 deposition 1986Apr27 - 1986May14; measured, control run, and modified cloud base run.

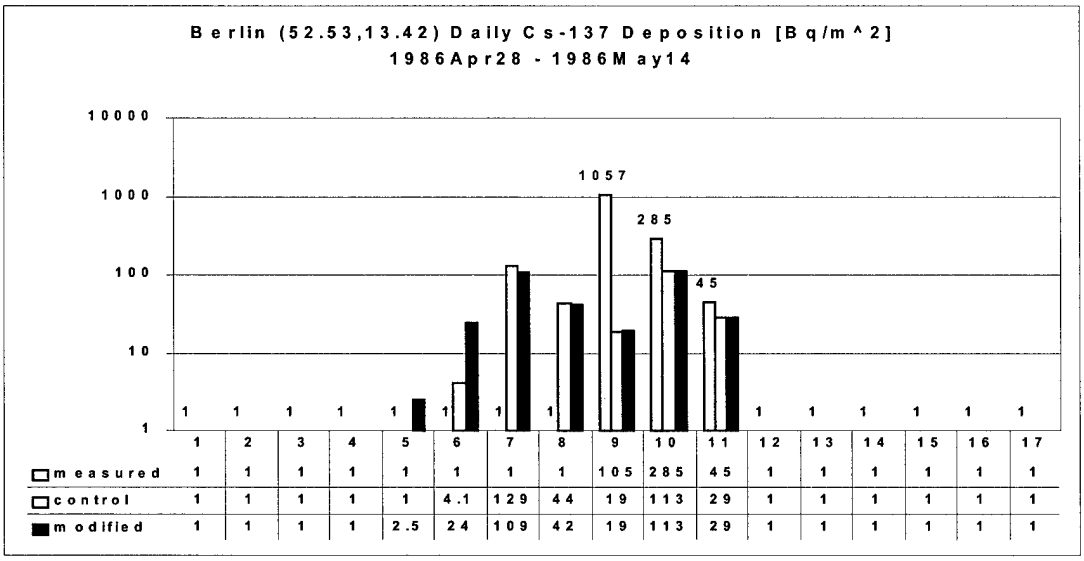


Figure 55 Summary of Berlin (Lat,Lon in decimal degrees) daily total Cs-137 deposition 1986Apr27 - 1986May14; measured, control run, and modified cloud base run.

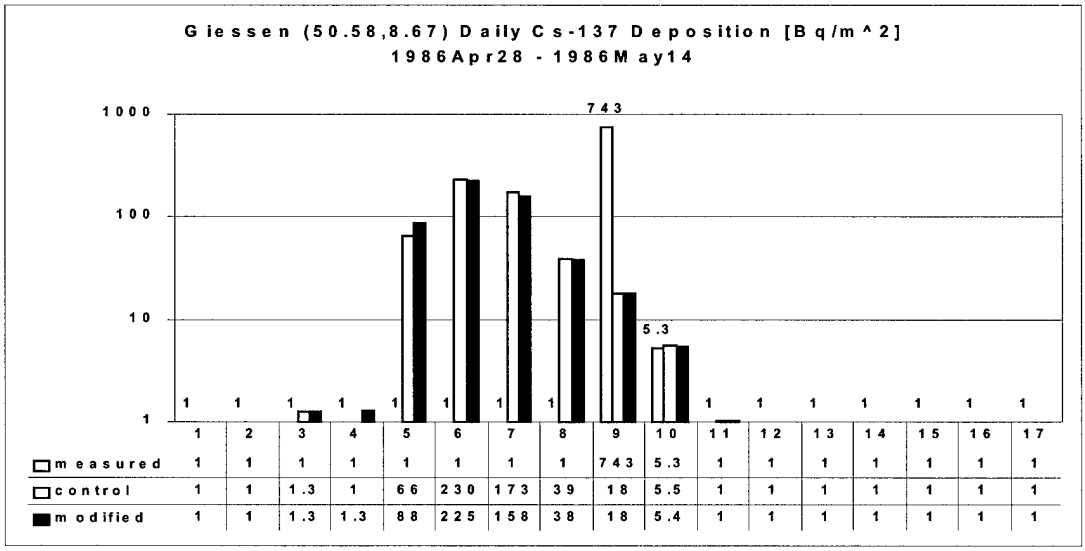


Figure 56 Summary of Giessen (Lat,Lon in decimal degrees) daily total Cs-137 deposition 1986Apr27 - 1986May14; measured, control run, and modified cloud base run.

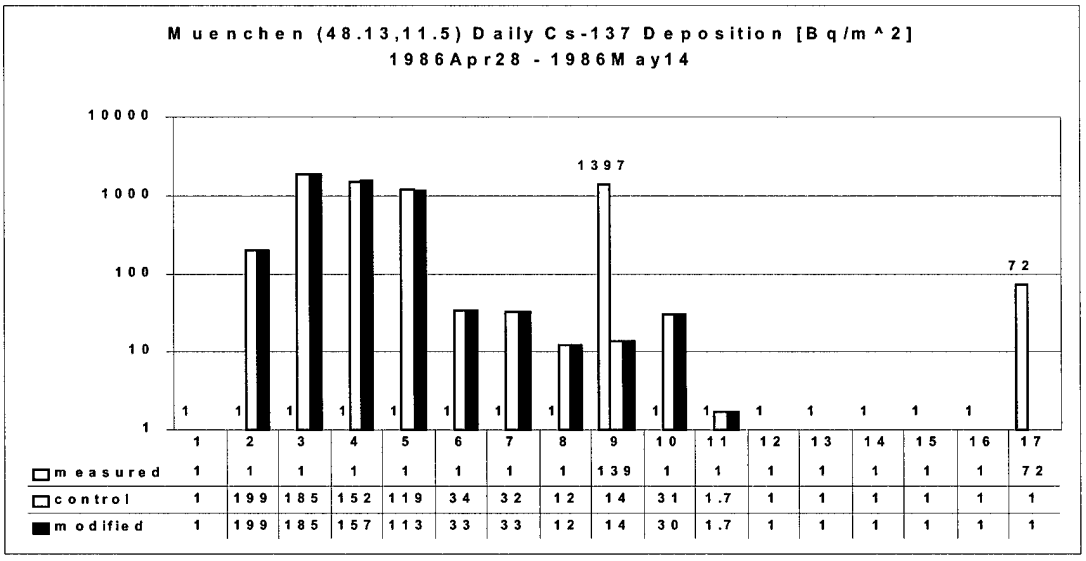


Figure 57 Summary of Muenchen (Lat,Lon in decimal degrees) daily total Cs-137 deposition 1986Apr27 - 1986May14; measured, control run, and modified cloud base run.

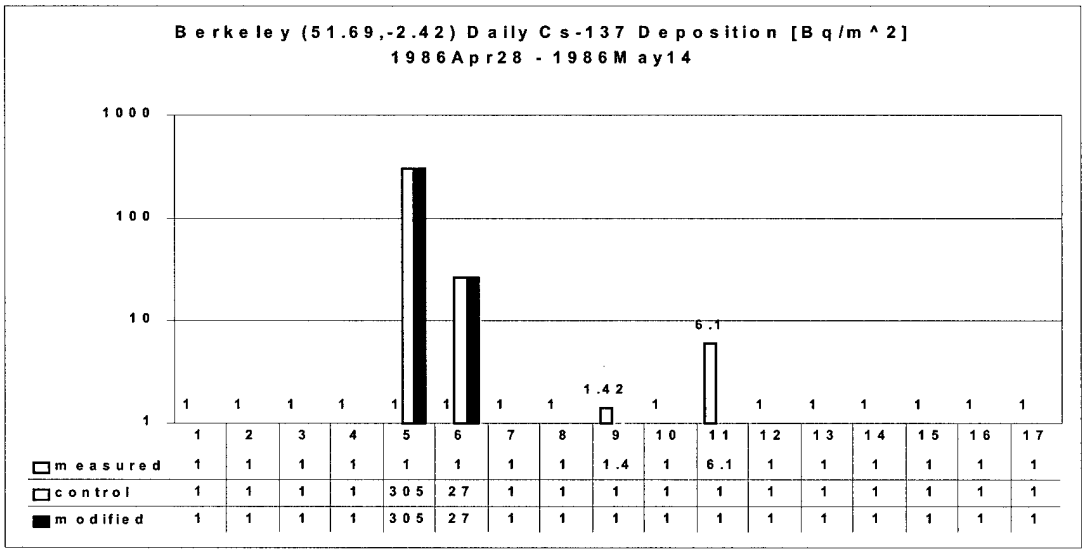


Figure 58 Summary of Berkeley (Lat,Lon in decimal degrees) daily total Cs-137 deposition 1986Apr27 - 1986May14; measured, control run, and modified cloud base run.

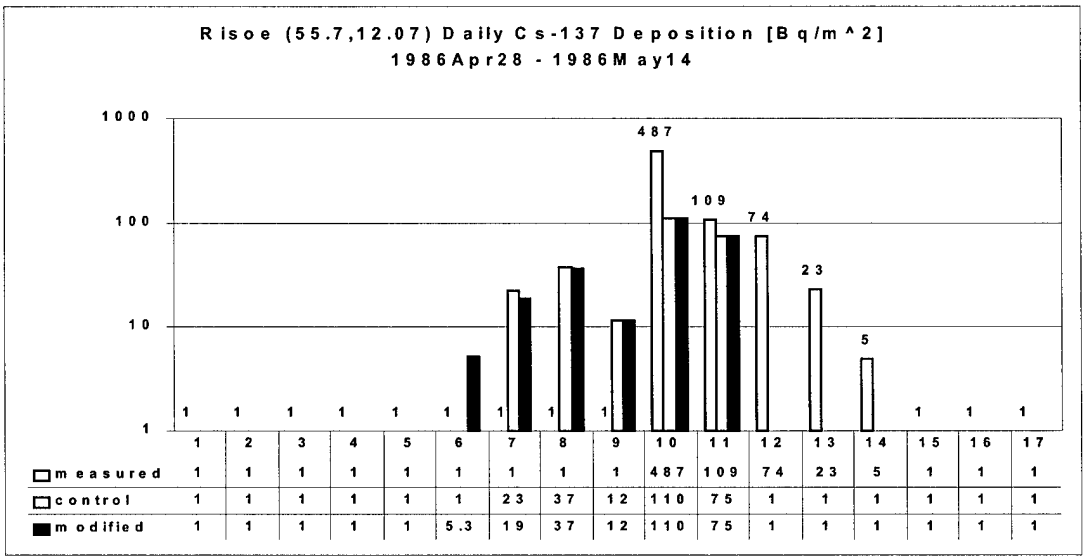


Figure 59 Summary of Risoe (Lat,Lon in decimal degrees) daily total Cs-137 deposition 1986Apr27 - 1986May14; measured, control run, and modified cloud base run.

*4.2.2 Modified-Cloud-Base Performance in April Over Germany/Austria.*

Herein are described the results of two 5-*day* Chernobyl plume simulations and their deposition in Germany/Austria. The first simulation is an April deposition control run using default Chernobyl settings as described in Section 3.5.4. The second simulation is an April deposition cloud base modification run identical to the April deposition control run, except with 75%-RH cloud bases over land, instead of the default 80%. Deposition contours from the April deposition control run over the selected region are depicted in Figure 60. Total deposition from the April deposition cloud base modification run is shown in Figure 61. The modified-cloud-base deposition pattern exhibits generally greater deposition than the control run. Also, the contours are less smooth, indicating higher variability. The difference between the two fields, displayed in Figure 62, confirms the general increase in deposition with a lowered cloud base. A quantitative analysis is presented next, then qualitative analysis of major features of Figure 62.

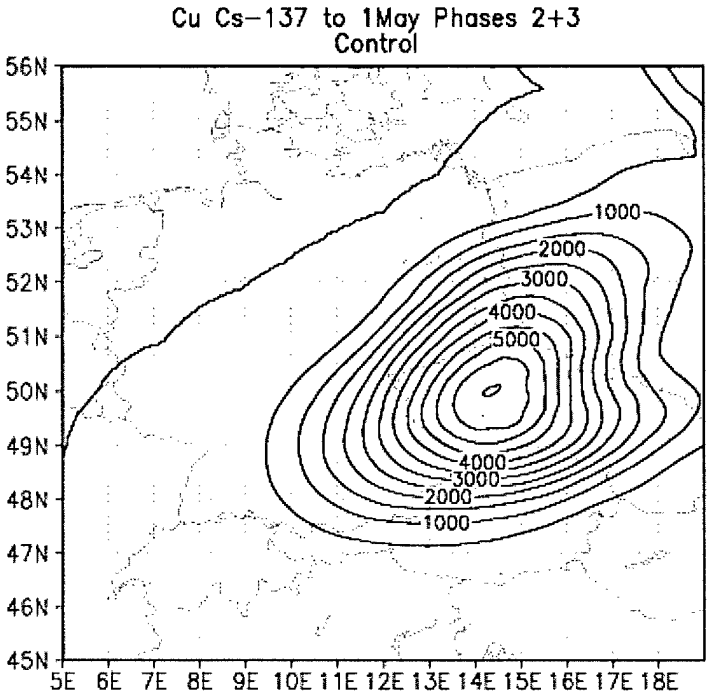


Figure 60 April deposition control run. Modeled Chernobyl Cs-137 deposition concentration $[Bq/m^2]$ accumulated over 86.04.26.00Z - 86.05.01.00Z.

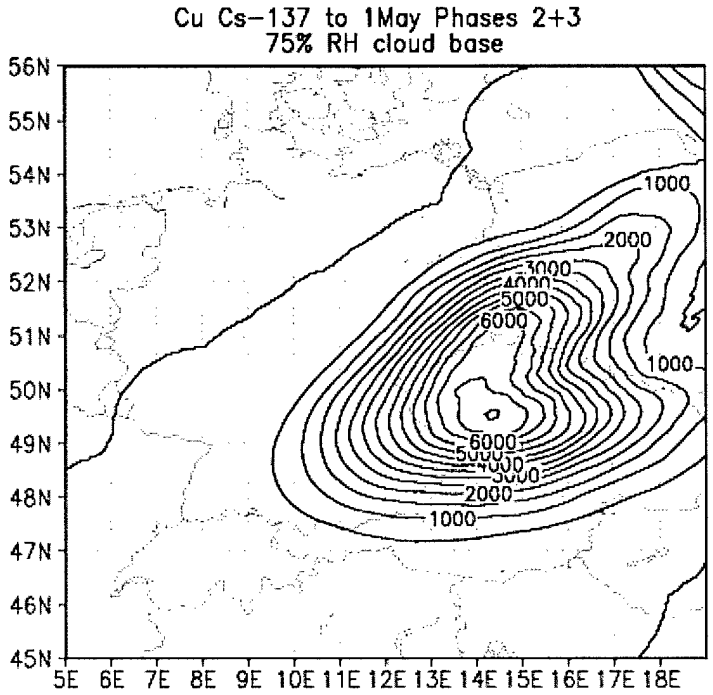


Figure 61 April deposition modified cloud base run. Modeled Chernobyl Cs-137 deposition concentration $[Bq/m^2]$ accumulated over 86.04.26.00Z - 86.05.01.00Z.

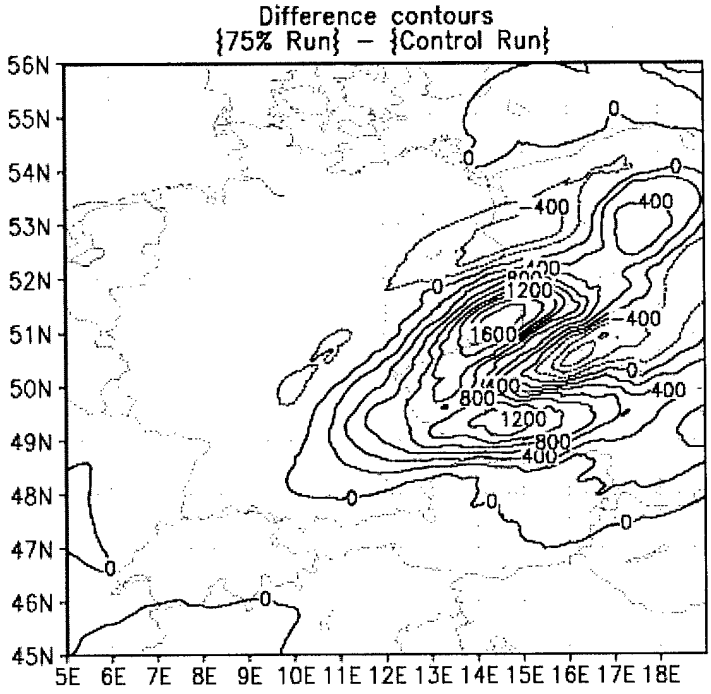


Figure 62 Difference in modeled Chernobyl Cs-137 deposition concentration $[Bq/m^2]$ between cloud-base-modified run April deposition and control run April deposition (modified run deposition minus control run deposition), accumulated over 86.04.26.00Z - 86.05.01.00Z.

Concentrations from each run are extracted at points corresponding to the 395 April-cumulative measurement sites (Subsection 3.5.4) and are compared to the measurements. As may be suspected from earlier explanations, the cloud base modification is a relatively subtle adjustment and its impact in a Chernobyl simulation is masked by large errors in other parameters. For display and statistical purposes, a value of 1 was added to avoid taking the logarithm of zero, then the base-10 logarithm was taken at each data point, measured and modeled. Adding a constant to a distribution does not at all affect its correlation with another variable. A normal probability plot of log-transformed measured deposition values, Figure 63, strongly confirms the assertion by Rodriguez et al. that the distribution of surface concentration is log-normal (Rodriguez 95:811). Measurements were of total deposition, including any Cs-137 deposits prior to the Chernobyl accident. To adjust modeled quantities for pre-Chernobyl deposition the lesser of the corresponding measurement value or $2500 Bq$ was added to each modeled data point. No null measurements are found in the REM database, so the data is log-transformed without adding a value of 1 to each data point. Correlation is 0.6059 for a point by point comparison of the log transformed 5-*day* Cs-137 measurements in Germany/Austria to log transformed deposition from the April deposition control run. Correlation is 0.5843 for the same comparison to the modified-cloud-base run. So, a slightly lower correlation to measurements is observed using modeled cloud bases lowered to the 75% humidity threshold. While cloud base parameterization improvement has not been shown for 5-day Chernobyl deposition in Germany and Austria, qualitative analysis of the results does unearth some clues to the possible role of wet deposition mechanisms at work in the Chernobyl case.

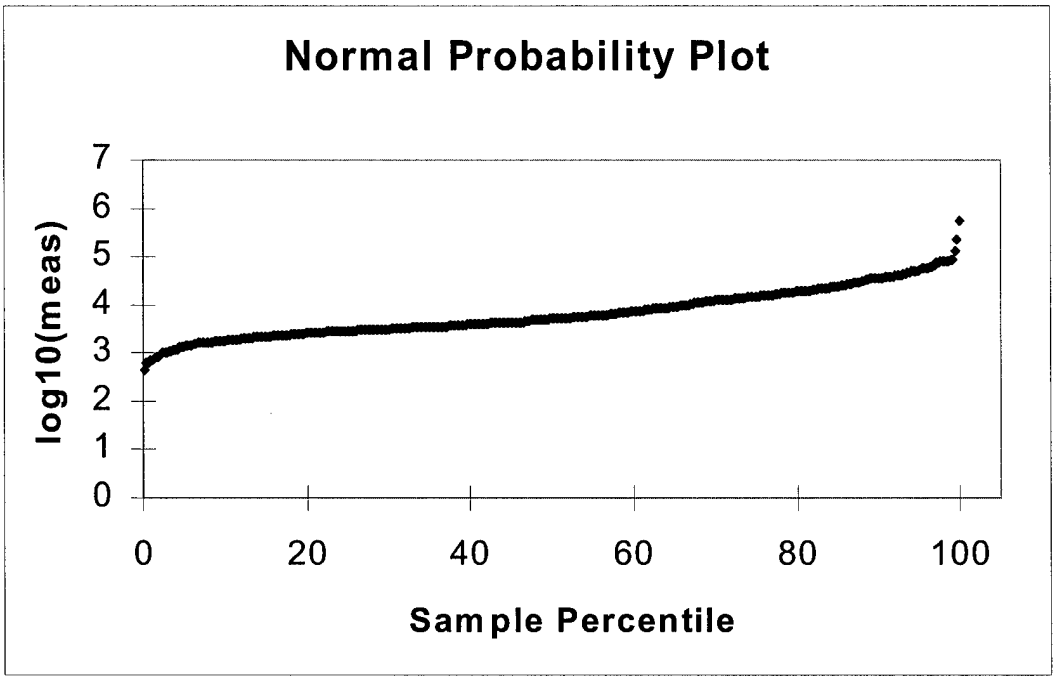


Figure 63 Normal Probability Plot of Log Transformed April Cumulative Cs-137 Deposition Measurements in Germany and Austria

The change from 80% to a 75% RH continental cloud base threshold in effect lowers the cloud base over land without changing the cloud top, the plume height, or the horizontal pattern of precipitation. In the sensitivity studies in Subsection 4.1.1, the BCS rate was left undisturbed. With the cloud base lower, as long as the plume is near the cloud base, more of the pollutant will be within the cloud and less will be below it. So, for modified-cloud-base simulation runs, BCS applies to less of the plume, and ICS applies to more of the plume. BCS is dependent on rain duration which, in the model, is always $6hrs$. ICS is dependent on rain amount which varies with each gridpoint, therefore, more variability appears in the modified-cloud-base run deposition pattern because more ICS is occurring relative to April deposition control run ICS. Since ICS always counts more in the cloud base modification run relative to the control run, the sign of the change in deposition

depends on which scavenging provided more deposition, ICS or BCS. The fact that an overall increase in deposition is observed for a lowered cloud base indicates that modeled ICS is removing more Cs-137 overall than modeled BCS over Germany in April, 1986. While ICS is proportional to total amount of rain, BCS is proportional to the amount of time it rains. ICS tends to dominate the wet deposition from a ten-minute downpour, and BCS is the predominate deposition mechanism for a 3-day drizzle.

The general precipitation pattern over the sampled domain for late April is heaviest over Austria and gradually diminishing northward (Appendix C). The best opportunity for BCS to dominate ICS is where the model precipitation is lightest, north in this case. The patch of negative deposition difference values over the north half of the Germany/Poland border in Figure 62 is consistent with this thinking. Since this area is the most likely place for ICS to apply to more of the plume at the expense of the more dominant BCS. The other negative anomaly, over the heart of Czechoslovakia, is more difficult to assess. Since, between April deposition control and April deposition modified-cloud-base runs, no changes in scavenging occur above the 80%-RH level or below the 75%-RH level, one only needs to assess what happens in the layer between those levels. Perhaps, during one or more precipitation events in the April deposition control run, BCS only slightly reduces pollutant concentration in the 75%-80% layer, leaving plenty of pollutant in the layer for deposition in a downstream location. Then, in a parallel April deposition modified-cloud-base run, during the same precipitation events, ICS depletes the 75%-80%-RH layer completely. So, the downstream location will have less pollutant available for scavenging, therefore, deposition will amount to less than that in the April deposition control run, as in the Czechoslovakia negative feature in Figure 62. If the April deposition modified-cloud-base run were truth, and the April deposition control run included the exact scavenging error, the SECP would be somewhere upstream from the negative feature.

# V. Conclusions

## 5.1 Sensitivity Runs

It has been observed that for a 6-$hr$ time step and a polar stereographic computational grid as coarse as $60km$ in resolution, a HySPLIT transport and deposition simulation requires over $6hrs$ (one time step) to produce a realistic deposition pattern. Anomalous modeled deposition occurs within $100km$ of the source and is probably an artifact of interpolations used to initialize the pollutant plume. It has been shown that relative changes in deposition due to altering the ICS efficiency parameter in HySPLIT are nearly proportional to the ICS efficiency alteration. In other words, when the efficiency of ICS is doubled, a doubling of rain-out deposition is the result as long as pollutant concentrations are not significantly reduced. The acronym, SECP (Scavenging Error Crossover Point), has been coined describing the location at which the effect of scavenging errors on plume concentration bottoms out and begins to have the opposite effect. For example, over-scavenging initially produces excess deposition, but at the SECP no excess deposition occurs because the plume concentration has dropped enough. Downstream from the SECP, deposition is underestimated as the plume concentration continues to drop too fast. ICS efficiency sensitivity test simulations were run out to $12hrs$ and $600km$ in light rain (approximately $1mm$ per $6hrs$). At these limits, no SECP was apparent in the deposition pattern. Future studies may help refine the understanding of the SECP in general and of its possible range of influence on Chernobyl simulations.

## 5.2 Cloud Base Modification Runs

The predictive ability of HySPLIT appears to improve very slightly when modified to model continental cloud bases at 75% RH instead of its default 80%. The slight improvement is based on a higher correlation with measured data (0.5050) of the total bulk results of a modified-cloud-base daily deposition run than that

(0.5037) of the total bulk results of the control daily deposition run. Given the combined severe uncertainties of Chernobyl emissions, of model precipitation and wind fields, and of the measurements themselves, and given that a 0.50 Pearson correlation is equivalent to raw guessing, the results in this format are inconclusive. However, an interesting clue arises from a city-by-city analysis. When correlation coefficients are calculated for each city, a trend of degraded predictive ability with time emerges. Figures 64 and 65 summarize the correlation of both control run and modified-cloud-base runs with measured data. The cities are in order by plume arrival, i.e., by earliest non-zero measurement recorded at each city. The cities where the modified cloud base has improved HySPLIT's predictive ability were Helsinki, Hof, Schwandorf, Hradec Kralov, Budapest, and Mol. There is virtually no change in predictive ability at Bratislava, Moravsky Krumlov, Passau, or Kosice (map of daily deposition cities in Section 3.5.3, Figure 12). So, the modified cloud base has performed slightly better than the control at the cities nearest Chernobyl (Figure 64, except for Harwell) and the same as, or worse than, the control run at the cities furthest from Chernobyl (Figure 65, and Harwell). This trend could be an indication that the modified cloud base has induced an actual predictive ability that degrades, as expected, with distance from the source.

Comparisons of HySPLIT control and cloud-base-modified runs of deposition in Germany and Austria in April, 1986 indicate a decrease in the predicitive ability of a HySPLIT Chernobyl simulation. Evidence of a SECP just upstream from Germany was examined in Section 4.2.2. These results are not inconsistent with the daily deposition run results since the modified-cloud-base run decreased accuracy at three of five German cities.

By means of a HySPLIT cloud base parameterization revision (75%-RH continental cloud bases), very small improvement has been demonstrated in the accuracy of a HySPLIT Chernobyl Cs-137 daily deposition simulation, while a decrease in accuracy has resulted from a 5-*day*-cumulative Chernobyl deposition simulation over

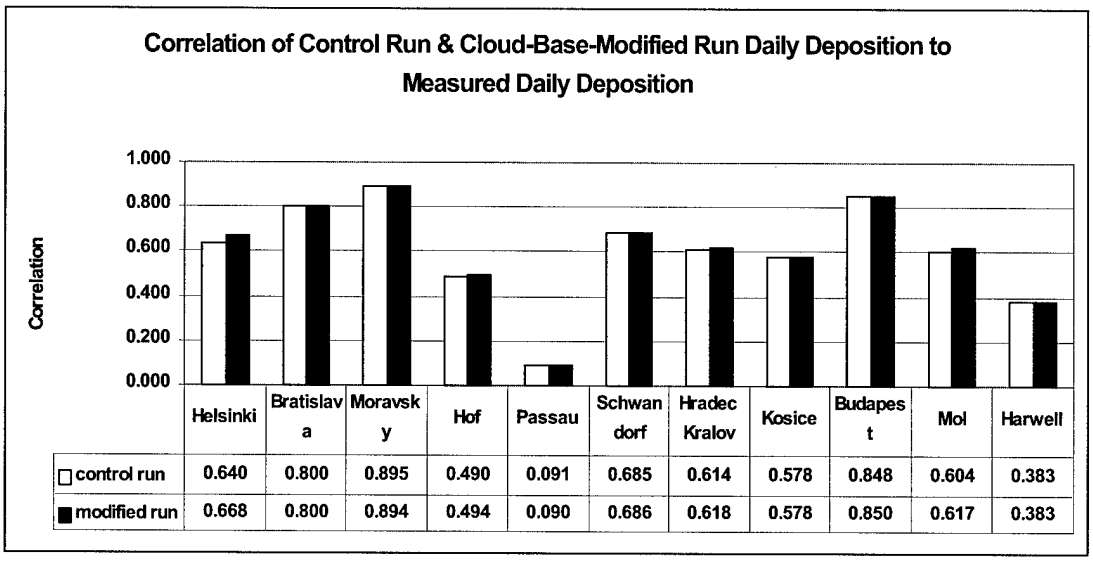


| | Helsinki | Bratislava | Moravsky | Hof | Passau | Schwandorf | Hradec Kralov | Kosice | Budapest | Mol | Harwell |
|---|---|---|---|---|---|---|---|---|---|---|---|
| control run | 0.640 | 0.800 | 0.895 | 0.490 | 0.091 | 0.685 | 0.614 | 0.578 | 0.848 | 0.604 | 0.383 |
| modified run | 0.668 | 0.800 | 0.894 | 0.494 | 0.090 | 0.686 | 0.618 | 0.578 | 0.850 | 0.617 | 0.383 |

Figure 64 Set 1. Pearson correlation coefficients of modeled Chernobyl Cs-137 daily deposition (control run and modified-cloud-base run) against measured Chernobyl Cs-137 daily deposition, by city. In order by earliest deposition measurement at each city.

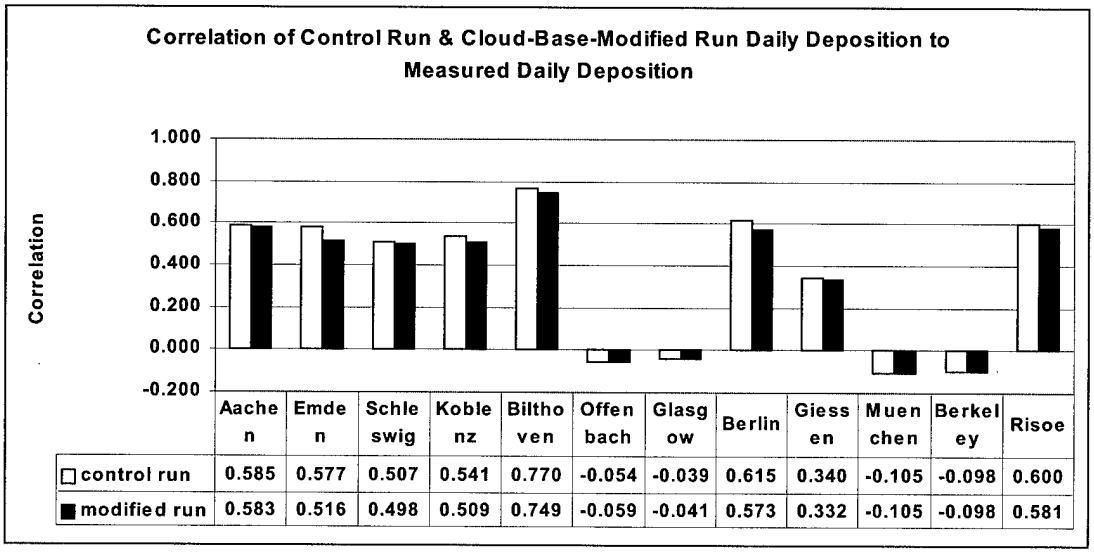


| | Aachen | Emden | Schleswig | Koblenz | Biltho ven | Offenbach | Glasgow | Berlin | Giessen | Muenchen | Berkeley | Risoe |
|---|---|---|---|---|---|---|---|---|---|---|---|---|
| control run | 0.585 | 0.577 | 0.507 | 0.541 | 0.770 | -0.054 | -0.039 | 0.615 | 0.340 | -0.105 | -0.098 | 0.600 |
| modified run | 0.583 | 0.516 | 0.498 | 0.509 | 0.749 | -0.059 | -0.041 | 0.573 | 0.332 | -0.105 | -0.098 | 0.581 |

Figure 65 Set 2. Pearson correlation coefficients of modeled Chernobyl Cs-137 daily deposition (control run and modified-cloud-base run) against measured Chernobyl Cs-137 daily deposition, by city. In order by earliest deposition measurement at each city.

Germany and Austria. The slightly improved HySPLIT performance in the daily deposition case does not prove indisputably that a 75%-RH continental cloud base is more true to the Chernobyl environmental conditions. A credible source term construction could be artificially devised such that 80%-RH continental cloud bases would produce the more "accurate" daily deposition. The 50% margin of error in Chernobyl's estimated daily emissions provides wide latitude to do so. Simulations of atmospheric plume transport and deposition are vulnerable to limitations in the representation of several aspects of the problem. These aspects include the particle size distribution and its space and time variations, turbulence, atmospheric instability, and other dry transport processes, the solubility of the particles, cloud formation and dissipation processes, fog deposition, and particle resuspension (Knap 88:48). Cumulative measurements representing all or several days of the Chernobyl deposition are likely to have a large positive bias since Cs-137 deposition measurement locations would tend to be where the highest radioactivity levels had been detected. The slightly positive results from the daily deposition simulation should in no way, then, be taken as proof of a general improvement in modeled cloud base. One can expect much larger gains in the accuracy of wet deposition modeling by improving the location, timing, and amount of precipitation inputs. It appears, in fact, that verifiable improvements to wet deposition parameterizations must wait both for increased resolution and accuracy of precipitation modeling, and for an experimental wet deposition case with more precise emission specifications and more homogeneous, higher resolution deposition measurements. Although the specific wet deposition parameterization test yielded no conclusive evidence of either better or worse performance, the exercise constitutes a meaningful starting point for a researcher interested in either refining the Chernobyl source term, or using Chernobyl data for validating transport or deposition mechanisms in a model where wet deposition is a factor, or learning how to use the HySPLIT model and becoming familiar with its capabilities and limitations.

### *5.3 Future Research Opportunities*

HySPLIT lacks the modeling of fog deposition. No clouds (fog) are diagnosed in the surface layer in HySPLIT, so only dry deposition occurs within the surface layer in the model. Modification of HySPLIT to include accurate fog modeling and the increased surface layer deposition that results, especially in up-slope wind instances, and investigation into its impact on Chernobyl could bring model results more in line with Chernobyl deposition measurements. Fog parameterization is an even larger challenge than cloud parameterization, so unless approached carefully, adding fog deposition to a model could easily hurt the accuracy of modeled deposition more than it helps. One could probably make the same argument about cloud parameterization. Until liquid and ice cloud water content variables are available routinely from meteorological models, transport model cloud parameterization in general would still benefit from more accurate cloud diagnosis. The MRF model run by the National Weather Service (NWS) in addition to treating clouds differently over land and sea, makes finer cloudiness distinctions by relative humidity in predefined latitude regions and in four predefined vertical layers based on Real Time Nephanalysis (RTNEPH) data from USAF (NWS 01). Slingo (Slingo 87) poses and validates a more complex diagnostic cloud parameterization scheme accounting for relative humidity, vertical velocity and static stability (specifically, potential temperature change in the vertical). His approach holds promise for improving regional deposition distinctions between cumuliform and stratiform precipitation events.

Further model comparisons to Chernobyl deposition should include as much measurement data as possible, increasing the span and resolution of observations in space and in time to strengthen confidence in results. Since surface-based observations near the source are scarce, aerial gamma spectrometry measurements taken over Russia could serve that purpose (DeCort 98). Even though there was about 2000 - 3000$Bq/m^2$ of Cs-137 from weapons fallout on the ground before the accident, these readings could help improve model representation of the Chernobyl plume early

in the accident because millions of $Bq/m^2$ of Cs-137 were deposited on Ukraine and Belarus (DeCort 98). The difficulties of source term uncertainty are not unique to Chernobyl. Transport analysts responding to any urgent, short-notice call for an emission simulation normally have only a crude estimation of the source term. Since the effective release height is highly dependent on static stability, one could investigate the modeled vertical profiles at Chernobyl and the nearest observed atmospheric soundings. Principles developed in this project could be applicable and valuable to operational simulations. The future of transport modeling, like the future of general meteorological forecasting, may look like ensemble forecasting. Motivated by a statistical view on stochastic processes like weather, an ensemble forecast is a set of simulations made up of a best-guess control run and a set of perturbation runs, each with a slightly different reasonable departure from the control run. An ensemble of forecasted patterns should provide helpful information about the spectrum of possible outcomes and about the confidence of any particular run (Draxler 00b). This method also provides an ongoing opportunity to generate further clues about which variables are important under specific synoptic regimes.

## *Appendix A. Glossary of Acronyms*

- AFTAC - Air Force Technical Applications Center
- AGL - Above Ground Level
- ARL - Air Resources Laboratory
- ATMES - Atmospheric Transport Model Evaluation Study
- BCS - Below-Cloud Scavenging
- CEC - Commission of the European Communities (or just EC, European Commission )
- EC - European Commission (see CEC)
- ECMWF - European Centre for Medium-range Weather Forecasts
- ETA - Not an acronym; weather model named after coordinate system with vertical coordinate, eta (the Greek letter, $\eta$)
- GRADS - GRidded Analysis Display System
- GRIB - GRIdded Binary format
- HTML - HyperText Markup Language
- HySPLIT - Hybrid Single-Particle Lagrangian Integrated Trajectories
- ICS - In-Cloud Scavenging
- JRC - Joint Research Centre
- NEA - Nuclear Energy Agency
- NOAA - National Oceanographic and Atmospheric Administration
- NCAR - National Center for Atmospheric Research
- REM - Radioactivity Environmental Monitoring
- RH - Relative Humidity

- RTNEPH - Real Time Nephanalysis
- SECP - Scavenging Error Crossover Point
- UCAR - University Corporation for Atmospheric Research
- USAEDS - United States Atomic Energy Detection System
- USAF - United States Air Force

# *Appendix B. Radioactivity Primer*

## *B.1 Ionizing Radiation*

A radioactive atom is an unstable isotope characterized by the high-energy radiation its nucleus emits upon spontaneous decay (or disintegration) to a more stable state. This "ionizing radiation" packs enough energy to strip electrons from materials it hits. Ionizing radiation from a radioactive atom can take the form of:

1. an alpha particle (2 protons with 2 neutrons, i.e., an electron-stripped helium nucleus)

– can be shielded by a few inches of air

2. a beta particle (stripped electron)

– can be shielded by several inches of plastic

3. gamma ray or x-ray (high-frequency electromagnetic wave)

– can penetrate lead

4. a neutron (stripped)

– can penetrate thick lead shields

Figure 66 (UIC 00) illustrates typical shielding requirements for each of the four types of ionizing radiation.

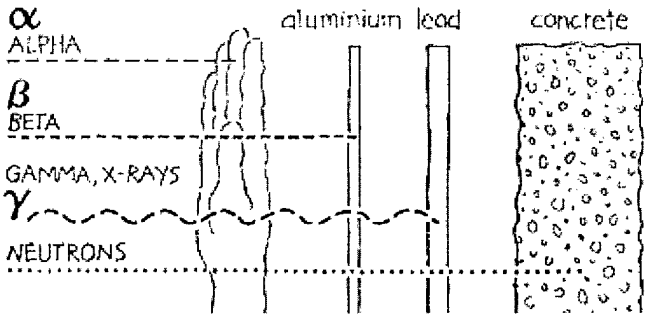


Figure 66 Typical Shielding Requirements for Different Ionizing Radiation Types from UIC, 00

There are (at least) three ways to measure ionizing radiation.

- Radiation Activity, a measure of the number of atomic disintegrations per unit time [e.g., in $Bq = s^{-1}$]
- Radiation Exposure, a measure of the amount of gamma or x-rays present [e.g., in *coulombs/kg*]
- Radiation Dose, a measure of the amount of radiation absorbed by a subject [e.g., in *sieverts*]

- See http://physics.nist.gov/cuu/Units/SIdiagram.html for an extensive summary of SI (International System) units.

*B.2 Cesium-137*

The becquerel is a common unit of Cs-137 deposition radioactivity. One becquerel of Cs-137 is the amount of Cs-137 substance in which 1 unstable cesium atom per second undergoes atomic disintegration (emitting a beta particle and gamma radiation) (MSE 00). The average radiation dose in 1998 from $1kBq/m^2$ of Cs-137 deposited in 1986 is about 1 to $2\mu Sv$. Where soils are more conducive to human exposure, the average dose is closer to $20\mu Sv$ (DeCort 98:22). Radioactive xenon

gas, an abundant product of nuclear fission, decays to Cs-137 which then readily condenses onto particles present (Glasstone 77:389). Cs-137 decays to barium-137 (Ba-137) with an ionizing radiation (beta particles and gamma rays) of $0.662MeV$ per decay (Serway 92). The effective dose is highly dependent on the pathway (respiratory system, skin, digestive system). Although the health effects of exposure to Chernobyl's fallout should not be trivialized, to date the only clear evidence for a confirmed correlation between Chernobyl fallout dose and illness is thyroid cancer in children induced by exposure to the iodine isotope, I-131. Because the detrimental health effects of Cs-137 are not sudden, and because of deficient human health records before the accident, it is difficult to isolate the effects of exposure to Chernobyl accident radiation from the existing widespread decline in the Russian population's general health.

For emergency planning purposes (one application of atmospheric transport modeling), the uncertain concentration effects of local land use, runoff, and population habits (DeCort 98:22), combined with the uncertain health effects of radionuclide exposure/ingestion introduce enough uncertainty to cloud the relative importance of the magnitude of operational concentration estimates and the location and timing of radionuclide deposition. To illustrate, consider the evacuation planner who may be much more interested in which side of a mountain (and when) a radioactive plume may settle than in exactly how much fallout will land in a certain neighborhood.

## *Appendix C. Reanalyzed Precipitation Fields from the ECMWF Model*

To facilitate informal diagnosis of wet deposition in simulations within this thesis, 6-*hrly* model precipitation contours are furnished on the following pages. The valid time for each plot is the end of the six-hour accumulation. Graphics are produced with display.exe utility included with HySPLIT software. 86/04/31/00 UTC implies 86/05/01/00 UTC.

Table 1 Reanalyzed ECMWF 6-Hour Precipitation Fields 1986Apr25.

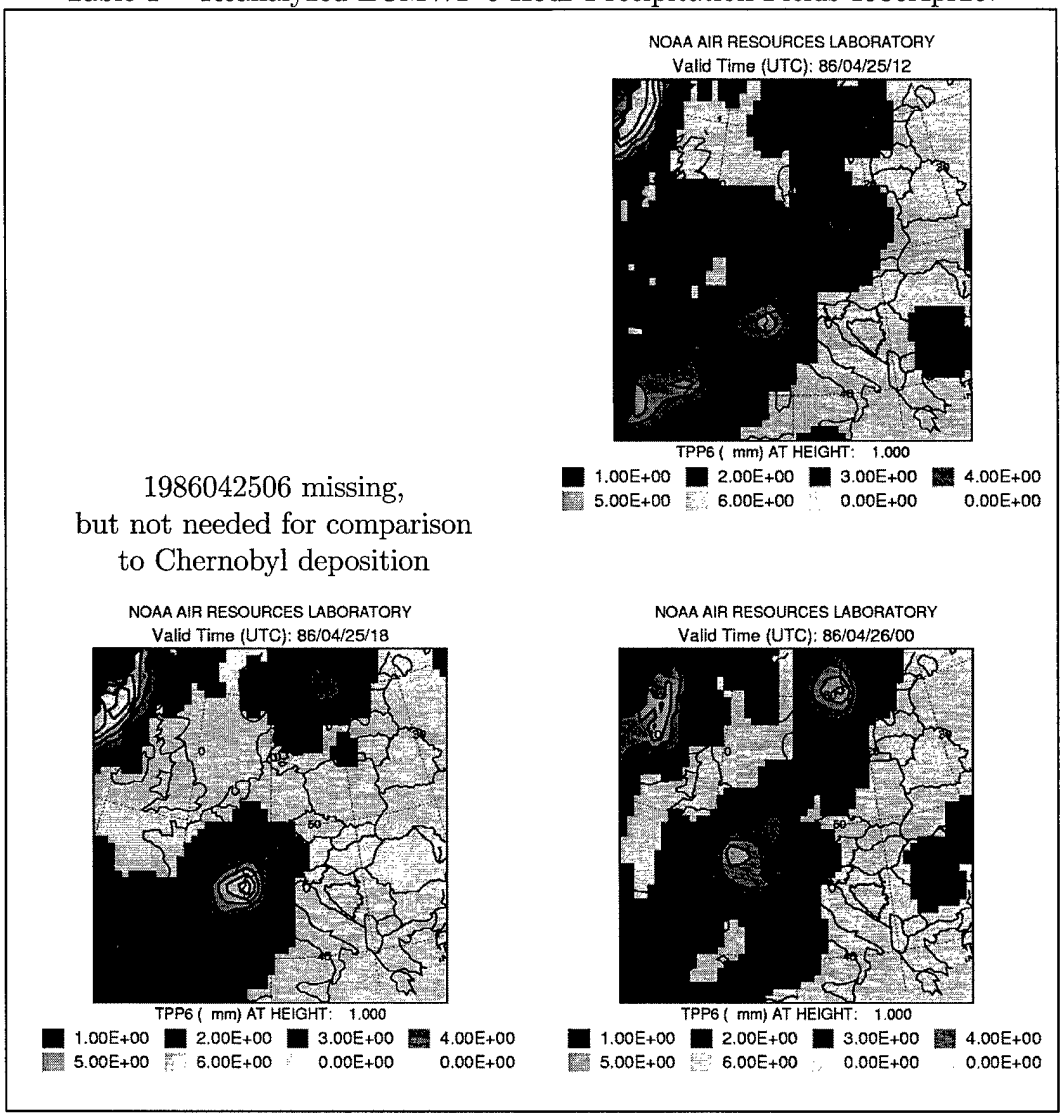

Table 2 Reanalyzed ECMWF 6-Hour Precipitation Fields 1986Apr26.

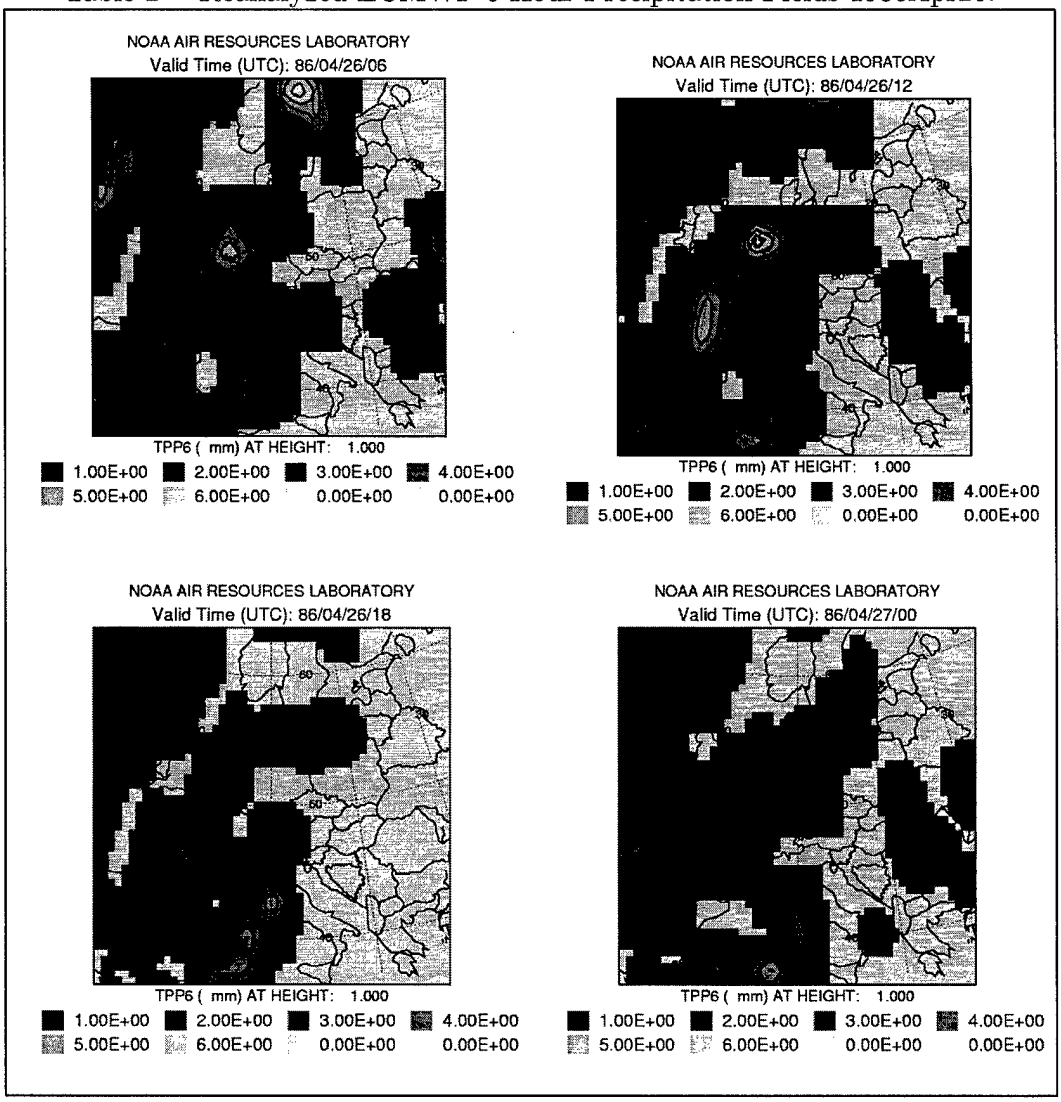

Table 3 Reanalyzed ECMWF 6-Hour Precipitation Fields 1986Apr27.

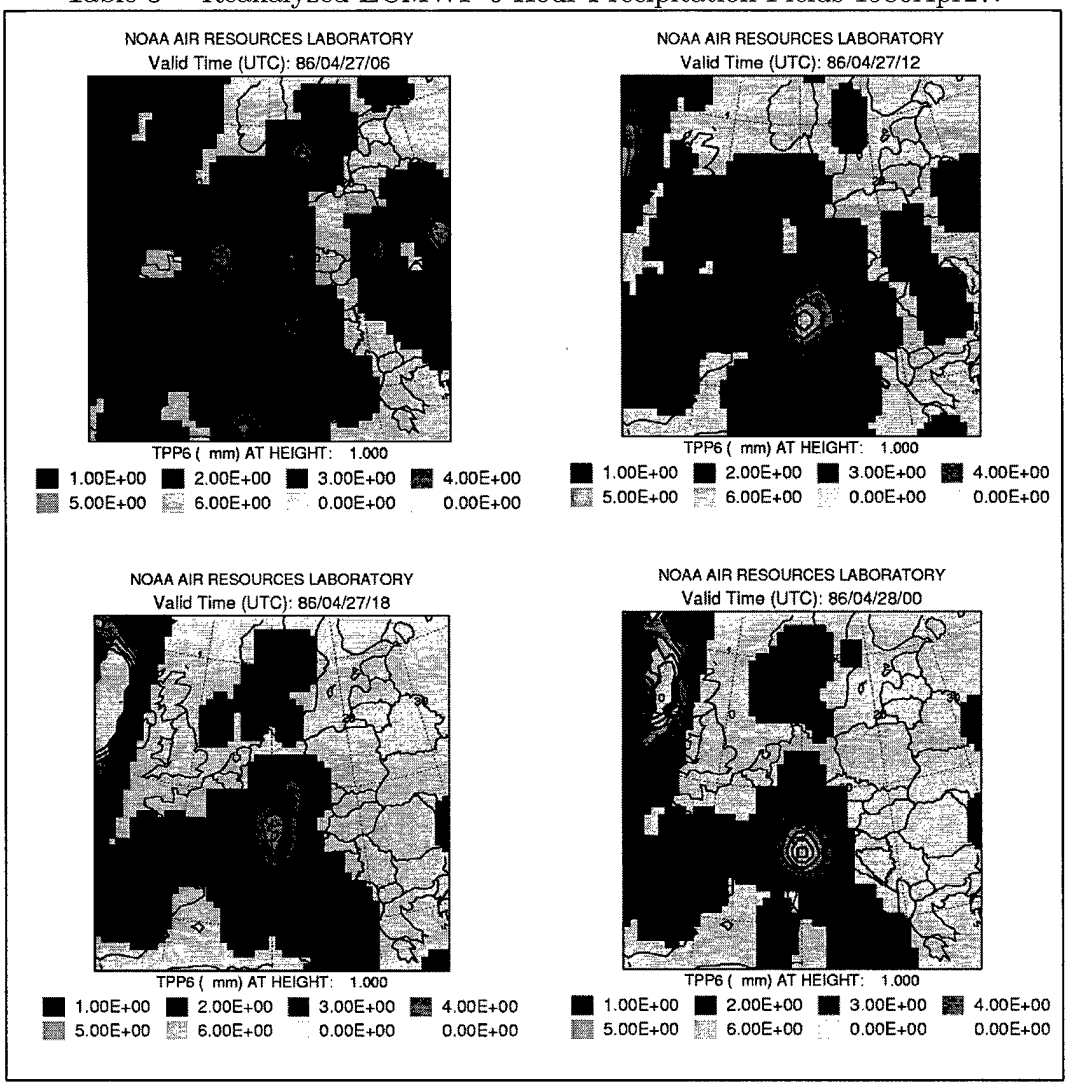

Table 4 Reanalyzed ECMWF 6-Hour Precipitation Fields 1986Apr28.

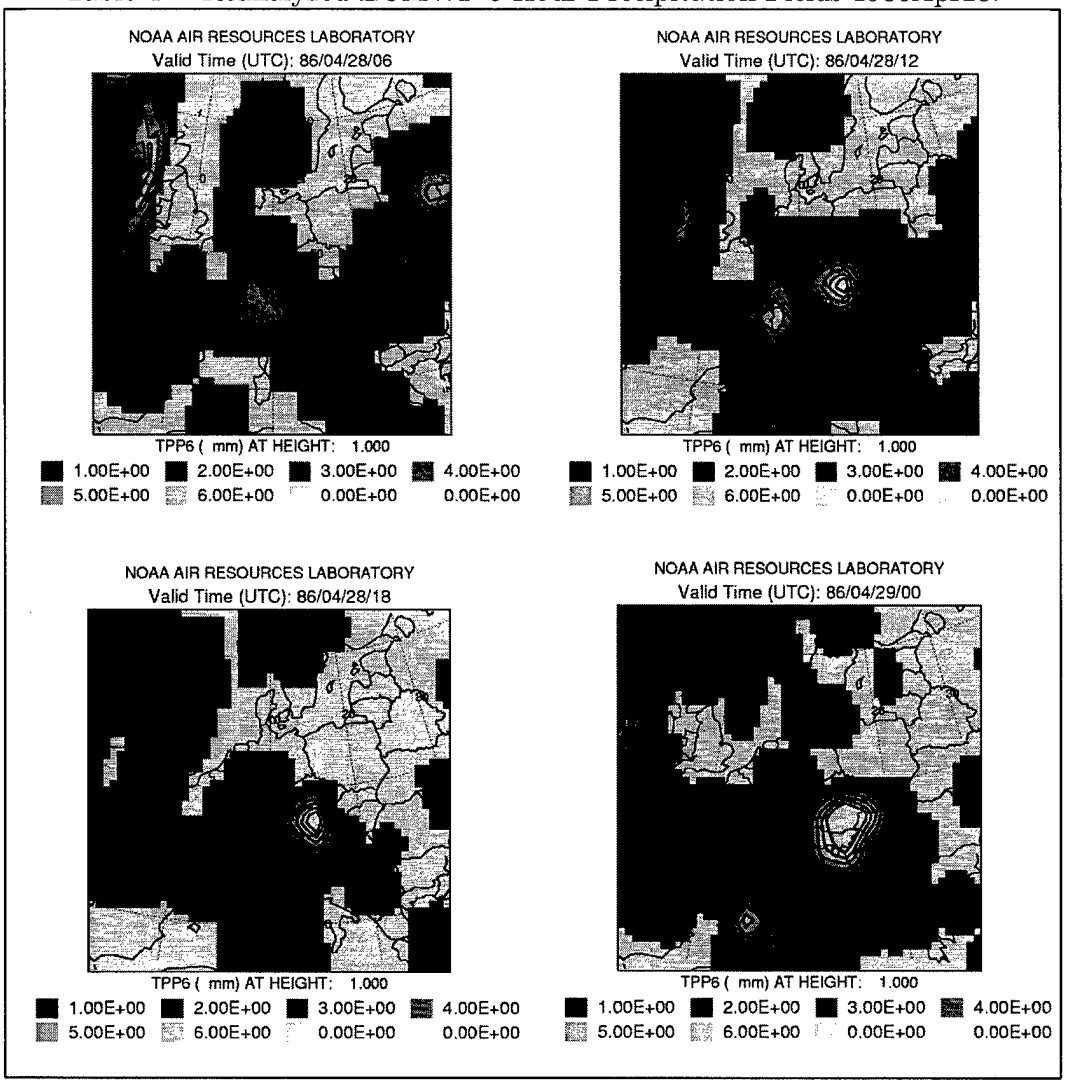

Table 5 Reanalyzed ECMWF 6-Hour Precipitation Fields 1986Apr29.

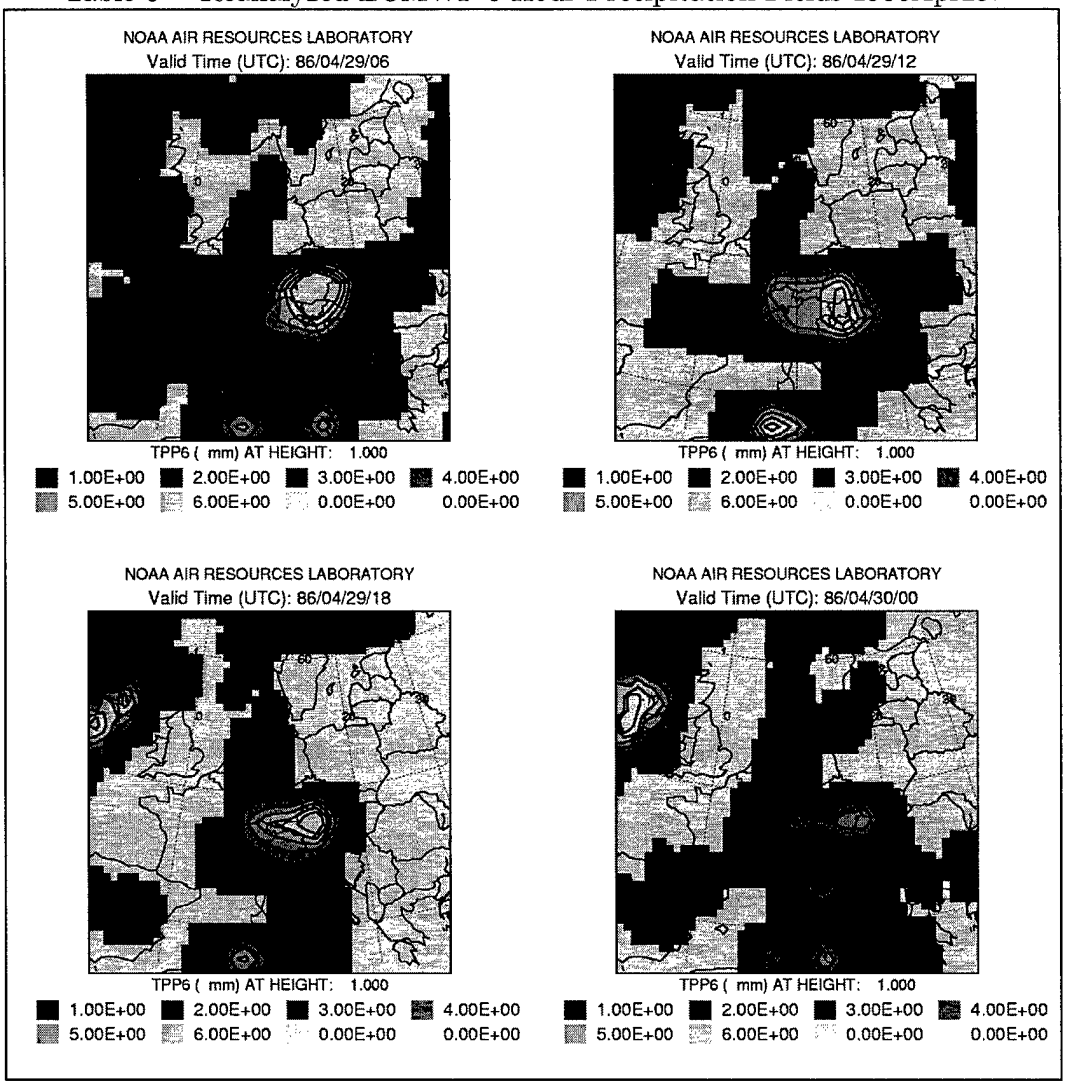

Table 6 Reanalyzed ECMWF 6-Hour Precipitation Fields 1986Apr30.

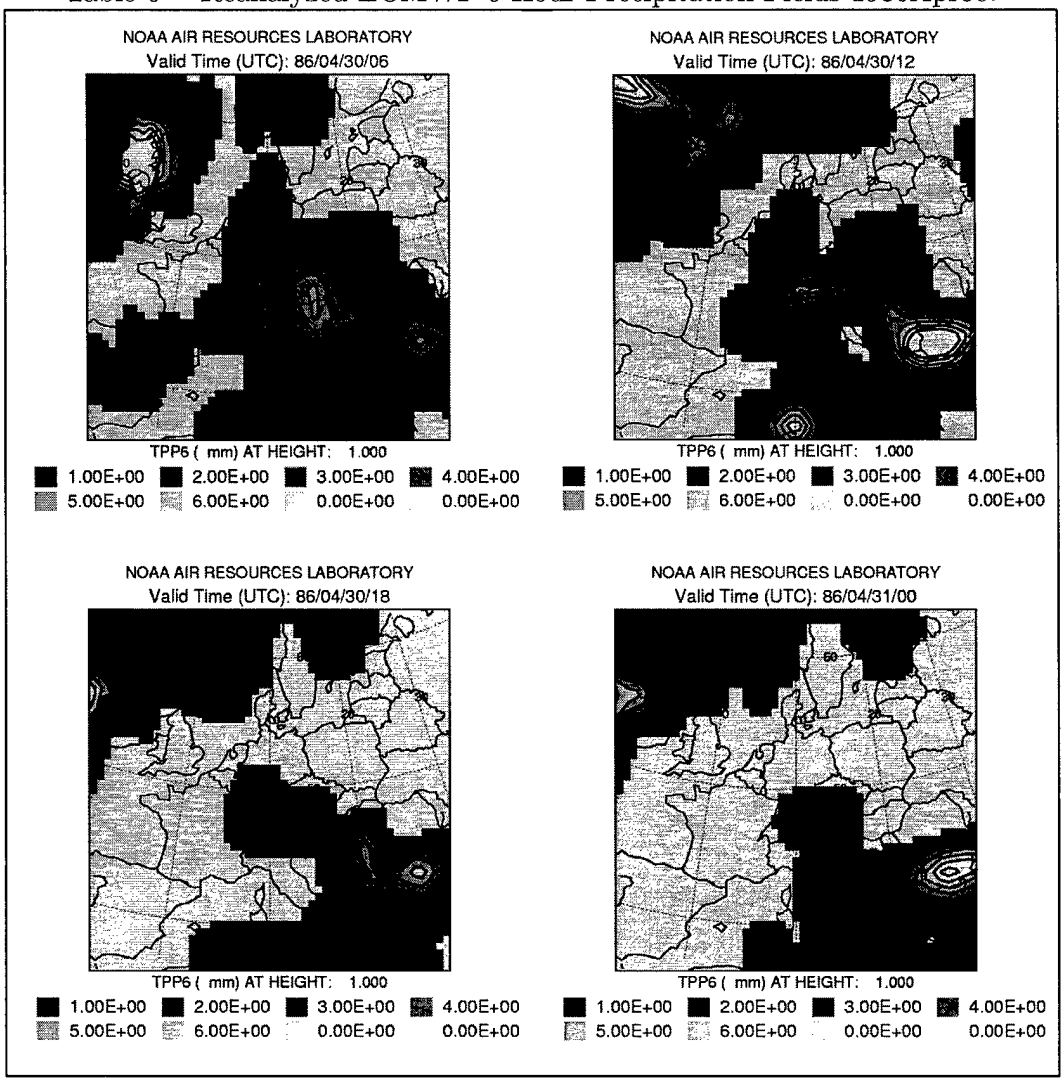

# *Appendix D. HySPLIT Settings*

This appendix provides exact HySPLIT model settings for all representative simulations run for this thesis. An attempt has been made to provide enough supplementary comments to enable the reader to reproduce the simulations in this thesis with a functioning version of HySPLIT. Australian Meteorological Magazine carried an article covering the general capabilities of HySPLIT Version 4, the transport modeling software used for this thesis (Draxler 98b). A complete description of the model including dispersion equations is available in NOAA Technical Memorandum ERL ARL-224 (Draxler 98a). The HySPLIT executable program and documentation is available for download at the following website:

http://www.arl.noaa.gov/ss/models/gethysplit.html

Initial settings for HySPLIT runs are adapted from settings used for Chernobyl simulation by Air Resources Laboratory. Some details are available online at:

http://www.arl.noaa.gov/ss/transport/chernobyl.html

## *D.1 Release Height Sensitivity Runs*

Following this paragraph is a line-by-line breakdown of the 'Control' file settings for the HySPLIT diagnostic run from Section 2.5 with a 1500-$m$ point source. HySPLIT 'Control' file (an ordinary text file) format requires that each numbered item appears (without the number) on a new line in the 'Control' file. Each numbered item below is followed by its description. Zeroes in line 27 would trigger calculations of gaseous emissions. The nominal 1.0 values in line 27 signal to the model that the pollutant is in particle form. A specified non-zero deposition velocity in line 28 eliminates the need for the model to calculate fall speed from particle attributes in line 27. See the HySPLIT User's Guide (Draxler 99) for more details

on the 'Control' file settings. The only changes for the 3000-$m$, 4000-$m$, and 5000-$m$ release height sensitivity simulations are the release heights in line 3 and unique output grid names in line 20.

1. **86 4 25 21**

   Simulation Starting Time [*yy mm dd hh*]

2. **1**

   **Number** of Emission Starting Locations (double it for uniform vertical line sources)

3. **51.38 30.1 1500.0**

   Emission **Latitude** [decimal *degrees*] **Longitude** and Emission **Height** [$m$ AGL]

4. **123**

   Total Simulation Run **Time** [*hours*]

5. **0**

   Vertical Coordinate **Type** for Simulation Run (0 defaults to met. model's)

6. **10000.0**

   Ceiling, or **Top** of Model [$m$ AGL]

7. **1**

   **Number** of Setup Meteorology Files

8. **D:/HySPLIT/hysplit4/metdata/ChernMet/**

   **Path** to Meteorology File

9. **analysisp.bin**

   **Filename** of Meteorology File

10. **1**

**Number** of Pollutants

11. **Cs**

    Pollutant **Identification**

12. **6.65E+14**

    Pollutant Emission **Rate** $[hr^{-1}]$ (Concentration $[m^{-3}]$ or Deposition $[m^{-2}]$ output will be in these units)

13. **24**

    **Hours** of Emission

14. **86 4 25 21 23**

    Release Start **Time** [*yy mo dd hh mn*]

15. **1**

    **Number** of Output Grids to Generate

16. **48.0 13.0**

    Center of Output Grid **Latitude** [decimal *degrees*] **Longitude**

17. **0.5 0.5**

    Spacing (Resolution) of Output Grid **Latitude** [decimal *degrees*] **Longitude**

18. **26.0 36.0**

    Span (Length and Width) of Output Grid **Latitude** [decimal *degrees*] **Longitude**

19. **./**

    **Path** Specification for Output Grid File

20. **1500_m**

    Output Grid **Filename**

21. **1**

**Number** of Vertical Levels in Output Grid

22. **0**

**Height** of Level [$m$ AGL] (0 Triggers Deposition Calculation)

23. **86 4 26 0 0**

Output Grid Sampling **Start** [*yy mo dd hh mn*]

24. **86 5 1 0 0**

Output Grid Sampling **End** [*yy mo dd hh mn*]

25. **0 120 0**

Output Grid Concentration **Type** (0=Average or 1=Snapshot) and **Interval** [*hh mn*]

26. **1**

**Number** of Deposition Setups (Must Match Number of Pollutants)

27. **1.0 1.0 1.0**

Particle **Diameter** [$\mu m$], **Density** [$g/cc$] and **Shape** Factor

28. **0.0001 0.0 0.0 0.0 0.0**

Deposition **Velocity** [$m/s$], Molecular Weight [$g$], **A-Ratio**, **D-Ratio**, and Effective **Henry's** Constant

29. **0.0 3.2E+05 5.0E-05**

Actual **Henry's** Constant [$M/atm$], In-cloud Scavenging Efficiency **Ratio** [$L/L$], and Below-cloud Scavenging **Rate** [$s^{-1}$]

30. **10976.0**

Pollutant Radioactive Decay **Half-life** [*days*] (Airborne and Deposited)

31. **0.0**

**Resuspension** Factor $[m^{-1}]$

*D.2 Comparison to ARL Chernobyl Simulation*

The following HySPLIT control file contents correspond to those used by ARL (ARL 00a) and discussed in Section 3.3.

86 4 25 21, 2, 51.38 30.1 750.0, 51.38 30.1 1500.0, 123, 0, 10000, 1, I:/, forecast.bin, 1, C137, 1.00E+15, 24, 86 4 25 21 0, 1, 50.0, 10.0, 0.5 0.5, 30.0 40.0, ./, dup, 1, 0, 86 4 27 0 0, 99 12 31 24 60, 0 84 0, 1, 1.0 1.0 1.0, 0.0001 0.0 0.0 0.0 0.0, 0.0 3.2E+05, 5.0E-05, 10976, 0

*D.3 In-Cloud Scavenging Sensitivity Control Run*

The following HySPLIT control file contents are used for the ICS sensitivity control run described in Section 3.4.

86 4 25 21, 2, 48.0 11.0 1250.0, 48.0 11.0 1750.0, 147, 0, 10000.0, 2, E:/, apr86.bin, E:/, may86.bin, 1, cs, 6.65E+14, 7.0, 86 4 25 21 0, 2, 50.5 12.0, 0.5 0.5, 11.0 14.0, ./, s3dn6, 1, 0, 86 4 26 0 0, 86 4 27 0 0, 0 6 0, 50.5 12.0, 0.5 0.5, 11.0 14.0, ./, s3dn24, 1, 0, 86 4 27 0 0, 99 12 31 24 0, 0 24 0, 1, 1.0 1.0 1.0, 0.0001, 0.0 0.0 0.0 0.0, 0.0 3.2E+05 5.0E-05, 10976.0, 0.0

*D.4 Daily Deposition Control Run*

The following HySPLIT control file contents are used for the cloud base modification control run described in Section 3.5.3.

86 4 25 21, 2, 51.38 30.1 1250.0, 51.38 30.1 1750.0, 483, 0, 10000.0, 2, E:/, apr86.bin, E:/, may86.bin, 1, Cs, 6.65E+14, 7.0, 86 4 25 21 0, 1, 54.0 10.0, 1.0, 1.0, 14.0 32.0, ./, dly01.hyc, 1, 0, 86 4 27 0 0, 99 12 31 0 0, 0 24 0, 1, 1.0 1.0 1.0, 0.0001 0.0 0.0 0.0 0.0, 0.0 3.2E+05 5.0E-05, 10976.0, 0.0

### *D.5 Chernobyl Control Run - Cumulative Deposition on Germany and Austria to 00Z, 1986May01*

The following HySPLIT control file contents are used for the cloud base modification control run described in Section 3.5.4. Control run resolution increased to 0.05 deg lat & lon for compatibility with display software, GRADS.

Phase II Germany/Austria Control Run HySPLIT Settings

86 4 26 4, 2, 51.38 30.1 350.0, 51.38 30.1 850.0, 116, 0, 10000.0, 1, E:/Chernmet/, analysisp.bin, 1, Cs, 8.8E+14, 20.0, 86 4 26 4 0, 1, 45.5 18.0, 0.05 0.05, 21.0 26.0, ./, cuall2, 1, 0, 86 4 26 4 0, 86 5 1 0 0, 0 116 0, 1, 1.0 1.0 1.0, 0.0001 0.0 0.0 0.0 0.0, 0.0 3.2E+05 5.0E-05, 10976.0, 0.0

Phase III Germany/Austria Control Run HySPLIT Settings

86 4 27 0, 2, 51.38 30.1 350.0, 51.38 30.1 850.0, 96, 0, 10000.0, 1, E:/Chernmet/, analysisp.bin, 1, Cs, 2.92E+14, 24.0, 86 4 27 0 0, 1, 45.5 18.0, 0.05 0.05, 21.0 26.0, ./, cuall3, 1, 0, 86 4 27 0 0, 86 5 1 0 0, 0 96 0, 1, 1.0 1.0 1.0, 0.0001 0.0 0.0 0.0 0.0, 0.0 3.2E+05 5.0E-05, 10976.0, 0.0

### *D.6 Greece Diagnostic Run HySPLIT Settings - Emission 10m to 1750m*

The following HySPLIT control file contents, and minor variations on it, are used for the April Greece omission diagnostic runs in Appendix G.

86 4 25 21, 2, 51.38 30.1 10.0, 51.38 30.1 1750.0, 123, 0, 10000, 1, E:/Chernmet/, analysisp.bin, 1, Cs, 7.66E+13, 123, 86 4 25 21 0, 1, 45.5 18.0, 0.5 0.5, 21.0 26.0, ./, t1750b10, 1, 0, 86 4 25 21 0, 86 5 1 0 0, 0 123 0, 1, 1.0 1.0 1.0, 0.0001 0.0 0.0 0.0 0.0, 0.0 3.2E+05 5.0E-05, 10976, 0

## *Appendix E. Political Map of Europe*


Figure 67 Current Political Map of Europe

## *Appendix F. HySPLIT Source Code Modification*

HySPLIT is configured to handle up to eleven land use types, i.e. one water type (type number 7), and ten terrestrial types. HySPLIT source code was provided for this thesis courtesy of Roland Draxler at ARL. Modifying the HySPLIT source code for the cloud base split parameterization requires a simple code change. The following is an excerpt from the HySPLIT subroutine, 'depelm.f' with all necessary modification. Additions to the original code include all full lines preceded with 'CCC' and one 'CCC' at the start of the line following 'O L D  C O D E.'

```
C test for wet removal processes
IF(DIRT(KT)%DOWET.AND.RAIN.GT.0.0)THEN
C determine bottom and top of the precip layer (80% to 60%)
CCC ******************************************************
CCC with modification: (BASE AT 75% OVER LAND, 80% OVER SEA)
CCC ******************************************************
KBOT=0
KTOP=NLVL
DO K=1,NLVL
KRH=QQ(K)*100.0+0.5
CCC ******************************************************
CCC CLOUD BASE MODIFICATION PROPOSED BY aaron@gimail.af.mil
CCC SEE: http://nimbo.wrh.noaa.gov/wrhq/96TAs/TA9629/ta96-29.html
CCC WESTERN REGION TECHNICAL ATTACHMENT
CCC NO. 96-29
CCC NOVEMBER 19, 1996
```

```
CCC THE EXPLICIT CLOUD PREDICTION SCHEME IN
CCC THE MESO ETA MODEL
CCC Mike Staudenmaier, Jr. - WRH-SSD/NWSFO SLC
CCC * * * * * *  O L D  C O D E  * * * * * *
CCC IF(KBOT.EQ.0.AND.KRH.GE.80)KBOT=K
CCC * * * * * *  N E W  C O D E  * * * * * *
IF(LAND.EQ.7.AND.KBOT.EQ.0.AND.KRH.GE.80)KBOT=K
IF(LAND.NE.7.AND.KBOT.EQ.0.AND.KRH.GE.75)KBOT=K
CCC ****************************************************
IF(KBOT.NE.0.AND.KTOP.EQ.NLVL.AND.KRH.LE.60)KTOP=K
END DO
```

## *Appendix G. Investigation of Greece Exclusion from Modeled April Cs-137 Deposition*

Since several cumulative Cs-137 concentration measurements exceeding $10^5 Bq/m^2$ were recorded in Greece on 1986May01, the conspicuous omission of Greece from April deposition patterns in this thesis bears investigation. No other simultaneous sources of atmospheric Cs-137 are documented, and Cs-137 arrives in Greece in the model early in May, so it is safe to assume that the measured deposition came from Chernobyl. This investigation considers three other possible explanations for the Greece exclusion from the cumulative control run. The first possibility is an over-estimated deposition velocity, i.e. the modeled dry fall speed is too fast. The distribution of particle sizes is not known nor is the change of the distribution in space and time, yet the modeled constant deposition velocity implies a uniform modeled size distribution. It's conceivable that actual particles of smaller aerodynamic diameter could have been carried further than the modeled plume before depositing. Another possible reason the model failed to show transport to Greece is trajectory looping of the actual plume, i.e. pollutant could leave the model domain and return (HySPLIT ignores particles that leave the domain of the meteorological model). Figure 17 suggests this is a strong possibility since the air parcels 'disappear' from the simulation (i.e, HySPLIT omits particles from any further calculations) when they cross the meteorological grid boundary at about 40.5 degrees longitude. The third possible reason for a modeled Cs-137-free Greece is a combination of modeled wind direction error and modeled wind speed error. Direction errors (especially near the source) or speed errors (especially in the vertical) could prevent the model from transporting pollutant to Greece by 0Z, May 1. Since no compelling evidence for control run adjustments has come to light, settings for the simulation should not be tuned solely to provide for April deposition in Greece, and the data is ignored. Modeled emission release heights of up to $2990m$ and $9000m$ in diagnostic

simulations yielded deposition nearer to Greece, but not in Greece. The first (wet) part checks different source term profiles in the vertical to isolate control run release heights that could result in Cs-137 deposited in Greece; none do. The second (dry) part employs the ultimate source term profile in the vertical to isolate control run plume layers that could result in Cs-137 deposited in Greece; none do. Reference Appendix E for a map of Europe with political boundaries and designations.

### *G.1 Evaluation of Source Term Height - Wet*

Since the source term height is uncertain, it is prudent to see if an error in the modeled source term height could be the cause of the Grecian deposition omission. Three diagnostic simulations are presented. Figure 68 is the result of a run set up the same as the 5-day cumulative control run, but with the emission in a uniform vertical line from $10m$ to $1750m$. If the reason for Greece's omission was a control run plume base estimate that was too high, then a plume base low enough would lead to model deposition in Greece. Figure 69 checks the effects of centering, for the run's duration, the uniform vertical line source at $1500m$, the recommended center of mass for the first six hours of emission (Klug 92:358). Figure 70 checks the effects of a source term extending to $9000m$. None of these diagnostic simulations deposit pollutant in Greece.

The contents of the HySPLIT Control file for the simulation in Figure 68 are recorded in Section D.6. Control file settings for the other two diagnostic simulations simply reflect the revised top of emission in line 4, and output grid filename in line 21. For a summary of all primary settings in this thesis see Appendix D. For full details on settings see the HySPLIT User's Guide (Draxler 99).

### *G.2 Evaluation of Source Term Height - Dry*

The exclusion of the Greece region from the model's control run output deposition fields is not a result of the model over-scavenging the plume by precipitation

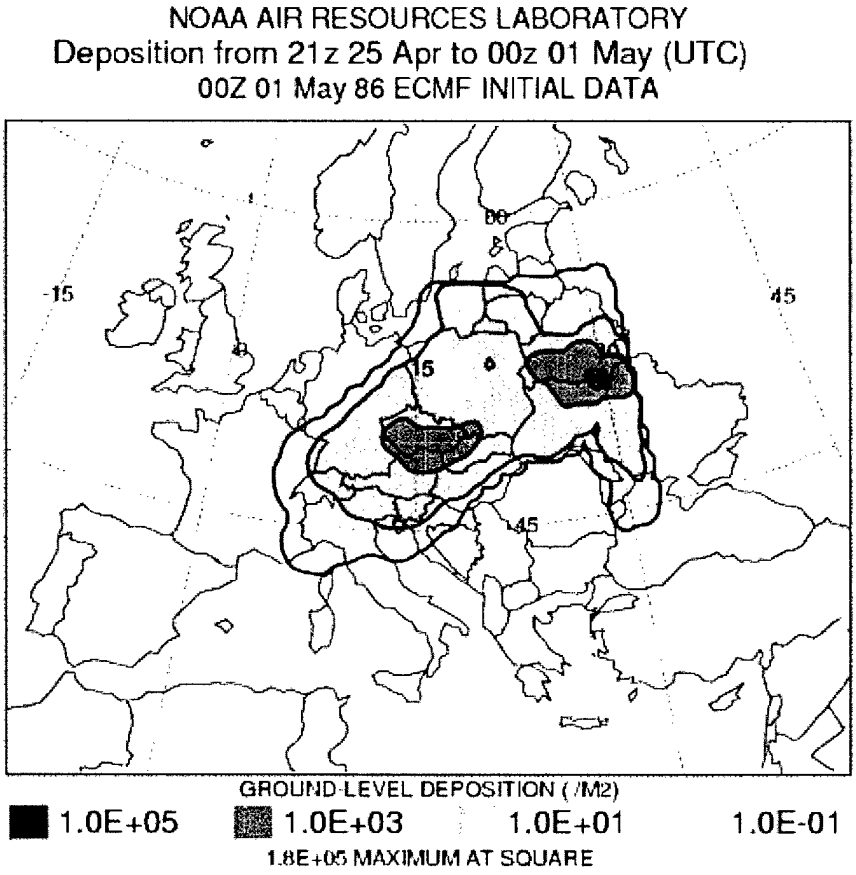


Figure 68 Greece Diagnostic Run, Cumulative April Deposition $[Bq/m^2]$, Release Height Profile from $10m$ to $1750m$

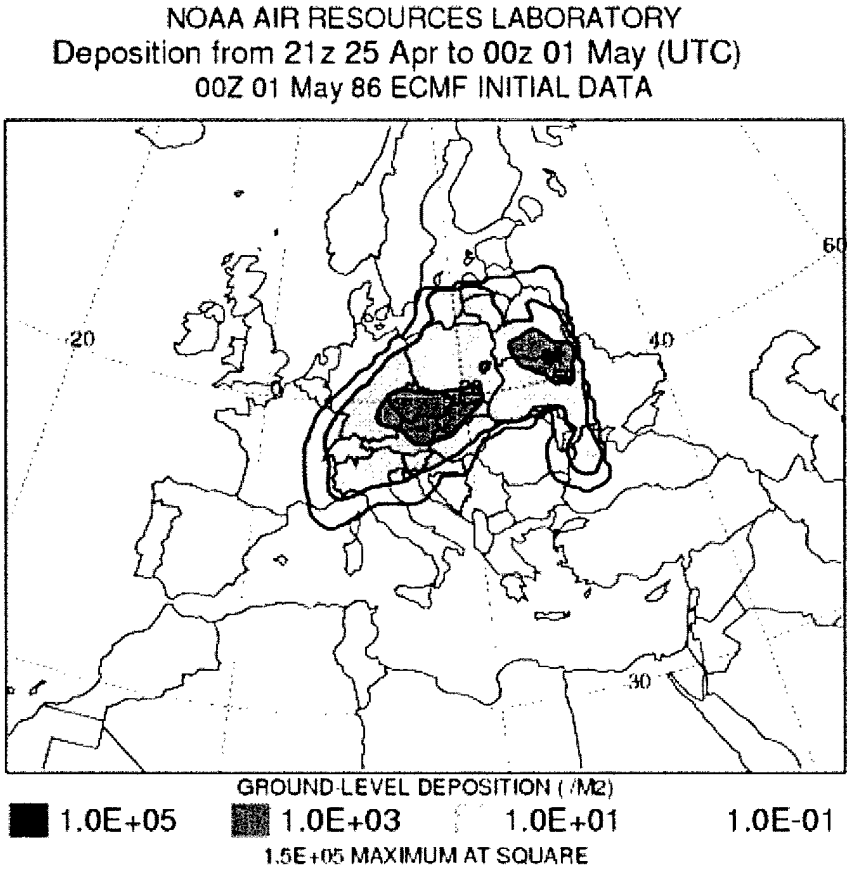


Figure 69 Greece Diagnostic Run, Cumulative April Deposition $[Bq/m^2]$, Release Height Profile from $10m$ to $2990m$

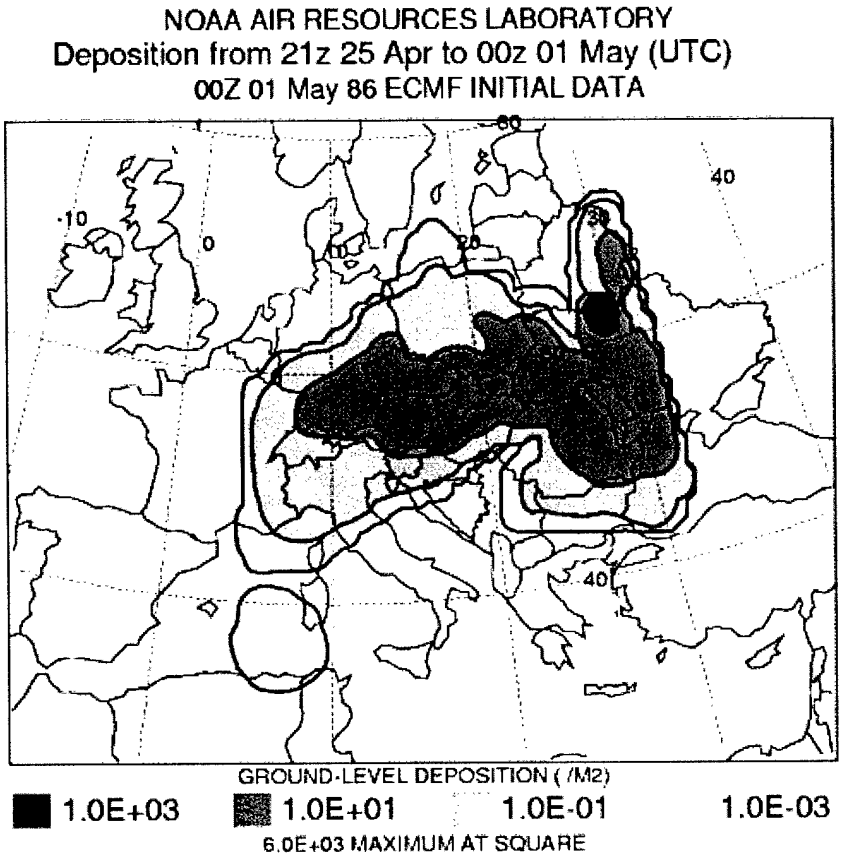


Figure 70 Greece Diagnostic Run, Cumulative April Deposition $[Bq/m^2]$, Release Height Profile from $10m$ to $9000m$

washout upstream. Dry model runs (i.e., with precipitation fields absent from the meteorological input file) indicate that the modeled pollutant plume (even with a vertical line source from 10 to 14000$m$) did not reach Greece. Figures 71 through 76 display slices of the total 5-day-averaged dry plume at several vertical levels. The output grids of this simulation imply that no particle emitted from Chernobyl at any height between 10$m$ and 14000$m$ at any time between 21Z1986Apr25 and 24Z1986Apr30 floated over Greece. This result is consistent with the null Greece deposition of the 'wet' runs, because the meteorological model contains significant precipitation Greece-wide, especially late in the simulation (see precipitation fields in Appendix C).

The dry runs were identical to the moist with these exceptions:

- The input meteorological model lacked precipitation fields (identical otherwise).
- All runs used the same source term layer (10$m$ to 14000$m$).
- The transport model top (ceiling) was set at 20000$m$ instead of at 10000$m$ (the default).
- Each run recorded an average concentration field at a different level (one at 0$m$, i.e., deposition, as in the wet runs).
- 2000 particles were tracked in each simulation instead of the default 500 (set in file 'setup.cfg').

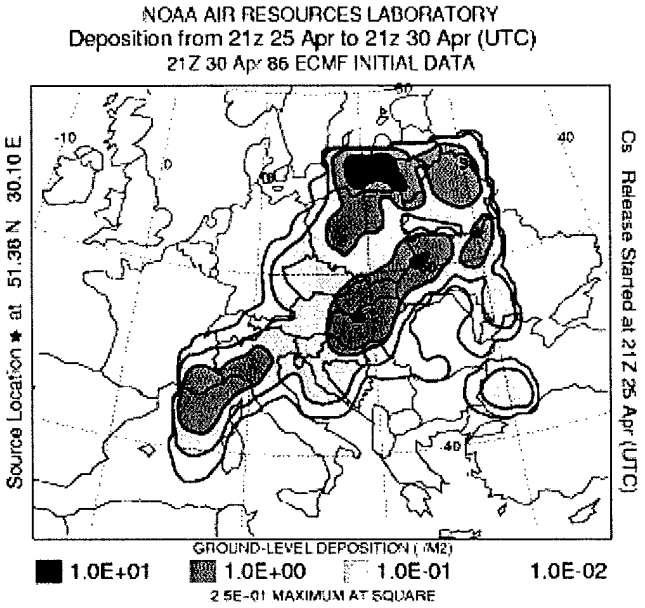


Figure 71 Five-day accumulated deposition due to Phase I emissions modeled as vertical line source from $10m$ to $14000m$. Precipitation turned off.

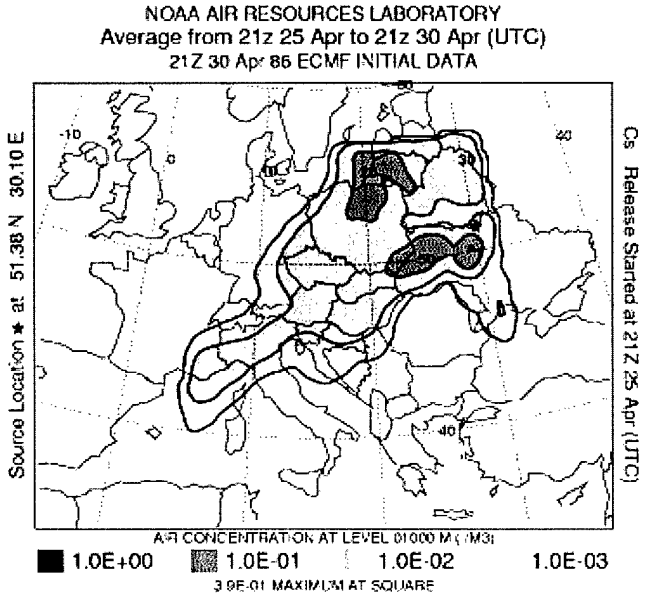


Figure 72 Five-day average concentration at $1000m$ due to Phase I emissions modeled as vertical line source from $10m$ to $14000m$. Precipitation turned off.

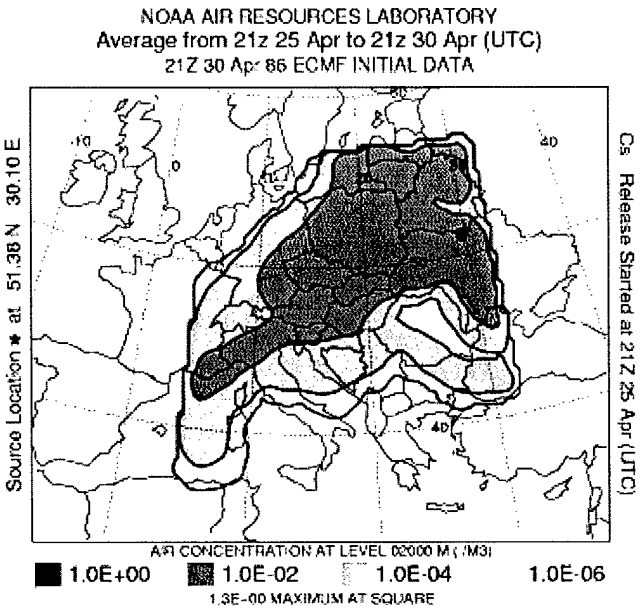


Figure 73 Five-day average concentration at $2000m$ due to Phase I emissions modeled as vertical line source from $10m$ to $14000m$. Precipitation turned off.

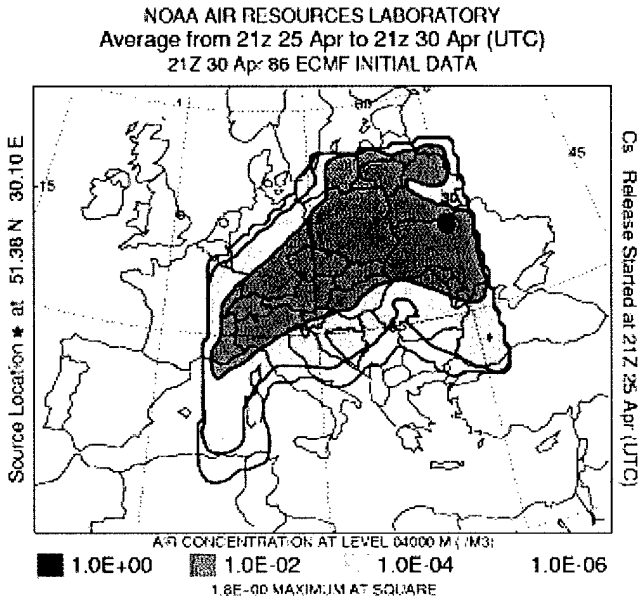


Figure 74 Five-day average concentration at $4000m$ due to Phase I emissions modeled as vertical line source from $10m$ to $14000m$. Precipitation turned off.

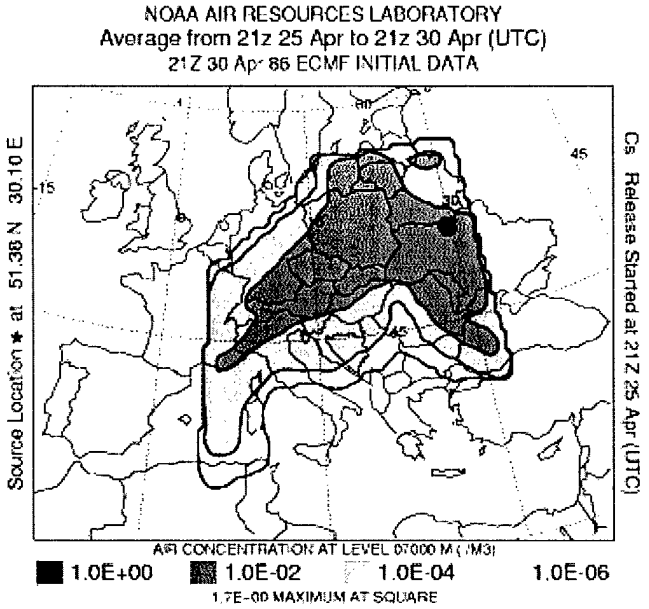


Figure 75 Five-day average concentration at $7000m$ due to Phase I emissions modeled as vertical line source from $10m$ to $14000m$. Precipitation turned off.

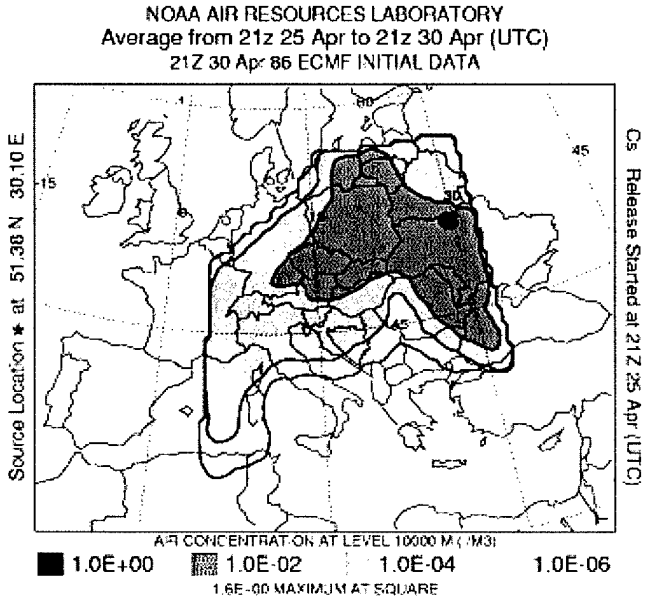


Figure 76 Five-day average concentration at $10000m$ due to Phase I emissions modeled as vertical line source from $10m$ to $14000m$. Precipitation turned off.

## *Bibliography*


ARL 00a. ARL. *The Chernobyl Reactor Accident.* http://www.arl.noaa.gov/ss/transport/chernobyl.html, October 2000. Air Resources Laboratory, Transport Modeling and Assessment - Silver Spring, MD.

ARL 00b. ARL. *ETEX Simulations Using HYSPLIT4.* http://www.arl.noaa.gov/ss/transport/etex.html, October 2000. Air Resources Laboratory.

DeCort 90. M. DeCort, G. Graziani, F. Raes, D. Stanners, G. Grippa & I. Ricapito. *Radioactivity Measurements in Europe after the Chernobyl Accident, Part II, Fallout and Deposition.* Rapport technique EUR 12800 EN, Commission of the European Communities Joint Research Centre - Ispra Site, 1990.

DeCort 98. M. DeCort, G. Dubois, Sh D. Fridman & M. G. Germenchuk et al. *Atlas of Caesium Deposition on Europe After the Chernobyl Accident.* Luxembourg, Office for the Official Publications of the European Communities, 1998. 176 pp.

Draxler 98a. Roland R. Draxler & G. D. Hess. *Description of the HYSPLIT4 modeling system.* Rapport technique NOAA Tech. Memo. ERL ARL-224, National Oceanographic and Atmospheric Administration, December 1998.

Draxler 98b. Roland R. Draxler & G.D. Hess. *An overview of the HYSPLIT4 modelling system for trajectories, dispersion and deposition.* Aust. Met. Mag., vol. 47, pages 295–308, 1998.

Draxler 99. Roland R. Draxler. *Hybrid single-particle Lagrangian integrated trajectories (HY-SPLIT): Version 3.0 – User's guide and model description.* Rapport technique NOAA Tech. Memo. ERL ARL-195, National Oceanographic and Atmospheric Administration, 5285 Port Royal Rd, Springfield, VA 22161, 1999. Available from National Technical Information Service, 5285 Port Royal Road, Springfield, VA 22161.

Draxler 00a. Roland Draxler, 2000. Electronic Message, 19Sep2000, ARL, Silver Spring, Maryland.

Draxler 00b. Roland Draxler, 2000. Personal Communication, 23March2000, Air Force Technical Applications Center, Patrick AFB, Florida.

Glasstone 77. Samuel Glasstone & Philip J. Dolan. *The Effects of Nuclear Weapons, 3rd edition.* United States Department of Defense and United States Department of Energy, 1977. 653 pp.

Graziani 97. Giovanni Graziani. *European Tracer Experiment.* http://www.ei.jrc.it/etex/, August 1997.

Graziani 00. Giovanni Graziani, 2000. Electronic Message, 18sep2000, JRC, Ispra, Italy.

Hagans 00. Fred Hagans. http://www.aftac.gov/mission.htm, 2000.

Hicks 86. Bruce B. Hicks. *Differences in wet and dry particle deposition parameters between North America and Europe.* Aerosols: Research, Risk Assessment, and Control Strategies, pages 973–982, 1986. Atmospheric Turbulence and Diffusion Division, Air Resources Laboratory, ERL/NOAA, Oak Ridge, TN – Lewis Publishers, Chelsea, MI.

IGES 01. IGES. *GRid Analysis and Display System.* http://grads.iges.org/grads/, January 2001. Institute of Global Environment and Society.

Klug 92. W. Klug, G. Graziani, G. Grippa, G. D. Pierce & C. Tassone. *ATMES Report, Evaluation of long range atmospheric transport models using environmental radioactivity data from the Chernobyl accident.* Elsevier Science Publishers, England, 1992. 366 pp.

Knap 88. Anthony H. Knap. *The Long-Range Atmospheric Transport of Natural and Contaminant Substances.* Kluwer Academic Publishers, 1988. NATO Advanced Science Institutes Series C: Mathematical and Physical Sciences - Vol. 297, 321 pp.

Lauritzen 99. B. Lauritzen & T. Mikkelson. *A probabilistic dispersion model applied to the long range transport of radionucleides from the Chernobyl accident.* Atm. Environ., vol. 33, pages 3271–3279, 1999. Riso National Laboratory, 4000 Roskilde, Denmark.

Métivier 95. Henri Métivier. *Chernobyl Ten Years On, Radiological and Health Impact.* http://www.nea.fr/html/rp/chernobyl/allchernobyl.html, November 1995. OECD Nuclear Energy Agency.

MSE 00. *Curie (measurement) Microsoft Encarta Online Encyclopedia 2000.* http://encarta.msn.com 1997-2000 Microsoft Corporation. All Rights Reserved, 2000.

NWS 01. *The Medium-Range Forecast Model status as of January 09, 2001.* http://sgi62.wwb.noaa.gov:8080/research/mrf.html, 2001. National Weather Service.

Persson 87. C. Persson, H. Rodhe & L. E. De Geer. *The Chernobyl accident – a meteorological analysis of how radionuclides reached and were deposited in Sweden.* Ambio, vol. 16, pages 20–31, 1987.

Pöllänen 97. Roy Pöllänen, Ilkka Valkama & Harri Toivonen. *Transport of radioactive particles from the Chernobyl accident.* Atm. Environ., vol. 31, pages 3575–3590, 1997. Finnish Centre for Radiation and Nuclear Safety (STUK), P.O. Box 14, 00881 Helsinki, Finland; and Finnish Meteorological Institute (FMI), P.O. Box 503, 00101 Helsinki, Finland.

Rodriguez 95. D. Rodriguez, H. Walker, N. Klepikova, A. Kostrikov & Y. Zhuk. *Evaluation of two pollutant disperson models over continental scales.* Atm. Environ., vol. 29, no. 7, pages 799–812, 1995. University of California, Livermore, CA 94550, U.S.A.; and Institute of Experimental Meteorology, Obninsk, Kaluga Region 249020, Russia.

Seinfeld 86. J. H. Seinfeld. *Atmospheric Chemistry and Physics of Air Pollution.* John Wiley and Sons, New York, 1986. 324 pp.

Serway 92. Raymond A. Serway. *Physics for Scientists and Engineers with Modern Physics, 3rd edition.* Saunders College Publishing, 1992. 1444 pp.

Slingo 87. J. M. Slingo. *The development and verification of a cloud prediction scheme for the ECMWF model.* Quart. J. Roy. Meteor. Soc., vol. 113, pages 899–927, 1987. European Centre for Medium Range Weather Forecasts, Reading, England.

Staudenmaier 96. Mike Staudenmaier Jr. *The explicit cloud prediction scheme in the Meso ETA model.* Rapport technique Western Region Technical Attachment 96-29, National Weather Service Western Region Headquarters, Salt Lake City, 1996.

Tiedke 93. M. Tiedke. *Representation of Clouds in Large-Scale Models.* Mon. Wea. Rev., vol. 121, pages 3040–3061, 1993. European Centre for Medium-Range Weather Forecasts, Reading, Berkshire, England.

UIC 00. UIC. *Radiation and Life.* http://www.uic.com.au/ral.htm, 2000. URANIUM INFORMATION CENTRE, Ltd., A.C.N. 005 503 828.

## *Vita*

Captain Aaron M. Kinser was born in Kettering, Ohio in 1966, and was raised in nearby Centerville. Centerville High School granted him a diploma in May, 1984. In 1989 he enlisted in the US Air Force as a computer operator and served one tour assigned to the 354th Communications Squadron, Eielson AFB, Alaska. While assigned there he was selected for the Airmen Education and Commissioning Program (AECP) administered by the Air Force Institute of Technology (AFIT), Wright Patterson AFB, Ohio. Per AECP, Captain Kinser earned a Bachelors Degree in Atmospheric Sciences in 1996 from the University of Arizona in Tucson, Arizona and graduated from Officer Training School at Maxwell AFB, Alabama on December 6, 1996. He then served as wing weather officer for the 57th Operational Support Squadron at Nellis AFB, Nevada until he was selected to earn a Masters Degree in Meteorology at AFIT starting in the Fall of 1999. Following graduation, Captain Kinser will be assigned to the Air Force Technical Applications Center (AFTAC), Patrick AFB, Florida. Captain Kinser can be contacted for the foreseeable future by text-only email at aaron@gimail.af.mil.

# REPORT DOCUMENTATION PAGE

*Form Approved*
*OMB No. 0704-0188*



**PLEASE DO NOT RETURN YOUR FORM TO THE ABOVE ADDRESS.**

| 1. REPORT DATE *(DD-MM-YYYY)* | 2. REPORT TYPE | 3. DATES COVERED |
|---|---|---|
| 03-2001 | Master's Thesis | Aug 2000 - Mar 2001 |

**4. TITLE AND SUBTITLE**

SIMULATING WET DEPOSITION OF RADIOCESIUM FROM THE CHERNOBYL ACCIDENT

**5a. CONTRACT NUMBER**

**5b. GRANT NUMBER**

**5c. PROGRAM ELEMENT NUMBER**

**6. AUTHOR(S)**

Kinser, Aaron, M., Captain, USAF

**5d. PROJECT NUMBER**

**5e. TASK NUMBER**

**5f. WORK UNIT NUMBER**

**7. PERFORMING ORGANIZATION NAME(S) AND ADDRESS(ES)**

Air Force Institute of Technology (AFIT/EN)
Bldg 640 Rm 100
2950 P St
Wright Patterson AFB, OH 45433-7765

**8. PERFORMING ORGANIZATION REPORT NUMBER**

AFIT/GM/ENP/01M-05

**9. SPONSORING/MONITORING AGENCY NAME(S) AND ADDRESS(ES)**

Air Force Technical Applications Center
Attn: Mr. Craig Sloan
1030 S. Highway A1A
Patrick AFB, FL 32925-3002 DSN: 854-7781

**10. SPONSOR/MONITOR'S ACRONYM(S)**

AFTAC/TMAR

**11. SPONSOR/MONITOR'S REPORT NUMBER(S)**

**12. DISTRIBUTION/AILABILITY STATEMENT**

APPROVED FOR PUBLIC RELEASE; DISTRIBUTION UNLIMITED.

**13. SUPPLEMENTARY NOTES**

**14. ABSTRACT**

In response to the Chernobyl nuclear power plant accident of 1986, a cesium-137 deposition dataset was assembled. Most of the airborne Chernobyl cesium was wet deposited, either via interception by falling raindrops or via absorption into cloud droplets destined to become raindrops. The Hybrid Single-Particle Lagrangian Integrated Transport (HYSPLIT) model, developed at Air Resources Laboratory, is used to simulate the transport and deposition of Chernobyl cesium-137. A cloud base parameterization modification is tested and appears to slightly improve the accuracy of one HYSPLIT simulation of daily Chernobyl cesium-137 deposition over the course of the accident at isolated European sites, and degrades the accuracy of another HYSPLIT simulation of deposition in Germany and Austria accumulated in the month of April 1986. Large uncertainties in the emission specifications, model precipitation fields, and deposition measurements prevent designating the results as conclusive, but most evidence points to improved performance within 500 kilometers of the emission source. Trial and error lessons learned from hundreds of preliminary model runs are documented, and the exact HYSPLIT settings of successful and meaningful simulations are appended.

**15. SUBJECT TERMS**

Hybrid Single-Particle Lagrangian Integrated Transport (HYSPLIT) model, atmospheric transport modeling, wet deposition, cesium-137 deposition, cloud base parameterization, Chernobyl

| 16. SECURITY CLASSIFICATION OF: | | | 17. LIMITATION OF ABSTRACT | 18. NUMBER OF PAGES | 19a. NAME OF RESPONSIBLE PERSON |
|---|---|---|---|---|---|
| a. REPORT | b. ABSTRACT | c. THIS PAGE | | | Lt Col Michael K. Walters, AFIT/ENP |
| U | U | U | UU | 123 | 19b. TELEPHONE NUMBER *(Include area code)* (937)237-7166 |